



**US Army Corps
of Engineers®**
Engineer Research and
Development Center



Report on Evaluation of Apartment Towers 1–4 and Parking Garages 1–4 at Camp Walker, Daegu, South Korea

C. Kennan Crane, Omar Esquilin-Mangual, Bradley W. Foust,
Andrew B. Groeneveld, William F. Heard, John M. Hoemann,
Kyle L. Klaus, Jason A. Morson, Robert D. Moser, James C.
Ray, M. Jason Roth, Cody M. Strack, Lucas A. Walshire,
Stephanie G. Wood, and Stanley C. Woodson

April 2022

The U.S. Army Engineer Research and Development Center (ERDC) solves the nation's toughest engineering and environmental challenges. ERDC develops innovative solutions in civil and military engineering, geospatial sciences, water resources, and environmental sciences for the Army, the Department of Defense, civilian agencies, and our nation's public good. Find out more at www.erdclibrary.on.worldcat.org/discovery.

To search for other technical reports published by ERDC, visit the ERDC online library at www.erdclibrary.on.worldcat.org/discovery.

Report on Evaluation of Apartment Towers 1–4 and Parking Garages 1–4 at Camp Walker, Daegu, South Korea

C. Kennan Crane, Omar Esquilin-Mangual, Bradley W. Foust, Brian H. Green, Andrew B. Groeneveld, William F. Heard, John M. Hoemann, Kyle L. Klaus, Jason A. Morson, Robert D. Moser, James C. Ray, M. Jason Roth, Cody M. Strack, Lucas A. Walshire, Stephanie G. Wood, and Stanley C. Woodson

*Geotechnical and Structures Laboratory
U.S. Army Engineer Research and Development Center
3909 Halls Ferry Road
Vicksburg, MS 39180*

Final report

Approved for public release; distribution is unlimited.

Prepared for Far East District, Pacific Ocean Division
U.S. Army Corps of Engineers
573 Bonney Loop, Building 525, Suite A300
Fort Shafter, HI 96858

Under Pacific Ocean Division (POD) funding

Abstract

In August of 2021, unexpected cracking was discovered in the concrete of newly constructed apartment towers and parking garages at Camp Walker, Daegu, South Korea. Initial evaluation by U.S. Army Corps of Engineers Far East District (USACE-POF) determined the towers to be safe for continued occupation. Out of an abundance of caution a team from the Engineer Research and Development Center (ERDC) conducted an independent evaluation of these structures to further verify life safety. Additionally, this evaluation sought to determine the potential causes of this cracking and remediation schemes both to inform future construction, but also to lay the groundwork for a more in-depth lifecycle evaluation by an Architectural/Engineering (AE) firm specializing in structural forensics.

The ERDC evaluation consisted of on-site inspection, non-destructive testing, materials sampling and testing, and review of particular design and construction documentation provided by the Far East District. The results of the evaluation confirmed the Far East District's findings that there was not a threat to life safety in these structures. Furthermore, the results of the ERDC evaluation indicated that drying shrinkage was the most likely causes of the observed cracking. In the areas where this cracking was the most severe, repair with epoxy injection was recommended for continued structural safety. In areas with moderate cracking, sealing of cracks was recommended to prevent long-term durability issues decreasing the lifespan of the structures.

DISCLAIMER: The contents of this report are not to be used for advertising, publication, or promotional purposes. Citation of trade names does not constitute an official endorsement or approval of the use of such commercial products. All product names and trademarks cited are the property of their respective owners. The findings of this report are not to be construed as an official Department of the Army position unless so designated by other authorized documents.

DESTROY THIS REPORT WHEN NO LONGER NEEDED. DO NOT RETURN IT TO THE ORIGINATOR.

Contents

Abstract.....	iii
Figures and Tables.....	vi
Preface.....	xv
Executive Summary.....	xvi
1 Introduction.....	1
2 Apartment Tower Evaluation.....	2
2.1 Observations from visual inspections of apartment towers.....	2
2.1.1 General tower observations.....	2
2.1.2 Tower 1 observations.....	3
2.1.3 Tower 2 observations.....	11
2.1.4 Tower 3 observations.....	22
2.1.5 Tower 4 observations.....	27
2.2 Analysis and findings.....	33
2.2.1 Geotechnical evaluation.....	33
2.2.2 Materials and construction evaluation.....	35
2.2.3 Structural evaluation.....	45
2.3 Conclusions and recommendations.....	47
3 Parking Garage Evaluation.....	48
3.1 Observations from visual inspections of parking garages.....	48
3.1.1 General garage observations.....	48
3.1.2 Garage 1 observations.....	51
3.1.3 Garage 2 observations.....	54
3.1.4 Garage 3 observations.....	56
3.1.5 Garage 4 observations.....	59
3.2 Analysis and findings.....	62
3.2.1 Geotechnical evaluation.....	63
3.2.2 Materials and construction evaluation.....	63
3.2.3 Structural evaluation.....	64
3.3 Conclusions and recommendations.....	66
4 Conclusions and Overall Recommendations.....	67
References.....	68
Appendix A: Geotechnical Evaluation Report.....	70
Appendix B: Additional Pictures from Visual Inspection of Towers and Parking Garages.....	86
Appendix C: Petrographic Analysis of Cores from Camp Walker, South Korea.....	136

Appendix D: Concrete Strength	186
Appendix E: Core Strength Report from Far East District	194
Appendix F: Initial ERDC Assessment Memorandum	195
Acronyms and Abbreviations	196
Unit Conversion Factors.....	197
Report Documentation Page	

Figures and Tables

Figures

Figure 1. Diagonal crack within the Tower 1 basement storage area (Section B of the floorplan insert). The widest section of the observed crack was 0.40 mm (crack gauge insert); however, the crack width narrows at the extents and does not intersect with the floor slab.....	4
Figure 2. Vertical crack within the Tower 1 basement storage area (Section A of the floorplan insert). The widest area of the observed crack was less than 0.40 mm and did not intersect the floor slab.	5
Figure 3. Wall cracks within the Tower 1 basement storage area (Section G of the floorplan insert). The widest observed crack width was less than 0.40 mm. The shown cracks were traced with a permanent marker to highlight typical locations, lengths, and spacing and are not representative of crack width.	6
Figure 4. Slab floor cracks within the Tower 1 basement storage area (Section C of the floorplan insert). The widest observed crack width was between 0.40 and 0.50 mm (crack gauge insert) with most observed cracks being hairline cracks of less than 0.25 mm.	7
Figure 5. Slab floor cracks within the Tower 1 basement storage area (Section C of the floorplan insert). The widest observed crack width was less than 0.25 mm.	7
Figure 6. Overhead (ceiling) slab cracks within the Tower 1 basement storage area (Section C of the floorplan insert). Widths of these cracks were not measured but approximate the size, patterns, and widths as other observed cracks in the floor slabs.	8
Figure 7. Cold joints within the Tower 1 basement shaft area (Section E of the floorplan insert). These cold joints were observed on bare concrete and were typical in the mechanical and electrical shaft areas in the upper floors.	9
Figure 8. Cracking over mudded walls (typical) within the nonbasement floors of Tower 1 (Section I of the floorplan insert).	10
Figure 9. Wall cracks within the Tower 1 attic elevator mechanical area (Section J of the floorplan insert). The widest observed crack width was less than 0.40 mm. The shown cracks were traced with a permanent marker to highlight typical locations, lengths, and spacing and are not representative of crack width.	11
Figure 10. Largest observed diagonal crack within the Tower 2 basement storage area (Section L of the floorplan insert). The widest section of the observed crack was 0.50 mm (crack gauge insert); however, the crack width narrows at the extents and does not intersect with the floor slab.	13
Figure 11. Typical observed diagonal cracking within the Tower 2 basement storage area (Section E of the floorplan insert). The widest area of the typical observed crack was less than 0.40 mm and did not intersect the floor slab. The crack shown here has been repaired; however, it is typical of orientation, location, and size of the Tower 2 diagonal cracking.	14
Figure 12. Wall cracks within the Tower 2 basement storage area (Section E of the floorplan insert). The widest observed crack width was less than 0.40 mm. The shown cracks were traced with a permanent marker to highlight typical locations, lengths, and spacing and are not representative of crack width.	15

Figure 13. Most severe observed vertical crack within the Tower 2 basement storage area (Section A of the floorplan insert). The widest section of the observed crack was 0.6 mm (crack gauge insert).....	16
Figure 14. Typical observed vertical cracking within the Tower 2 basement storage area (Section I of the floorplan insert). The widest area of the observed crack was less than 0.40 mm and did not intersect the floor slab (crack gauge insert).....	16
Figure 15. Wall cracks within the Tower 2 basement storage area (Section D of the floorplan insert). The widest observed crack width was less than 0.50 mm (crack gauge insert). The shown cracks were traced with a permanent marker to highlight typical locations, lengths, and spacing and are not representative of crack width.....	17
Figure 16. Typical observed repaired vertical cracking within the Tower 2 basement storage area (Section D of the floorplan insert). The repaired region has been intentionally widened with an angle grinder and filled with a polymer grout.....	18
Figure 17. Typical observed overhead (ceiling) slab cracks within the Tower 2 (Section Q of the 1st Floor floorplan insert).....	19
Figure 18. Observed cold joints within the Tower 2 elevator shaft area (Section H of the floorplan insert). These cold joints were observed on bare concrete and were typical in the elevator shaft areas in the upper floors.....	19
Figure 19. Cracking on bare concrete walls (typical) within the nonbasement floors of Tower 2 (Section R of the 2nd Floor floorplan insert). Majority of observed crack widths were less than 0.4 mm (insert depicts the largest observed of these cracks at a width of 0.6 mm).	20
Figure 20. Honeycombing within Tower 2 (Section TAA of the 12 th Floor floorplan insert). The honeycombing varied in severity but was typically located in areas of high rebar congestion and was often near cold joints.....	21
Figure 21. Cracks within the Tower 2 attic elevator mechanical area (Section AB of the floorplan insert). The widest observed crack width was less than 0.40 mm. The shown cracks were traced with a permanent marker to highlight typical locations, lengths, and spacing and are not representative of crack width.....	22
Figure 22. Representative diagonal crack within the basement area of Tower 3 (Indicated on floorplan insert). The widest section of the observed crack was 0.15 mm (crack gauge insert).....	23
Figure 23. Typical observed cold joints within Tower 3 elevator shaft area (floorplan insert).	24
Figure 24. Vertical crack in Tower 3 observed on bare concrete (Section A of the floorplan insert). The widest section of the crack was 0.35 mm (crack gauge insert).....	25
Figure 25. Representative diagonal crack within the nonbasement floors of Tower 3 (Apartment Section of the 1st Floor floorplan insert). The widest section of the crack was 0.15 mm (crack gauge insert).....	26
Figure 26. Observed cracking within Tower 3, 14th Floor stairwell (Stairway #2 of the floorplan insert). The widest area of the observed crack less than 0.25 mm. The crack did not intersect the ceilings, floors, or wall edges.	26

Figure 27. Typical diagonal cracking observed in the basement of Tower 4 (floorplan insert). The cracking was covered post placement but before visual inspections (insert shows the inspected crack on bare concrete without patch).....	28
Figure 28. Vertical cracking observed in the basement of Tower 4 (floorplan insert). The cracking was covered post placement but before visual inspections (insert shows observable crack after patch/paint removed).....	29
Figure 29. Observed vertical crack in Tower 4 (3rd Floor floorplan insert). The crack width was less than 0.20 mm (crack gauge insert).	29
Figure 30. Observed slab cracking in Tower 4 (floorplan insert). The crack widths were less than 0.15 mm (crack gauge insert).....	30
Figure 31. Observed cold joint in Tower 4 stairwell (floorplan insert).	31
Figure 32. Poor consolidation along bottom wall of Tower 4 balcony and adjacent columns (floorplan insert).....	32
Figure 33. Patching of voids in exterior concrete of Tower 4 (floorplan insert).	32
Figure 34. Nonuniformity in Tower 4 concrete wall (floorplan insert).	33
Figure 35. Concrete placement terminated within a slab. The person standing on the concrete indicates that this concrete has hardened.....	38
Figure 36. Reinforcement in Parking Garage 4 roof. The rebar placement was very precise in all areas observed.	40
Figure 37. Typical rebar placement showing intersection between slab and beam (Parking Garage 4).	41
Figure 38. Rebar congestion in slab-beam intersection in Parking Garage 4.....	41
Figure 39. Rebar congestion at intersection between beams and column in Parking Garage 4.....	42
Figure 40. Congested rebar around HVAC duct passthrough in Tower 4.....	42
Figure 41. Polished cross section of core T2-3 with locations of cracking through aggregates indicated.....	44
Figure 42. Comparison of crack pattern and width above and below coating in Garage 1. The crack patterns did not change when the surface coating was removed, and the widths were all within 0.05 mm of those measured on top of the coating.	49
Figure 43. Parallel diagonal cracks in beam on Column Line E between Column Lines 5 and 6 of upper floor of Garage 1.....	50
Figure 44. Typical diagonal crack in beam showing decrease in crack width at bottom and top of beam.	50
Figure 45. Diagonal cracks in beam and girder at the intersection of Column Lines E and 4 on the upper floor of Garage 1.	51
Figure 46. Ground level entrance to Parking Garage 1.	52
Figure 47. Diagonal cracks in first floor (basement) of Parking Garage 1.	53
Figure 48. Crack in roof beam over Parking Garage 1 ramp. Crack width was approximately 1.2 mm.	54
Figure 49. Typical diagonal cracking in girder of Parking Garage 2. Note the staining near a crack on the ceiling indicating water coming through from the upper floor.	55

Figure 50. Most severe diagonal crack noted in Parking Garage 2 (0.7 mm).	55
Figure 51. Multidirectional cracking extending from beams into ceiling slab of roof over ramp to floor 2.	56
Figure 52. Repaired wall of cracked stairwell in Parking Garage 3.....	57
Figure 53. Repaired diagonal concrete cracks visible beneath exterior coating on Parking Garage 3.....	58
Figure 54. Vertical cracking in stairwell wall of Parking Garage 4.....	60
Figure 55. Crack monitoring in Parking Garage 4.....	60
Figure 56. Crack in slab of Parking Garage 4 showing staining at location of water ingress.	61
Figure 57. Vertical crack in beam immediately adjacent to shoring. This shoring was in place continuously since concrete was cast.....	61
Figure 58. Diagonal cold joint under staircase in Parking Garage 4.....	62
Figure A1. Tower locations on Camp Walker, Daegu, South Korea (courtesy Google Earth).	73
Figure A2. Results of point load tests, reported as unconfined compression for A. Tower 1 and B. Tower 2.	78
Figure A3. Results of point load tests, reported as unconfined compression for A. Tower 3 and B. Tower 4.	78
Figure A4. Tower 4 laboratory testing results comparing unconfined compression test results to PLT derived unconfined compression.....	79
Figure A5. Load settlement curves from static load tests: A. Tower 1, B. Tower 2, C. Tower 3, and D. Tower 4.....	83
Figure B1. Cracking in walls of Tower 1.....	86
Figure B2. Honeycombing and cold joint in cored shaft of Tower 1.....	86
Figure B3. Cracking in mapped wall of elevator mechanical room in Tower 1.....	87
Figure B4. Cracking in concrete and cementitious coating in wall of Tower 1.....	88
Figure B5. Rebound hammer test locations in Tower 1—Basement through Floor 3.	88
Figure B6. Rebound hammer test locations in Tower 1—Floor 4.....	89
Figure B7. Rebound hammer test locations in Tower 1—Floor 5.	89
Figure B8. Rebound hammer test locations in Tower 1—Floors 6 through 9.....	90
Figure B9. Rebound hammer test locations in Tower 1—Floors 10 through 13.	90
Figure B10. Rebound hammer test locations in Tower 1—Floors 14 and 15.....	91
Figure B11. Coring activities in Tower 1.	92
Figure B12. Wall cracks with gauges in Tower 2 basement.....	93
Figure B13. Wall crack with gauge in Tower 2 basement.	93
Figure B14. Wall cracks with gauges in Tower 2 basement.....	94
Figure B15. Wall cracks with gauges in Tower 2 basement.....	94
Figure B16. Wall cracks with gauges in Tower 2 basement.....	95
Figure B17. Wall crack with gauge in Tower 2 basement.	96
Figure B18. Sealed cracks in Tower 2 basement.....	97

Figure B19. Mapped diagonal cracks in basement storage area of Tower 2.	97
Figure B20. Vertical and horizontal cracks in stairwell wall of Tower 2.	98
Figure B21. Cracks in basement mechanical room of Tower 2.	98
Figure B22. Wall cracks in shaft behind elevators in Tower 2.	99
Figure B23. Cold joints in shafts behind elevators in Tower 2.	99
Figure B24. Embedded rebar support (top left) and honeycombing and poor consolidation in shafts behind elevators in Tower 2.	100
Figure B25. Mapped wall cracks (top) and floor slab shrinkage cracks in elevator mechanical room in Tower 2.	101
Figure B26. Diagonal cold joint in wall of attic in Tower 2.	102
Figure B27. Rebound hammer test locations in Tower 2—Basement through Floor 3.	102
Figure B28. Rebound hammer test locations in Tower 2—Floors 4, 5, and 7.	103
Figure B29. Rebound hammer test locations in Tower 2—Floors 8, 9, and 10.	103
Figure B30. Rebound hammer test locations in Tower 2—Floors 12 through 15.	104
Figure B31. Vertical and horizontal cracks in basement wall of Tower 3.	105
Figure B32. Diagonal cracks in basement walls of Tower 3.	106
Figure B33. Cold joints in walls of shaft behind the elevators in Tower 3.	107
Figure B34. Rebound hammer test locations in Tower 3—Basement through Floor 3.	108
Figure B35. Rebound hammer test locations in Tower 3—Floors 5, 6, and 7.	108
Figure B36. Rebound hammer test locations in Tower 3—Floors 8 through 11.	109
Figure B37. Rebound hammer test locations in Tower 3—Floors 12, 14, and 15.	109
Figure B38. Coring activities in basement of Tower 3.	110
Figure B39. Diagonal cracks in basement walls of Tower 4.	111
Figure B40. Diagonal cracks in basement walls of Tower 4.	112
Figure B41. Cracks in walls of Tower 4.	112
Figure B42. Cold joints in walls of Tower 4.	113
Figure B43. Poor consolidation at balconies of Tower 4.	113
Figure B44. Nonuniformity (top) and staining (bottom) of concrete in Tower 4.	114
Figure B45. Rebound hammer test locations in Tower 4—Basement through Floor 3.	115
Figure B46. Rebound hammer test locations in Tower 4—Floors 4 through 7.	115
Figure B47. Rebound hammer test locations in Tower 4—Floors 8 through 11.	116
Figure B48. Rebound hammer test locations in Tower 4—Floors 12 through 14.	116
Figure B49. Wall reinforcement of Floor 15 in Tower 4.	117
Figure B50. Reinforcement on Floor 15 of Tower 4.	118
Figure B51. Diagonal cracks in girders and beams in Parking Garage 1.	119
Figure B52. Diagonal cracks in girders in Parking Garage 1.	120
Figure B53. Diagonal cracks in walls in Parking Garage 1.	121

Figure B54. Cracks in ceiling, beams, and wall of entrance to basement of Parking Garage 1.....	122
Figure B55. Mapped cracks in beam along column line 4 in Parking Garage 1.....	122
Figure B56. Mapped cracks in girder along column line E in Parking Garage 1.....	123
Figure B57. Removal of paint and top coating from girder and beam in Parking Garage 1. The girder is in line with column E, and the beam is in line with column 4 of the floor plan.....	123
Figure B58. Cracks in bare concrete of beam along column line 4 in Parking Garage 1.....	124
Figure B59. Cracks in bare concrete of girder along column line E in Parking Garage 1.....	124
Figure B60. Mapped cracks in bare concrete of beam along column line 4 in Parking Garage 1.....	125
Figure B61. Mapped cracks in bare concrete of girder along column line E in Parking Garage 1.....	125
Figure B62. Multidirectional cracks in ceiling and cracks in girder of entryway of Parking Garage 2.....	126
Figure B63. Diagonal cracks in girders and beams in Parking Garage 2.....	127
Figure B64. Diagonal cracks in girders and beams in Parking Garage 2.....	128
Figure B65. Vertical cracks manifest in surface architectural coating on exterior of Parking Garage 3.....	129
Figure B66. Diagonal crack in wall of stairwell in Parking Garage 3.....	130
Figure B67. Shoring for girders and beams throughout Parking Garage 4.....	131
Figure B68. Cold joints in walls in Parking Garage 4.....	132
Figure B69. Cracks with gauges and bugholes in walls in Parking Garage 4.....	133
Figure B70. Vertical cracks in beam in Parking Garage 4.....	134
Figure B71. Vertical crack in wall in Parking Garage 4.....	134
Figure B72. Cracks in exterior column and connected girder in Parking Garage 4.....	135
Figure B73. Rebound hammer test location in column in Parking Garage 4.....	135
Figure C1. As-received core T1-S1.....	140
Figure C2. Photo of bisected core T1-S1.....	140
Figure C3. Scanned image of polished sections from core T1-S1. Lettered boxes refer to locations of micrographs in Figure 4.....	142
Figure C4. Photomicrographs of T1-S1: (a) 5.0x photomicrograph of paste microstructure; (b) 10x photomicrograph showing crack extending from surface; (c) 15x photomicrograph showing crack along a coarse aggregate with changing width; (d) 30x photomicrograph of air voids within paste.....	143
Figure C5. Map of crack observed in T1-1.....	144
Figure C6. Low magnification montage electron photomicrograph of T1-S1 (200x magnification).....	145
Figure C7. Electron photomicrographs of T1-S1: (a) 1000x photomicrograph of paste microstructure; (b) 1000x photomicrograph of paste; (c) 4000x photomicrograph of paste; (d) 4000x photomicrograph of paste.....	146

Figure C8. As-received core T1-S2.....	147
Figure C9. Photo of bisected core T1-S2.....	147
Figure C10. Scanned image of polished sections from core T1-S2. Lettered boxes refer to locations of micrographs in Figure C11.	149
Figure C11. Photomicrographs of T1-S2: (a) 5.0x photomicrograph of paste microstructure; (b) 5.0x photomicrograph of paste microstructure with clusters of voids near an entrapped void; (c) 10x magnification showing vertical cracking with varied width; (d) 15X photomicrograph of air voids.	150
Figure C12. Map of crack observed in core T1-S2.....	151
Figure C13. Low magnification montage electron photomicrograph of T1-S2 (200x magnification).	152
Figure C14. Electron photomicrographs of T1-S2: (a) 1000x photomicrograph of paste microstructure; (b) 1000x photomicrograph of paste; (c) 4000x photomicrograph of paste; (d) 4000x photomicrograph of paste.	153
Figure C15. As-received core T1-3.....	154
Figure C16. Photo of bisected core T1-3.....	154
Figure C17. Scanned image of polished sections from core T1-3. Lettered boxes refer to locations of micrographs in Figure C18.	156
Figure C18. Photomicrographs of 220053-3: (a) 5.0x photomicrograph of paste microstructure showing large entrapped air void; (b) 5.0x photomicrograph showing paste microstructure; (c) 10x photomicrograph clusters of entrapped air along aggregate-paste boundary; (d) 15x photomicrograph of air voids within paste.	157
Figure C19. Low magnification montage electron photomicrograph of T1-3 (200x magnification).	158
Figure C20. Electron photomicrographs of T1-3: (a) 1000x photomicrograph of paste microstructure; (b) 1000x photomicrograph of paste; (c) 4000x photomicrograph of paste; (d) 4000x photomicrograph of paste.	159
Figure C21. Comparison of concrete phases in sample T1-3 with depth acquired during ASTM C-457 analysis. The x-axis represents traverse lines across the core, 3 of which equal approximately a centimeter.	160
Figure C22. As-received core T2-3.....	161
Figure C23. Photo of bisected core T2-3.....	161
Figure C24. Scanned image of polished sections from core T2-3. Lettered boxes refer to locations of micrographs in Figure C4.	163
Figure C25. Photomicrographs of T2-3: (a) 5.0x photomicrograph of paste microstructure and surficial paste discoloration; (b) 10x photomicrograph of rebar with voids present at paste boundary; (c) 10x magnification showing vertical crack through a coarse aggregate; (d) 10x photomicrograph vertical crack with varied width.....	164
Figure C26. Map of crack observed in core T2-3.....	165
Figure C27. Low magnification montage electron photomicrograph of T2-3 (200x magnification).	166

Figure C28. Electron photomicrographs of T2-3: (a) 1000x photomicrograph of paste microstructure; (b) 1000x photomicrograph of paste; (c) 4000x photomicrograph of paste; (d) 4000x photomicrograph of paste.	167
Figure C29. Comparison of concrete phases in sample T2-3 with depth acquired during ASTM C-457 analysis. The x-axis represents traverse lines across the core, 3 of which equal approximately a centimeter.	168
Figure C30. As-received core T3-3.	169
Figure C31. Photo of bisected core T3-3.	169
Figure C32. Scanned image of polished sections from core T3-3. Lettered boxes refer to locations of micrographs in Figure C33.	171
Figure C33. Photomicrographs of T3-3: (a) 5.0x photomicrograph of paste microstructure; (b) 5.0x photomicrograph of large entrapped air voids; (c) 10x magnification showing paste microstructure; (d) 15x photomicrograph showing air voids concentrated along aggregate boundaries.	172
Figure C34. Low magnification montage electron photomicrograph of T3-3 (200x magnification).	173
Figure C35. Electron photomicrographs of T3-3; (a) 1000x photomicrograph of paste microstructure; (b) 1000x photomicrograph of paste; (c) 4000x photomicrograph of paste; (d) 4000x photomicrograph of paste.	174
Figure C36. Comparison of concrete phases in sample T3-3 with depth acquired during ASTM C-457 analysis. The x-axis represents traverse lines across the core, 3 of which equal approximately a centimeter.	175
Figure D1. Average rebound numbers obtained on each floor for each tower.	187
Figure D2. Average rebound numbers obtained in each parking garage.	188
Figure D3. Prepared and cored (upper left insert) area of representative concrete in Tower 1. Red lines indicate locations of internal reinforcement.	189
Figure D4. Prepared and cored (upper left insert) area of wall containing a cold joint in Tower 1. Red lines indicate locations of internal reinforcement.	190
Figure D5. Prepared area for concrete coring in Tower 2. One core was taken over the crack, and two cores were taken to the sides of the crack to be representative concrete samples. Red lines indicate locations of internal reinforcement. Insert shows Schmidt hammer locations.	191
Figure D6. Prepared and cored (insert) area of representative concrete in Tower 3. Red lines indicate locations of internal reinforcement and numbers represent locations of Schmidt hammer testing.	191

Tables

Table 1. Mixture proportions used for Towers 1, 2, and 3.	36
Table A1. Documents reviewed.	74
Table A2. USACE-POF soil borings per structure.	75
Table A3. Rock Quality Designation (RQD) range per tower.	76
Table A4. Maximum allowable axial loads for 500-mm-diam piles.	80
Table A5. Results of allowable axial capacity design calculations from each foundation report.	81

Table A6. Results of the dynamic pile load test, allowable working loads presented from restrike testing.....	82
Table A7. Results of static load tests for Towers 1-4.....	84
Table C1. Summary of locations investigated, year constructed, corresponding CMB Serial No, and tests performed. T1, T2, and T3 sample identifiers correspond to Towers 1, 2, and 3, respectively.....	138
Table D1. Cored areas of each tower with corresponding wall designations.....	188
Table D2. Average rebound number, estimated compressive strength, and measured compressive strength for areas cored in each tower.	193

Preface

This study was conducted for the Far East District, Pacific Ocean Division, of the U.S. Army Corps of Engineers (USACE-POF). The technical monitors were Mr. Amro Habib (USACE-POF) and COL Cristopher Crary (USACE-POF).

The work was performed by the Geotechnical Engineering and Geosciences Branch (GSG), the Structural Engineering Branch (GSS), the Structural Mechanics Branch (GSM), the Survivability Engineering Branch (GSV), and the Research Group (GSR) of the Geosciences and Structures Division (GS), the Concrete and Materials Branch (GMC) and the Research Group (GMR) of the Engineering Systems and Materials Division (GM), and the Senior Scientists (GZA), U.S. Army Engineer Research and Development Center, Geotechnical and Structures Laboratory (ERDC-GSL). At the time of publication, Mr. Christopher G. Price was Chief, GSG; Ms. Mariely Mejias-Santiago was Chief, GSS; Mr. Bradford A. Steed was Chief, GSM; Mr. Omar G. Flores was Chief, GSV; Dr. Jameson Shannon was Chief, GMC; Mr. James L. Davis was Chief, GS; Mr. Justin S. Strickler was Chief, GM; and Ms. Pamela G. Kinnebrew, GZT, was the Technical Director for Military Engineering. The Deputy Director of ERDC-GSL was Mr. Charles W. Ertle II, and the Director was Mr. Bartley P. Durst.

COL Teresa A. Schlosser was the Commander of ERDC, and Dr. David W. Pittman was the Director.

Executive Summary

This report furnishes the ERDC Team's final findings on the structural condition of Family Housing Towers 1–4 and connected parking garages at Camp Walker, Daegu, South Korea. The Engineer Research and Development Center (ERDC) scope of work covers four areas: (a) the identification of any life safety concerns, (b) potential intermediate considerations for monitoring and additional analysis, (c) potential long-term durability concerns in the structures, and (d) support to U.S. Army Corps of Engineers Far East District (USACE)-POF as it seeks additional services for forensic analysis and repair activities. This report covers the first three areas: (a) life safety concerns, (b) intermediate structural and durability issues, and (c) long-term structural and durability issues. Area (d) support will be provided until USACE-POF no longer needs the ERDC Team assistance.

The ERDC Team evaluated Towers 1–4 and corresponding parking garages to assess the impact of observed cracking in the concrete structures, as initially reported by USACE-POF. The evaluation included on-site visual inspection of accessible areas, review of USACE-POF documentation on the structures' conditions, review of particular design and construction records, and materials testing. Nineteen ERDC engineers, scientists, and technicians with subject matter expertise in structural engineering, concrete materials, geotechnical engineering, forensic analysis, and construction practices have been engaged since 17 January 2022 to evaluate the available data and perform a thorough analysis. Four of these personnel, Dr. C. Kennan Crane, PE, Dr. Oliver-Denzil S. Taylor, PE, Dr. Stephanie G. Wood, and Mr. Jason A. Morson, deployed onsite at Camp Walker to conduct independent ERDC inspections and testing from 17 January to 5 February 2022.

Structural observations and findings

The structural designs for all four towers utilize cast-in-place reinforced concrete slab and wall construction with a centrally located elevator shaft. According to the design documentation, progressive collapse resistance was incorporated per the requirements of Unified Facilities Criteria 4-023-03. These important design features enhance overall structural robustness and provide redundancy and resilience for load transfer and load redistribution through the structures.

The on-site team was able to visually inspect all concrete not covered by architectural finishings in Towers 1–4. Cracking was observed in a

majority of the inspected areas and generally consisted of hairline cracks in multiple orientations with widths of 0.2 mm or less. Cracking was more prevalent in Tower 2 than in Tower 1. The on-site team did identify isolated cracks wider than 0.2 mm, but no crack widths were observed in excess of 0.7 mm. The predominantly narrow crack widths, distribution, and orientation is consistent with restrained drying shrinkage cracking and corroborates the findings of initial assessments made by USACE-POF. Drying shrinkage occurs when concrete contracts due to loss of water to the environment. When this shrinkage is restrained, cracking occurs. Materials testing, including nondestructive testing, concrete core compressive strength testing, and petrography, further supported the diagnosis of drying shrinkage. None of the cracks observed in the towers was of a size and location to create decreased structural performance. It is recommended that interior cracks larger than 0.3 mm should be V-cut and sealed with elastomeric polymer to prevent long-term deterioration.

The parking garages are cast-in-place reinforced concrete beam-column construction with monolithic slabs. The on-site team was able to visually inspect Parking Garages 1–4 and observed cracks in walls, beams, and slabs. In several instances within Parking Garages 1 and 2, crack widths exceeded the width above which long-term durability is a concern (i.e., 0.2 mm for outdoor structures). Field observations of concrete cracking in the parking garages indicated restrained shrinkage cracking. This finding was supported by analysis of construction documents and best practices for concrete construction. Team analysis suggests that these cracks were not caused by structural deficiencies. However, due to their nature and orientation, and to ensure that the structures continue to behave as designed, it is prudent to address the recommended repairs as noted in the USACE-POF memorandum dated 19 January 2022.

Materials observations and findings

Similar structural concrete was used across all structures and the reported Quality Assurance/Quality Control (QA/QC) testing results for these materials were in accordance with design specifications. Additional nondestructive testing as well as concrete core testing was conducted and confirmed that all concretes met the strength specification listed in the construction documents. The concrete mixture proportions as designed did not have clear indicators of potential severe shrinkage issues like those observed in the structures. Petrographic analysis did show internal variations in the concrete

composition due to segregation, which could lead to increased shrinkage. The observed shrinkage and resultant cracking are also the product of significant restraint provided by the heavily reinforced robust structural system coupled with placement and curing techniques that did not adhere to best practices. The ERDC Team's field observations, along with QA documentation, report extensive issues with concrete honeycombing and improper termination of concrete placements within walls and on slabs during construction, all of which have resulted in the presence of unintended cold joints in the columns and wall systems. However, this is largely a long-term durability concern rather than a structural concern.

Geotechnical observations and findings

The on-site team performed a visual geotechnical and foundation assessment of interior and exterior areas of Towers 1 and 2 and their parking garages for evidence of foundation distress. The ERDC Team also reviewed particular construction and design documents including the results of static and dynamic load tests performed on the pile foundations. The results of the foundation inspection and design review indicated that the cracking identified in these structures was not related to foundation distress or excessive settlement.

Recommendations

Based on the above observation and analysis, the ERDC Team has not observed any life safety concerns in Towers 1–4 or their connected parking garages. Cracking and defects observed in Towers 1–4 appear to be the result of restrained drying shrinkage cracking. Cracking observed in Parking Garages 1 and 2 do not present a life safety concern, but they should be addressed as noted within the USACE Far East District (USACE-POF) memorandum dated 19 January 2022. Parking Garages 3 and 4 have not exhibited cracking to date. Team members recommend that Parking Garages 3 and 4 be monitored on a 6- to 12-month cycle to determine if repair does eventually become necessary. The ERDC Team recommends that USACE-POF continues to work, as planned, to engage an expert structural forensics consultant to further assess long-term impacts of observed cracking on the service life of the structures and to develop remediation plans to ensure the designed performance level is maintained. Until the final report is provided by the forensic AE firm, cracks over 0.2 mm in parking garages (weather exposed) should be

visually inspected every 6 months and cracks over 0.3 mm in towers (not weather exposed) should be inspected every 12 months to ensure cracks remain unchanged.

1 Introduction

In October 2015, the U.S. Army Corps of Engineers Far East District (USACE-POF) broke ground on the first of a series of four residential apartment towers and four accompanying parking garages at Camp Walker, Daegu, South Korea. These towers are 15 stories each and will each house 90 Army families when completed. The first tower (and its accompanying parking garage) was completed and turned over from USACE-POF to the Garrison in February 2019. Since then, the second and third towers and garages have been completed and turned over to the Garrison. The fourth tower and parking garage were still under construction at the time of this report's publication.

In August 2021, unexpected cracking was discovered in the concrete of Parking Garage 3. Further inspection revealed additional cracking in all three towers and all three parking garages. While some cracking in concrete is expected, the extent of cracking was unusual given the young age of these structures. An evaluation and report by USACE-POF determined the towers and garages to be safe for continued occupation.

In early December 2021, USACE-POF contacted researchers in the Geotechnical and Structures Laboratory (GSL) of the U.S. Army Engineer Research and Development Center (ERDC) to perform an independent evaluation of these structures. This was done out of an abundance of caution to further verify life safety and to determine the probable causes of cracking in the structures. A team of four ERDC researchers and technicians deployed to Daegu in mid January 2022 to perform an on-site visual inspection. At the same time, 13 additional researchers at ERDC began review of particular design and construction documentation from these structures.

On 28 January 2022, the ERDC team submitted a memorandum to the USACE Pacific Ocean Division (CEPOD) confirming the initial finding of the USACE-POF report that the observed cracking did not pose a life safety concern. This report presents the complete findings of the ERDC evaluation of the towers and parking garages.

2 Apartment Tower Evaluation

Evaluation of the towers consisted of visual inspection of the structures as well as review of particular design and construction documentation and materials testing. The following sections detail those observations and analyses and provide conclusions and recommendations for the apartment buildings.

2.1 Observations from visual inspections of apartment towers

Visual inspection of the towers was performed by the ERDC on-site team between 18 and 31 January 2022. The inspection comprised visual examination of accessible concrete surfaces, measurement and photographic documentation of key observations, nondestructive testing using ground-penetrating radar (GPR) and Schmidt hammer testing, and concrete coring for mechanical and materials testing of the concrete. The following sections give general observations as well as specific observations from each tower.

2.1.1 General tower observations

The four towers exhibited significant similarities in their designs, constructions, and the types of observed cracking/cold joints. Particularly in the first three towers only the extents and specific locations of cracking varied, while the fourth tower was more difficult to directly compare due to its unfinished state.

In all the towers, concrete surfaces in public areas were covered with a thin layer of cementitious compound known generally as “mud.” The mud layer was then covered with paint. Bare unmudded concrete was observable in limited mechanical and electrical access shafts in various areas of the structures. Almost all the walls in the apartment spaces were sheetrock or sheetrock over concrete; therefore, the concrete in these areas was not observable.

Based on the consistency of crack types and locations in all observable areas, it was reasonably assumed that covered walls exhibited the same types and extents of cracking/cold joints as were observed in the rest of the structure. Similarly, mudded walls were observed to exhibit the same types and extents of cracking as were observed in the bare concrete walls. The assumption that

mudded and unmudded concrete showed cracks equally was verified by removal of the mud in several locations. In each of these locations, cracks through the mud matched cracks in the underlying concrete.

A few different types of cracks were prevalent in all the towers. Diagonal cracks in basement walls were often observed near corners where two walls intersected the floor. When cracks were observed in the exterior walls of the basements, no water intrusion or staining was observed despite these serving as retaining walls.

Vertical cracks were observed in many walls throughout the towers and were most often determined to be directly above vertical rebar locations*. Where floor/ceiling slabs were observable, they often exhibited random multidirectional cracking. In many locations, bare concrete walls exhibited diagonal cold joints where concrete setting between subsequent lifts prevented complete bonding along the joint. The following sections will provide details of where these and other features were observed on each tower.

2.1.2 Tower 1 observations

Apartment Tower 1, also known as Shilla (Bldg. 800), was the first tower constructed. Construction began on this tower in October 2015; it was turned over from USACE-POF to the Daegu Garrison in February 2019 and was occupied beginning in April 2019. The structure is 15 stories with a basement. It is a cast-in-place concrete slab and wall structure. Concrete surfaces were observable in all of the basement, in the public hallways of floors 1–15, and in the elevator mechanical room in the attic above floor 15.

Throughout Tower 1, cracks and cold joints were observed in multiple surfaces and orientations. The basement exhibited both vertical and diagonal cracking in the walls as well as cracks in the ceiling and floor. The bare concrete in the shafts of Tower 1 exhibited cold joints and vertical cracking. The walls in the upper floors and attic also showed cracking.

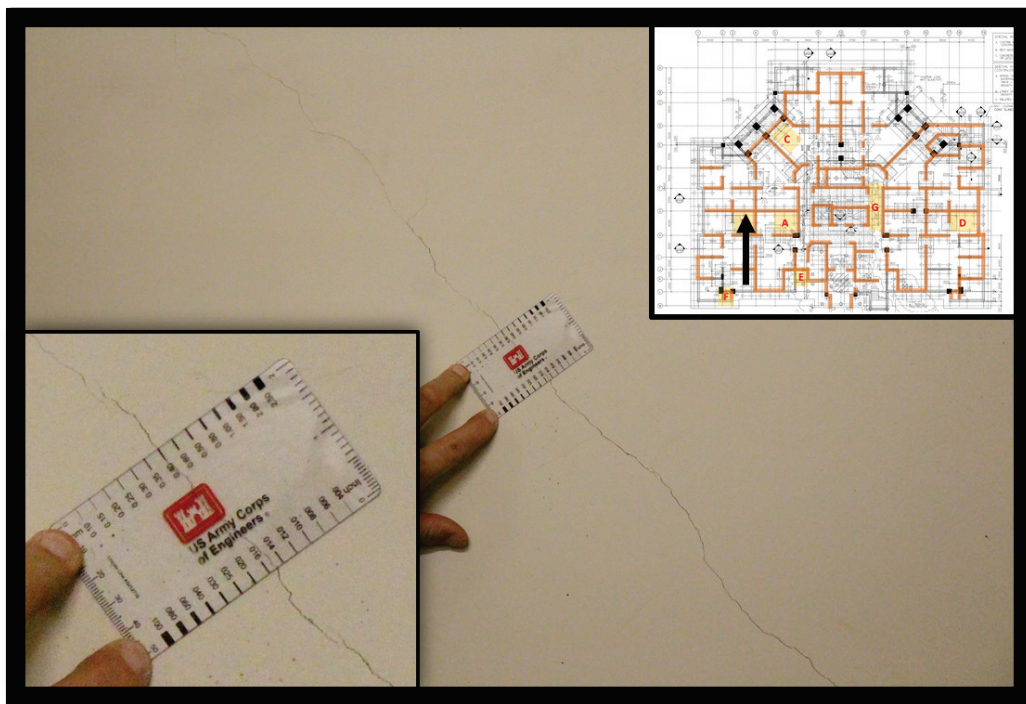
* This was not an unexpected location; because, when the concrete shrinks perpendicular to the orientation of the rebar, the rebar acts as a discontinuity and a likely place for crack formation. There were no noted occurrences of inadequate concrete cover, so these crack locations were not thought to be directly linked to improper rebar placement.

2.1.2.1 Basement diagonal cracks

Diagonal cracks were observed in multiple locations in the walls of the Tower 1 basement. These cracks were usually oriented sloping away from the bottom corners created when two walls and the floor intersected.

Figure 1 shows a typical diagonal crack seen in the basement of Tower 1. From the view in this figure, the corner would be down and to the left.

Figure 1. Diagonal crack within the Tower 1 basement storage area (Section B of the floorplan insert). The widest section of the observed crack was 0.40 mm (crack gauge insert); however, the crack width narrows at the extents and does not intersect with the floor slab.



2.1.2.2 Basement vertical cracks

Vertical cracks were observed in many locations in the walls in the basement of Tower 1. Later nondestructive testing (NDT) with a ground-penetrating radar showed that these cracks often occurred at the location of vertical rebar in the walls. Figure 2 shows one of the longest and widest such cracks observed in Tower 1. Figure 3 shows an area of one wall in the basement with the cracks traced to convey relative location and patterns.

Figure 2. Vertical crack within the Tower 1 basement storage area (Section A of the floorplan insert). The widest area of the observed crack was less than 0.40 mm and did not intersect the floor slab.

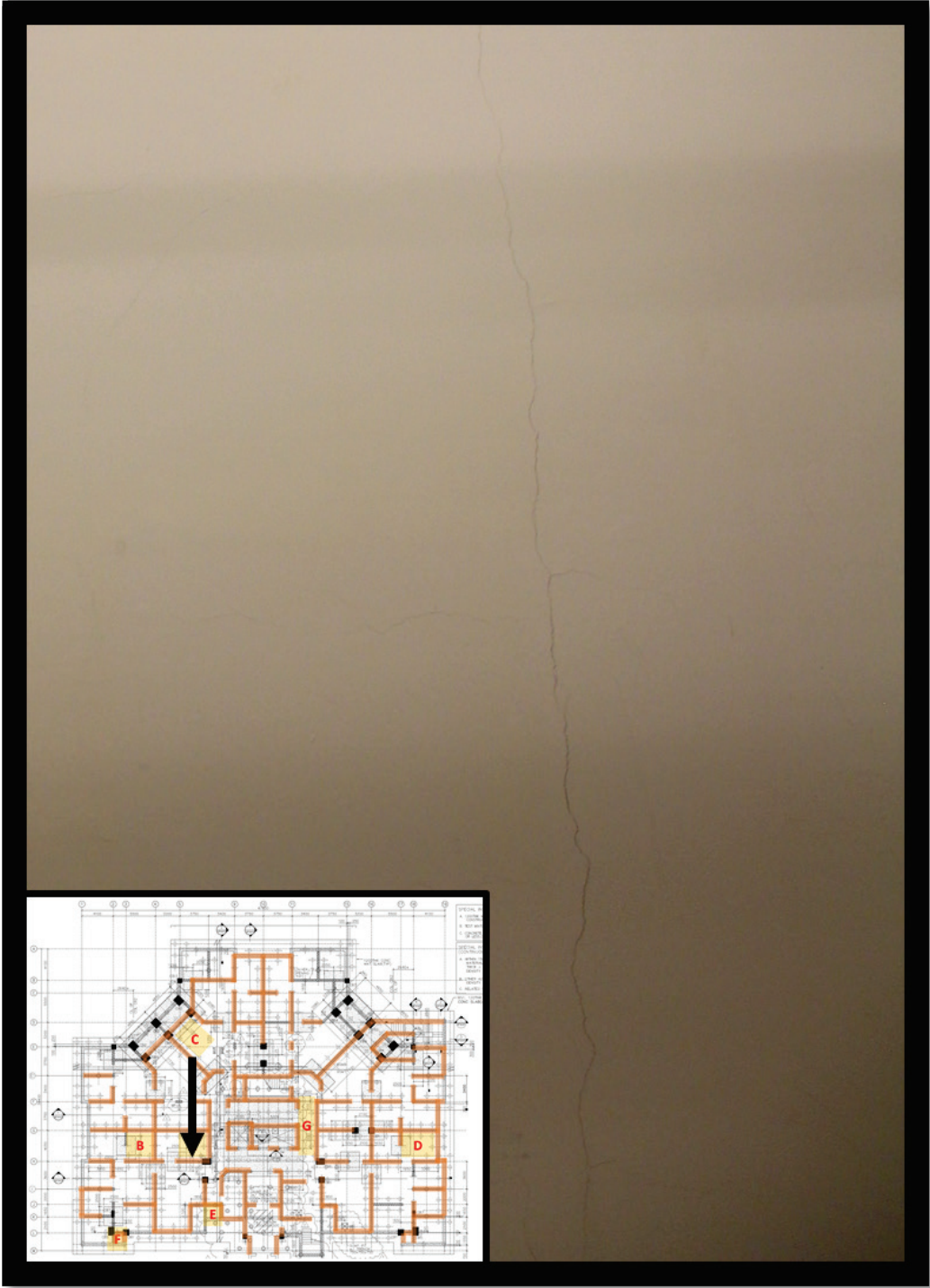
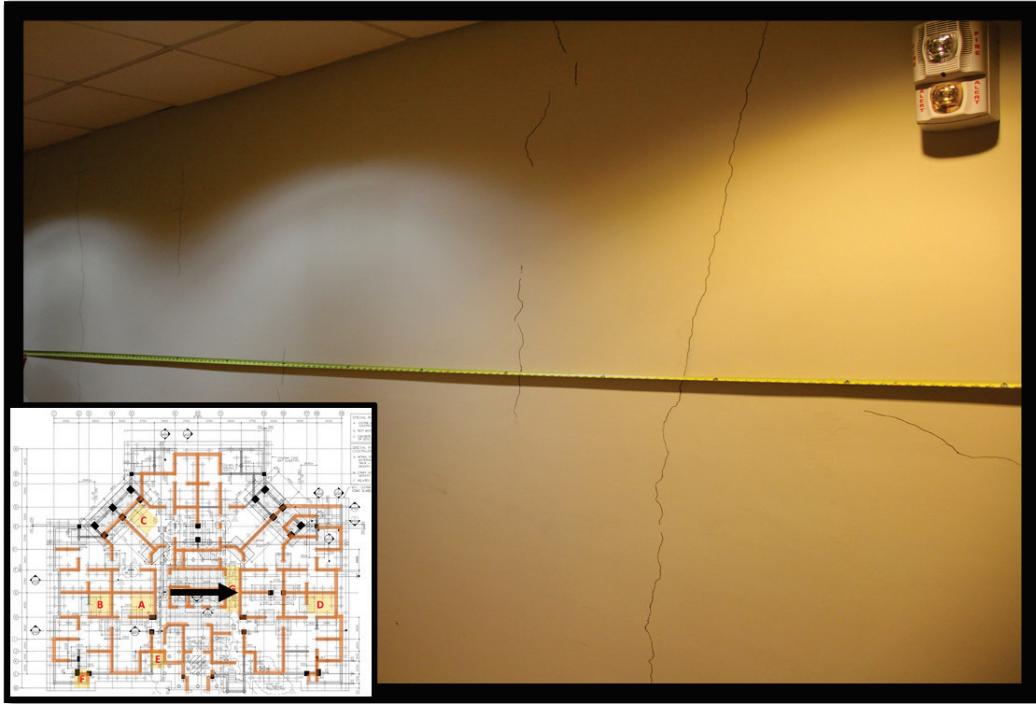


Figure 3. Wall cracks within the Tower 1 basement storage area (Section G of the floorplan insert). The widest observed crack width was less than 0.40 mm. The shown cracks were traced with a permanent marker to highlight typical locations, lengths, and spacing and are not representative of crack width.



2.1.2.3 Basement floor cracks

The basement of Tower 1 was one of the only areas where the bare concrete floor was visible. Figure 4 shows typical crack patterns and widths. This type of multidirectional cracking is often an indicator of poor concrete finishing practices or early-age plastic shrinkage. On a slab, this is often a sign of poor finishing or curing practices. Poor finishing can cause a thin surface layer that has a very high water to cement (w/c) ratio. In this case or in poor curing, as water is lost to evaporation, this surface layer shrinks causing cracking. Figure 5 shows additional views of similar cracking in the same area of the Tower 1 basement.

Figure 4. Slab floor cracks within the Tower 1 basement storage area (Section C of the floorplan insert). The widest observed crack width was between 0.40 and 0.50 mm (crack gauge insert) with most observed cracks being hairline cracks of less than 0.25 mm.

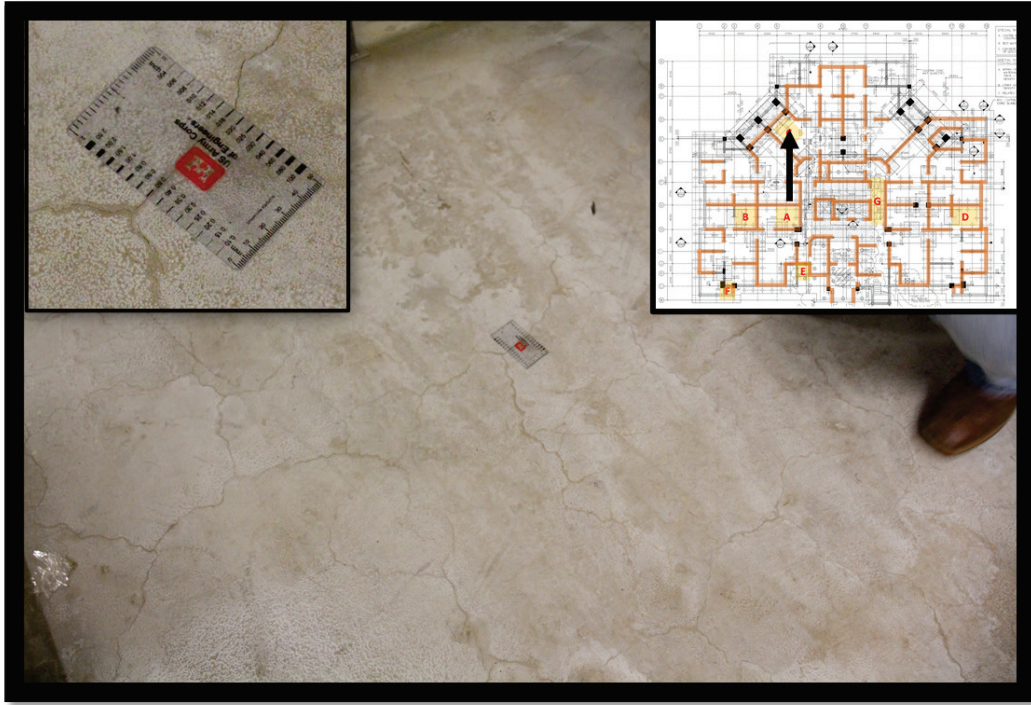
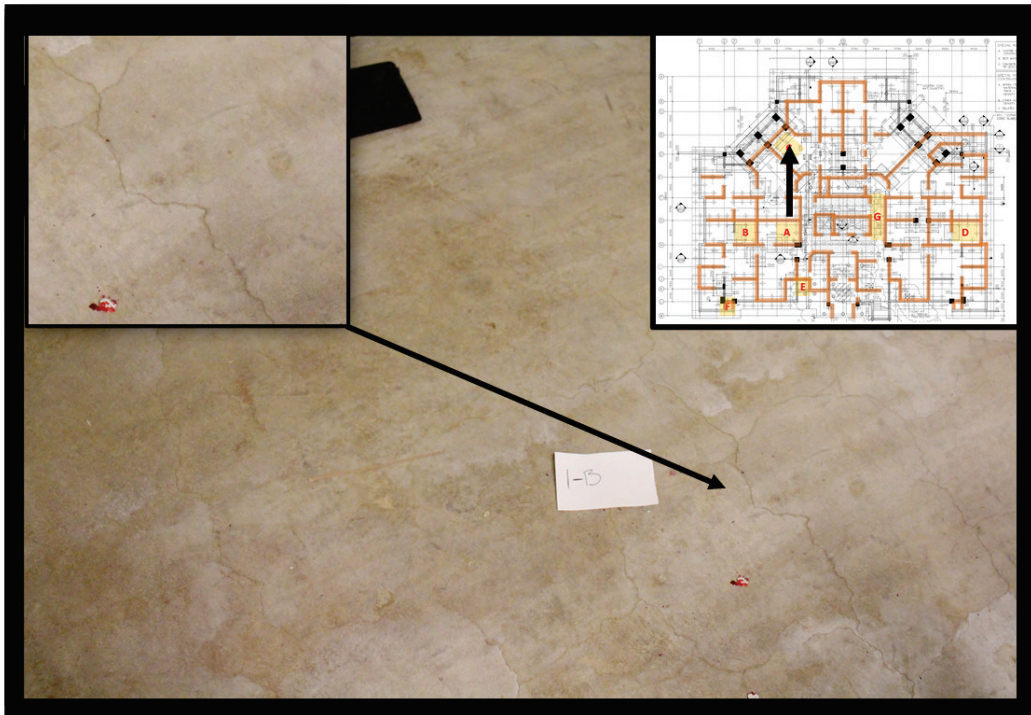


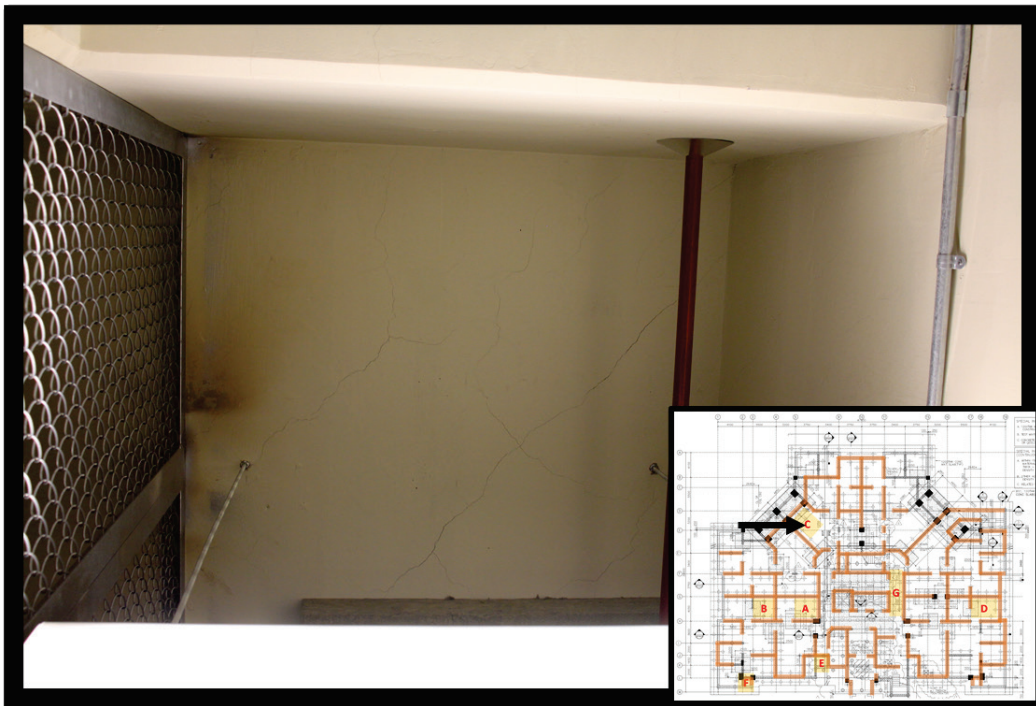
Figure 5. Slab floor cracks within the Tower 1 basement storage area (Section C of the floorplan insert). The widest observed crack width was less than 0.25 mm.



2.1.2.4 Basement ceiling cracks

In several areas of the basement cracking was observed in the overhead slab (ceiling). These cracks were random in orientation and often initiated/terminated at intrusions such as where electrical conduits, water lines, or other building systems came through the slab. Figure 6 shows a typical example of these cracks in the basement ceiling.

Figure 6. Overhead (ceiling) slab cracks within the Tower 1 basement storage area (Section C of the floorplan insert). Widths of these cracks were not measured but approximate the size, patterns, and widths as other observed cracks in the floor slabs.



2.1.2.5 Observed features in bare concrete

The only bare concrete that was accessible to inspection in Tower 1 was in the mechanical and electrical shafts. These locations demonstrated cracking similar to that observed elsewhere, but also showed the construction cold joints that existed throughout the building as seen in Figure 7.

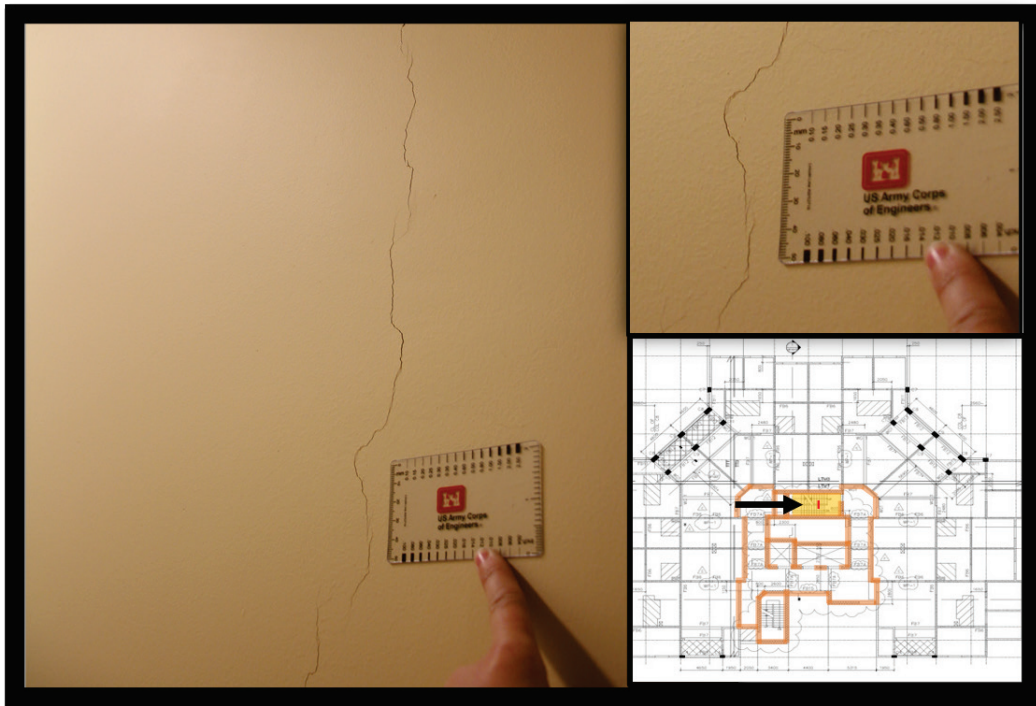
Figure 7. Cold joints within the Tower 1 basement shaft area (Section E of the floorplan insert). These cold joints were observed on bare concrete and were typical in the mechanical and electrical shaft areas in the upper floors.



2.1.2.6 Cracking in upper floors

In the upper floors, cracking was observed in the public hallway areas. These areas were mudded and painted and generally did not display a significant number of cracks. Where they did appear, they were generally vertical and were most often directly over reinforcing bars (see Figure 8). In a few areas, diagonal cracks were observed in walls near stairwells.

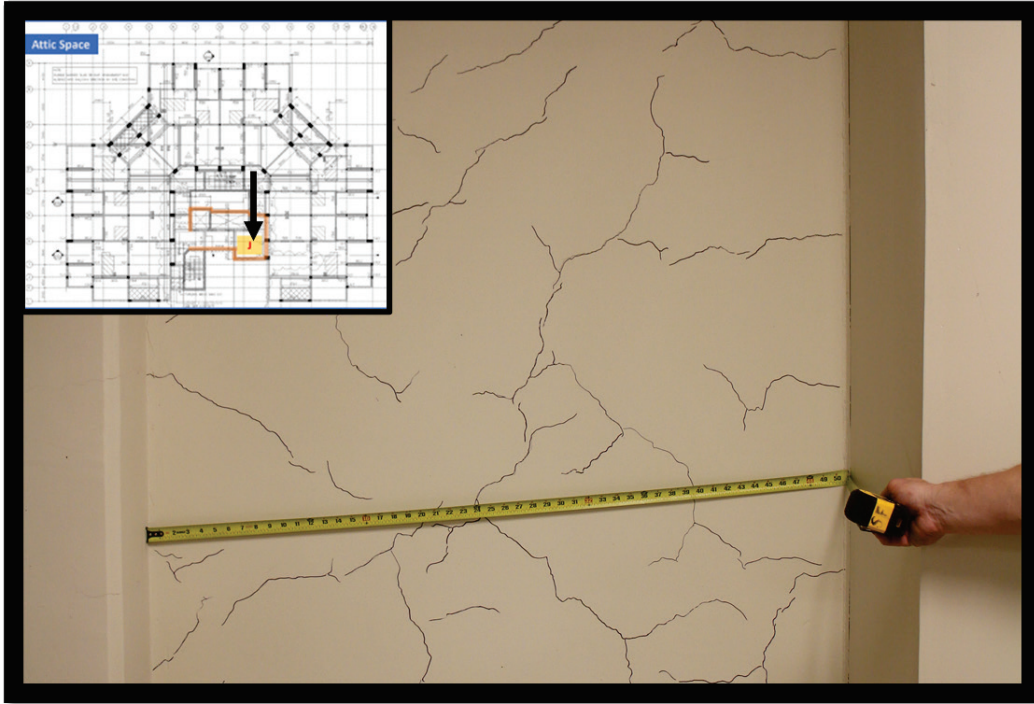
Figure 8. Cracking over mudded walls (typical) within the nonbasement floors of Tower 1 (Section I of the floorplan insert).



2.1.2.7 Cracking in attic areas

The attic area of Tower 1 houses the mechanical and electrical systems that operate the tower's three elevators. This area is not accessible to the public under normal circumstances. Multidirectional cracking was seen in the mudded walls throughout this area as seen in Figure 9 (note that these cracks are traced for visibility). The size of the cracks was not noticeably different from elsewhere in the structure, but there appeared to be a greater number of cracks. This may be due to a lessened emphasis on aesthetics, which meant apparent cracks were not remudded or repainted as they might have been in other areas.

Figure 9. Wall cracks within the Tower 1 attic elevator mechanical area (Section J of the floorplan insert). The widest observed crack width was less than 0.40 mm. The shown cracks were traced with a permanent marker to highlight typical locations, lengths, and spacing and are not representative of crack width.



Overall, observed cracking in Tower 1 was not a concern for life safety and was only a long-term durability concern in a few areas where crack widths exceeded 0.3 mm*. Even in these areas, the presence of climate control (specifically the lack of significant humidity) should allow for the structure to behave as designed through its stated design life.

2.1.3 Tower 2 observations

Apartment Tower 2, also known as Baekje (Bldg. 810), was the second tower constructed. Construction began in December 2016. Tower 2 was turned over from USACE-POF to the Daegu Garrison in August 2019 and was occupied beginning in September 2019. The structure is 15 stories with a basement. Like Tower 1, it is a cast-in-place concrete slab and wall structure. Concrete surfaces were observable in all of the basement, in the shaft behind the elevators on all floors, and in the elevator mechanical

* For a full list of the spelled-out forms of the units of measure used in this document, please refer to *US Government Publishing Office Style Manual*, 31st ed. (Washington, DC: US Government Publishing Office 2016), 248-52, <https://www.govinfo.gov/content/pkg/GPO-STYLEMANUAL-2016/pdf/GPO-STYLEMANUAL-2016.pdf>.

room in the attic above floor 15. Unlike Tower 1, the walls in the public hallways of floors 1–15 were covered in sheetrock.

The types of concrete features seen in Tower 2 were consistent with the general observations described in 2.1.1. Of the finished towers, Tower 2 exhibited the most extensive cracking in the observed concrete.

Throughout Tower 2, cracks and cold joints were observed in multiple surfaces and orientations. The basement exhibited both vertical and diagonal cracking in the walls as well as cracks in the ceiling and floor. The bare concrete in the shafts of Tower 1 exhibited cold joints and vertical cracking on the walls and multidirectional cracking on the slabs. The walls in the attic also showed cracking.

2.1.3.1 Basement diagonal cracks

Because of the more widespread presence of cracks in Tower 2 and their generally larger widths, crack gauges had been placed at multiple locations in the basement. The gauges were placed 13 AUG 2021 and the widths noted. No increase in crack width has been observed since placement of the crack gauges. Figure 10 shows the largest observed diagonal crack in the basement of Tower 2. Figure 11 shows a more typical diagonal crack with orientation as described in 2.1.2.1.

Figure 10. Largest observed diagonal crack within the Tower 2 basement storage area (Section L of the floorplan insert). The widest section of the observed crack was 0.50 mm (crack gauge insert); however, the crack width narrows at the extents and does not intersect with the floor slab.

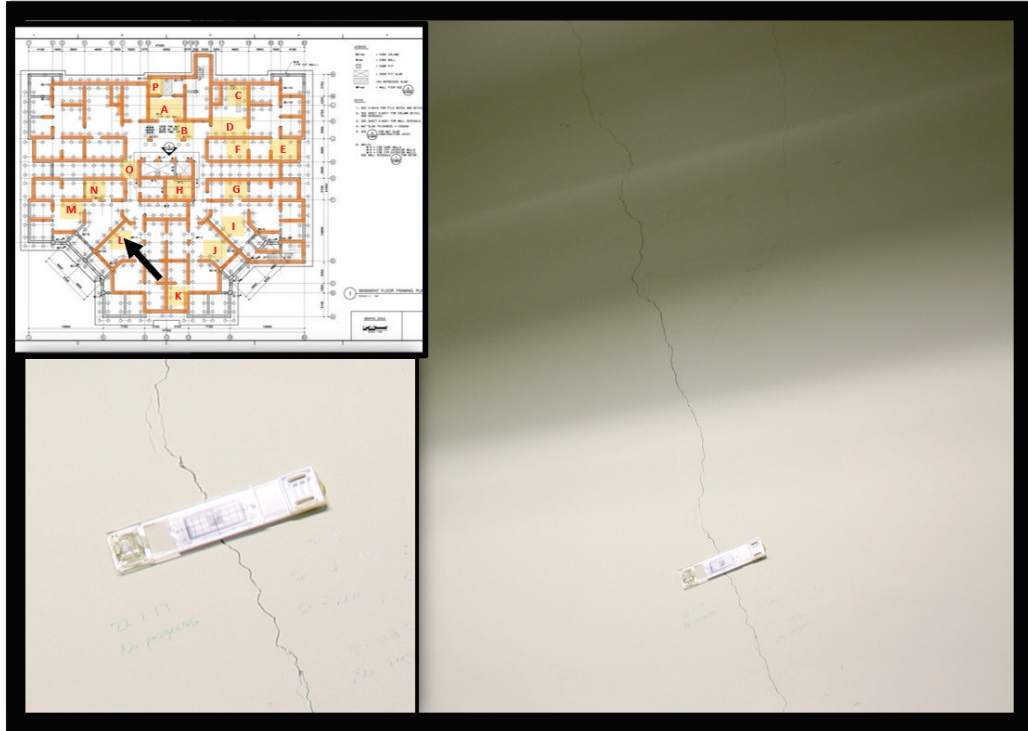


Figure 11. Typical observed diagonal cracking within the Tower 2 basement storage area (Section E of the floorplan insert). The widest area of the typical observed crack was less than 0.40 mm and did not intersect the floor slab. The crack shown here has been repaired; however, it is typical of orientation, location, and size of the Tower 2 diagonal cracking.

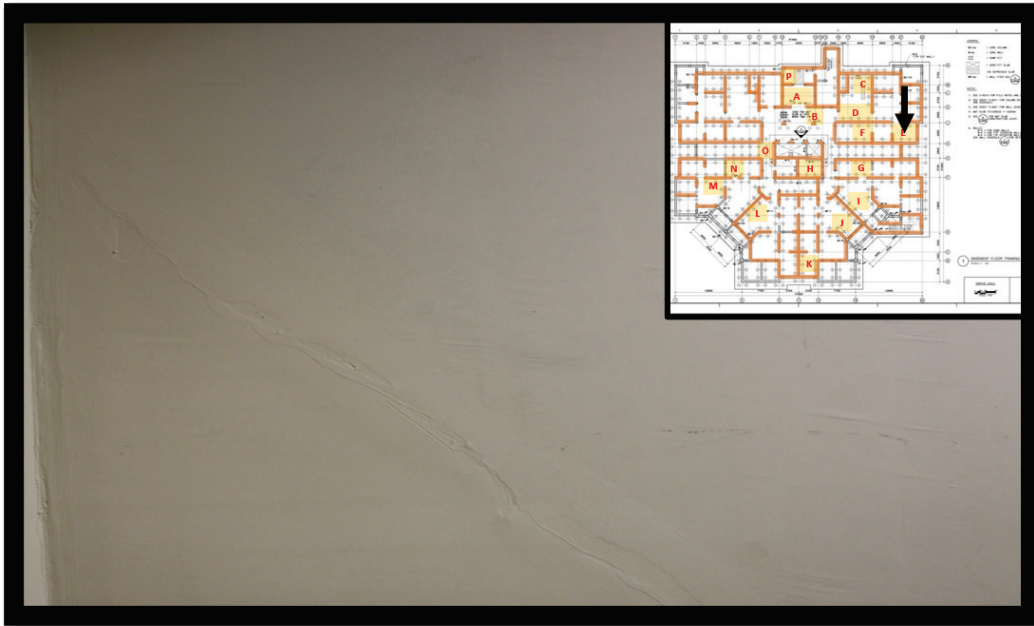
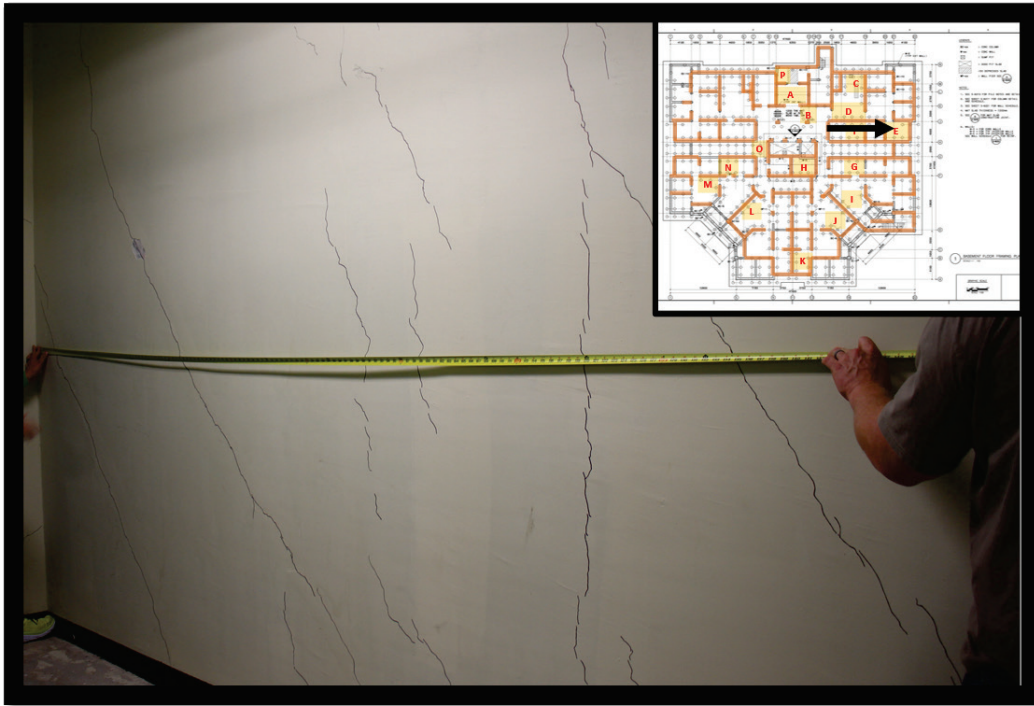


Figure 12 shows the crack pattern on a section of wall in the basement of Tower 2. This picture captures the mixture of diagonal and vertical cracking often present in this basement. It also demonstrates the relative spacings of these cracks. It should be noted that most of the cracks seen in this picture are hairline (<0.2 mm in width). The cracks have been traced for visibility, but the lines are not representative of crack widths.

Figure 12. Wall cracks within the Tower 2 basement storage area (Section E of the floorplan insert). The widest observed crack width was less than 0.40 mm. The shown cracks were traced with a permanent marker to highlight typical locations, lengths, and spacing and are not representative of crack width.



2.1.3.2 Basement vertical cracks

Vertical cracks were observed throughout the basement of Tower 2. As in Tower 1, these cracks occurred most often over vertical rebar. The size and number of these cracks were greater than in Tower 1. Figure 13 and Figure 14 show the most severe observed vertical crack and a typical vertical crack, respectively. Figure 15 shows the relative spacings and lengths of these cracks on a basement wall. All cracks are traced for visibility, and, thus, the figure should not be seen as indicative of crack widths.

Figure 13. Most severe observed vertical crack within the Tower 2 basement storage area (Section A of the floorplan insert). The widest section of the observed crack was 0.6 mm (crack gauge insert).

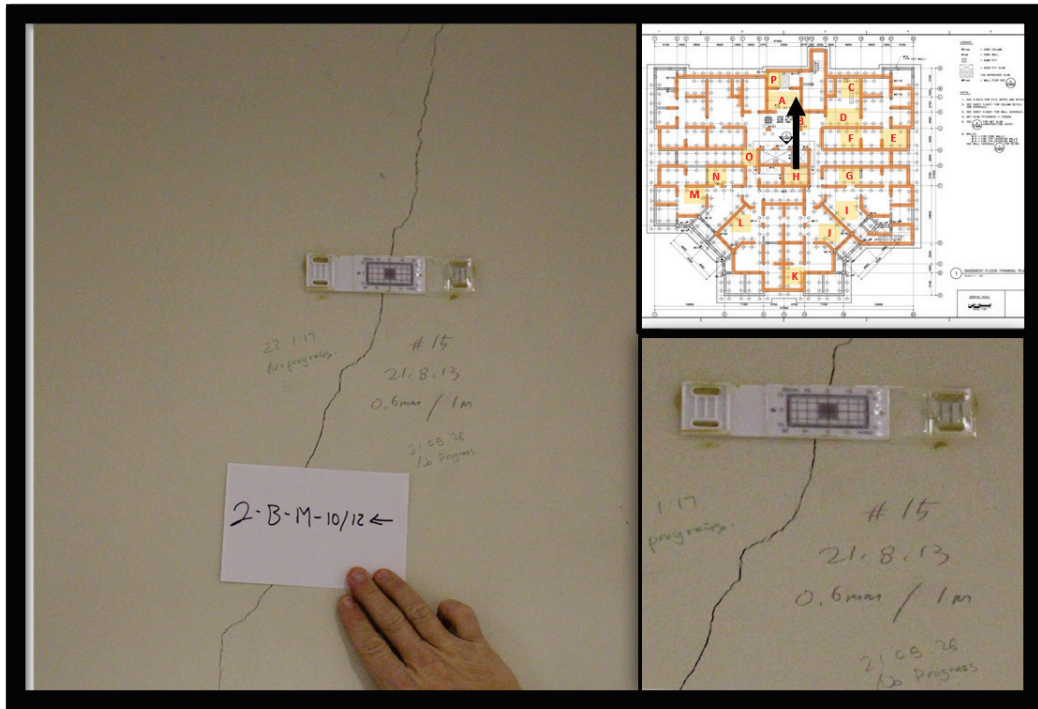


Figure 14. Typical observed vertical cracking within the Tower 2 basement storage area (Section I of the floorplan insert). The widest area of the observed crack was less than 0.40 mm and did not intersect the floor slab (crack gauge insert).

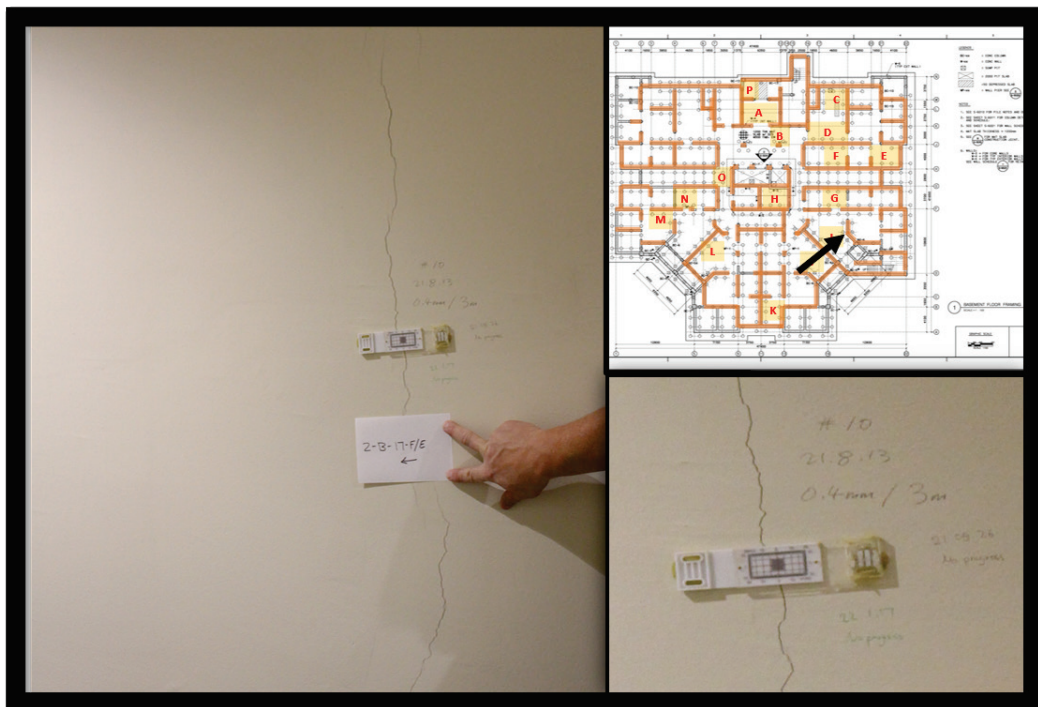
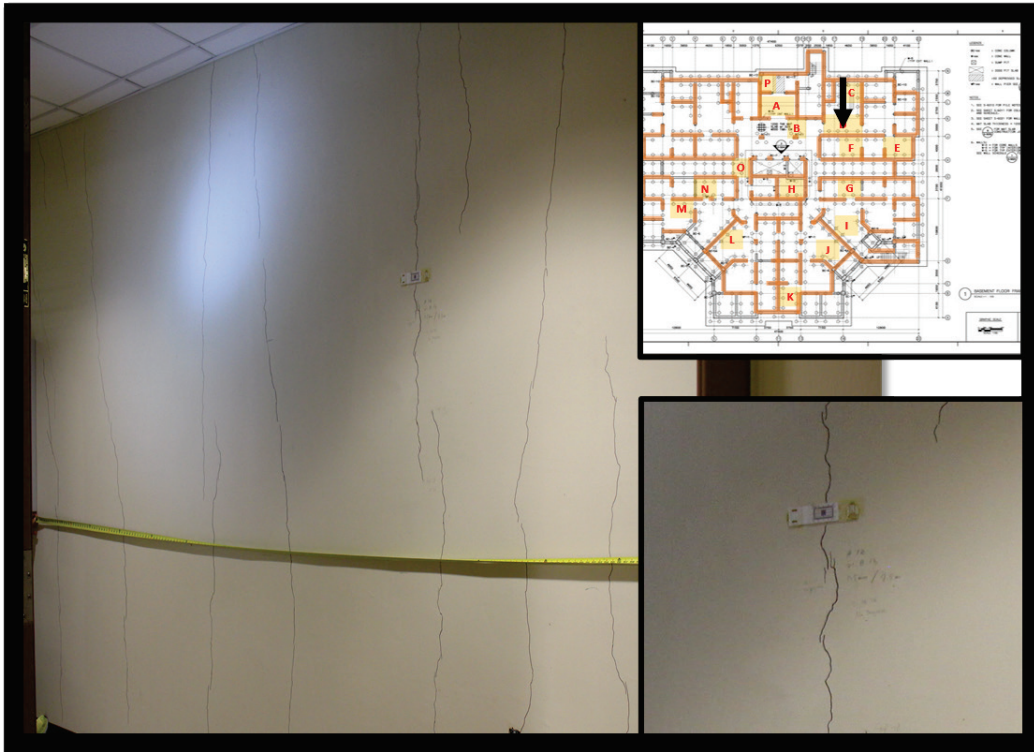
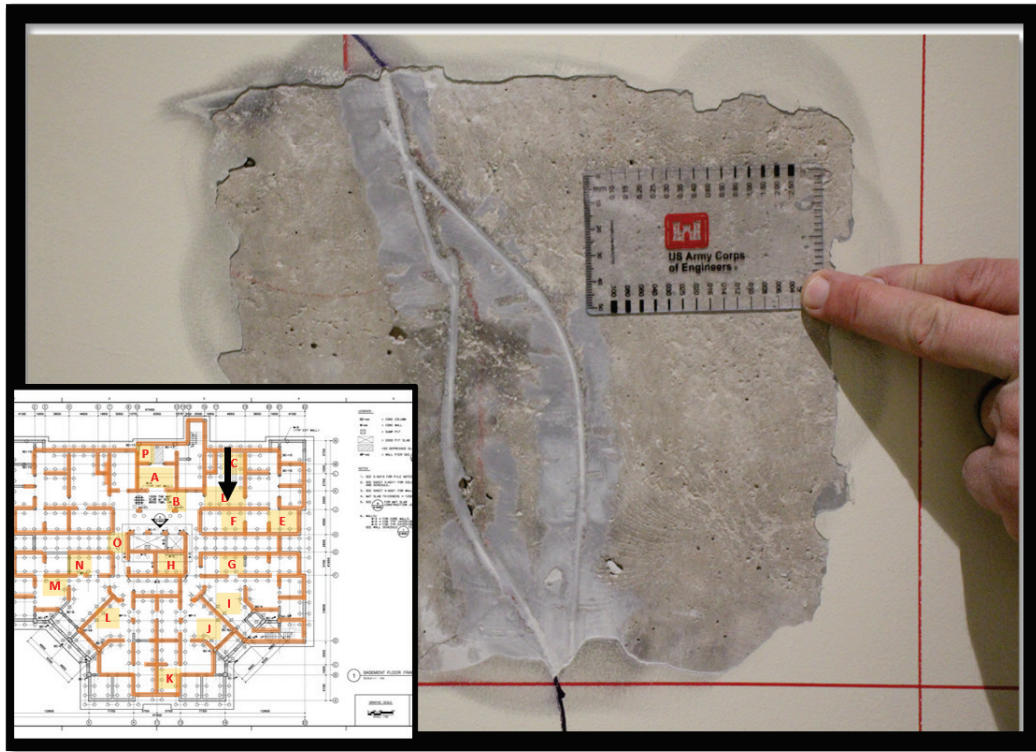


Figure 15. Wall cracks within the Tower 2 basement storage area (Section D of the floorplan insert). The widest observed crack width was less than 0.50 mm (crack gauge insert). The shown cracks were traced with a permanent marker to highlight typical locations, lengths, and spacing and are not representative of crack width.



In many areas, it was obvious that cracks had been repaired prior to the structure being turned over to the garrison. Figure 16 shows a typical example of these repairs under the mud and paint. These cracks were first opened and smoothed with a grinder and then infilled with an elastomeric polymer grout. This repair method is common and is useful for preventing water ingress and related durability issues, as well as improving aesthetics.

Figure 16. Typical observed repaired vertical cracking within the Tower 2 basement storage area (Section D of the floorplan insert). The repaired region has been intentionally widened with an angle grinder and filled with a polymer grout.



2.1.3.3 Observed features in bare concrete

In Tower 2, the majority of the bare concrete observed was in a large access shaft that was behind the elevator shafts on each floor. These small rooms had exposed concrete walls, floors, and ceilings. Figure 17 shows cracking on the ceiling of one of these rooms. In this location, white exudate staining can be seen around some of the cracks. This exudate was dry and did not appear recent. It was likely formed shortly after the concrete was cast prior to the building envelope being sealed against weather. If this is the case, it indicates that these cracks were present very early in the structure's life.

Figure 18 shows a cold joint observed in one of these access shafts. The concrete consistency is visibly different above and below this cold joint, which was typical of many cold joints observed in the towers. Figure 19 shows typical vertical cracking observed in the bare concrete. The extents and size of the cracking in bare concrete was comparable to that observed in mudded and painted concrete.

Figure 17. Typical observed overhead (ceiling) slab cracks within the Tower 2 (Section Q of the 1st Floor floorplan insert).



Figure 18. Observed cold joints within the Tower 2 elevator shaft area (Section H of the floorplan insert). These cold joints were observed on bare concrete and were typical in the elevator shaft areas in the upper floors.



Figure 19. Cracking on bare concrete walls (typical) within the nonbasement floors of Tower 2 (Section R of the 2nd Floor floorplan insert). Majority of observed crack widths were less than 0.4 mm (insert depicts the largest observed of these cracks at a width of 0.6 mm).

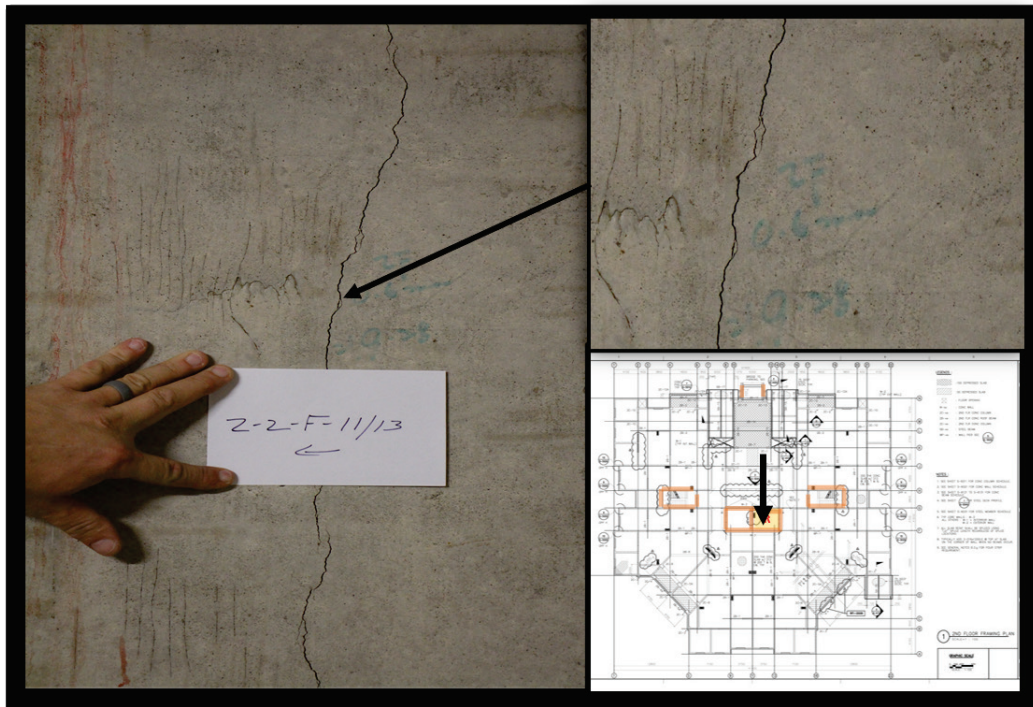


Figure 20 shows some of the worst honeycombing observed in the towers. There were several areas of bare concrete where concrete patching had been performed, but this area was unrepaired and unpatched. When honeycombing was observed, it was often near the bottom of walls and near areas of high rebar congestion. This is likely due to the difficulty of providing adequate concrete vibration in these areas, resulting in poor consolidation. These areas were also often near cold joints.

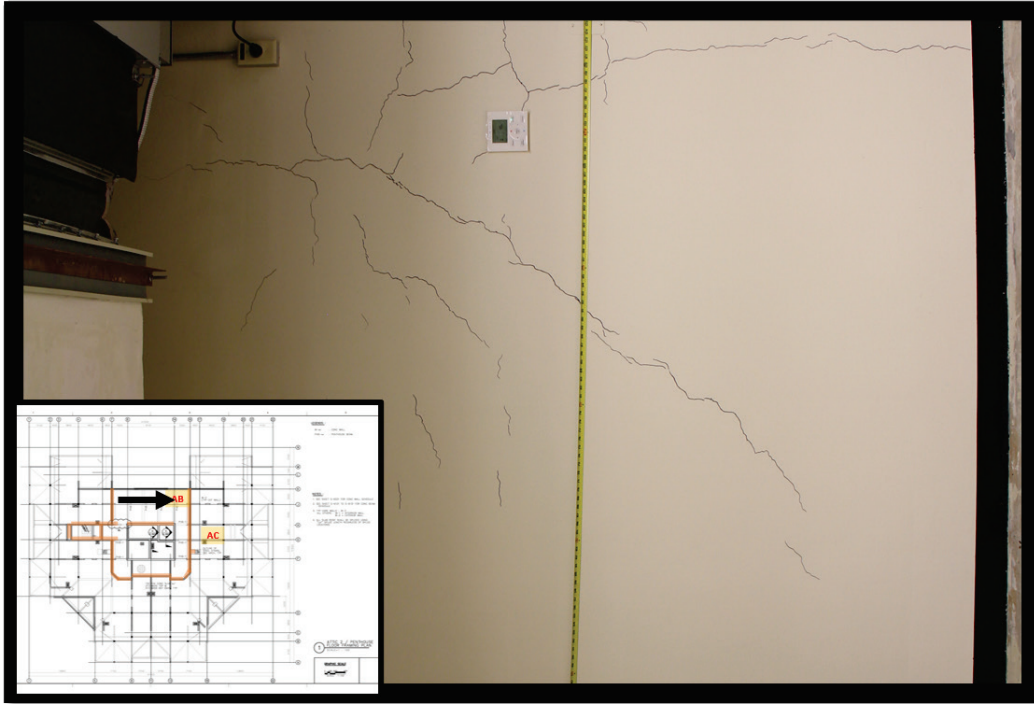
Figure 20. Honeycombing within Tower 2 (Section TAA of the 12th Floor floorplan insert). The honeycombing varied in severity but was typically located in areas of high rebar congestion and was often near cold joints.



2.1.3.4 Cracking in attic areas

As in Tower 1, the attic area of Tower 2 was observed to have multidirectional cracking as shown in Figure 21. These cracks were more obvious than many other areas of the structure, but this may be attributable to less aesthetic concerns in areas not accessible to the public.

Figure 21. Cracks within the Tower 2 attic elevator mechanical area (Section AB of the floorplan insert). The widest observed crack width was less than 0.40 mm. The shown cracks were traced with a permanent marker to highlight typical locations, lengths, and spacing and are not representative of crack width.



While Tower 2 did exhibit more cracking and cracks of greater width than either Tower 1 or Tower 3, all the cracks were consistent with shrinkage cracking. None of the cracks demonstrated any differential movement (shearing) along the crack length. Based on the crack gauges, the cracks have also not grown in width or length over the last 6 months.

2.1.4 Tower 3 observations

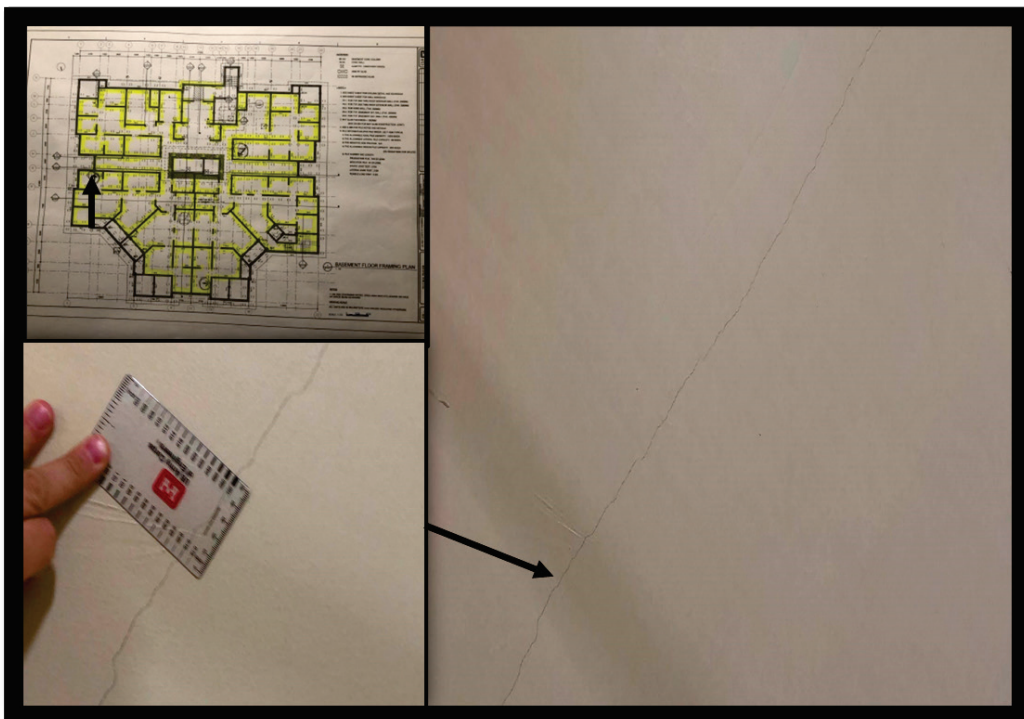
Apartment Tower 3, also known as Goguryeo (Bldg. 820), was the most recent tower to be completed. Construction began on this tower in July 2019, and it was turned over from USACE-POF to the Daegu Garrison in January 2022. The tower was tentatively set to be occupied in late April 2022. The structure is 15 stories with a basement. It is a cast-in-place concrete slab and wall structure. Concrete surfaces were observable in all of the basement, in the shaft behind the elevators on all floors, and in some apartment units (each unit had one small mechanical room). Unlike Tower 1, the walls in the public hallways of floors 1–15 were covered in sheetrock.

The same types of cracks and cold joints were observed in Tower 3 as had been in Towers 1 and 2, but the regularity and severity of these features was significantly less in Tower 3. Fewer photos were taken to document the cracking because there were so few areas that exhibited cracking. The cause of the significant decrease in cracking was unclear from observation. The following sections show examples of cracks and cold joints seen in Tower 3.

2.1.4.1 Basement cracks

As with Towers 1 and 2, the basement of Tower 3 was where the most concrete surfaces were accessible for inspection. The types of cracks (i.e., diagonal and vertical wall cracks, randomly oriented ceiling and floor cracks, etc.) were the same as seen in the previous two towers. The number and dimensions (both length and width) of cracks were significantly smaller than in either Tower 1 or 2. Figure 22 shows a representative diagonal crack from Tower 3. While representative cracks from Tower 1 and Tower 2 (Figure 1 and Figure 11) were measured at around 0.4 mm, the representative crack from Tower 3 in Figure 22 is only 0.15 mm.

Figure 22. Representative diagonal crack within the basement area of Tower 3 (Indicated on floorplan insert). The widest section of the observed crack was 0.15 mm (crack gauge insert).



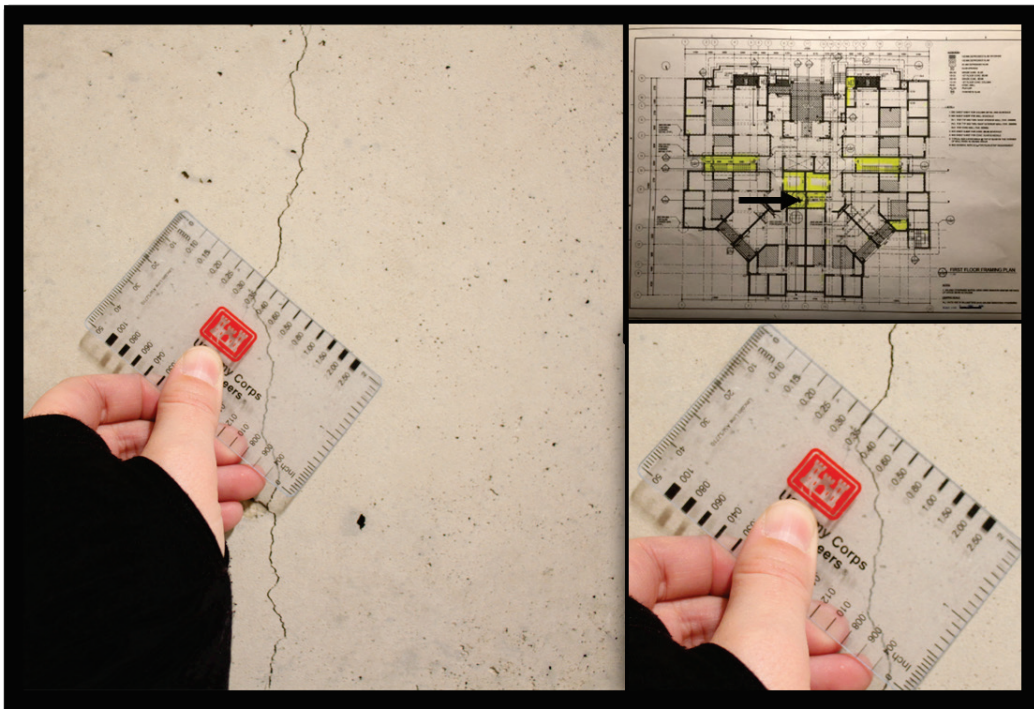
2.1.4.2 Observed features in bare concrete

Bare, unmudded concrete was only accessible in a few locations, mostly in the rooms behind the central elevator shafts. Figure 23 shows a typical cold joint in one of these locations. These cold joints were similar to those observed in Towers 1 and 2. Figure 24 shows a vertical crack on bare concrete observed in one of these areas. This crack measured 0.35 mm and was one of the larger cracks observed in Tower 3.

Figure 23. Typical observed cold joints within Tower 3 elevator shaft area (floorplan insert).



Figure 24. Vertical crack in Tower 3 observed on bare concrete (Section A of the floorplan insert). The widest section of the crack was 0.35 mm (crack gauge insert).



2.1.4.3 Cracking in upper floors

Due to Tower 3 not being occupied, several of the apartment units were open and available to be inspected. Each of these units housed a single mechanical room with mudded and painted concrete walls. Figure 25 shows one of these cracks. The cracks observed in these locations were typical in orientation, size, and number to those observed throughout the rest of the structure. Figure 26 shows cracking within Stairway No. 2.

Figure 25. Representative diagonal crack within the nonbasement floors of Tower 3 (Apartment Section of the 1st Floor floorplan insert). The widest section of the crack was 0.15 mm (crack gauge insert).

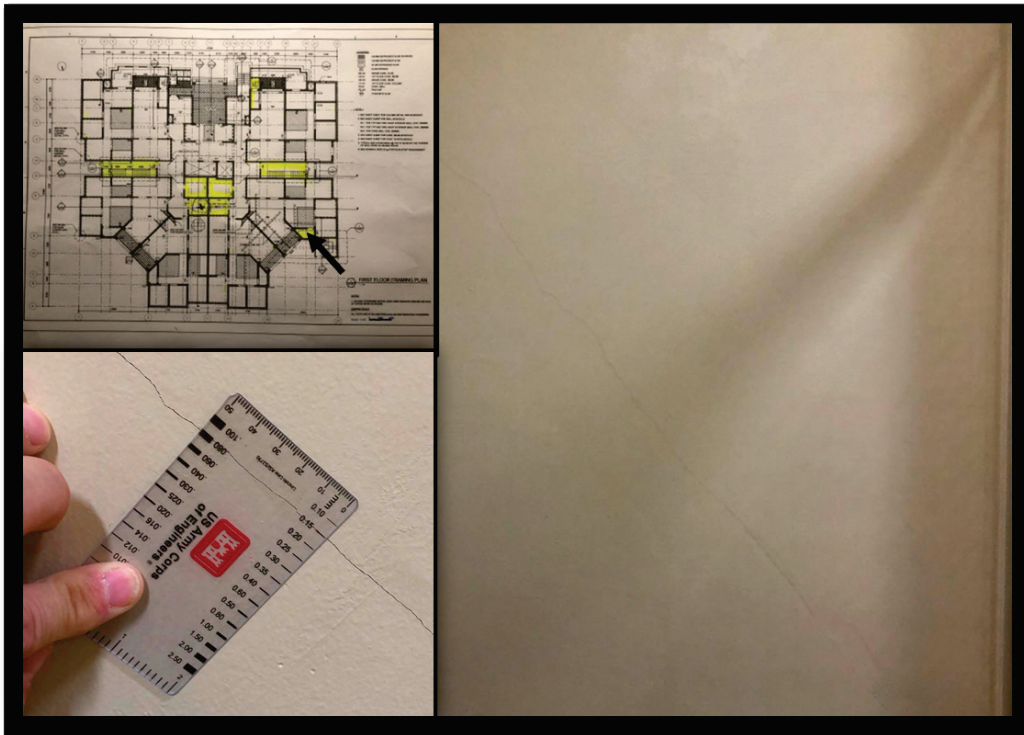
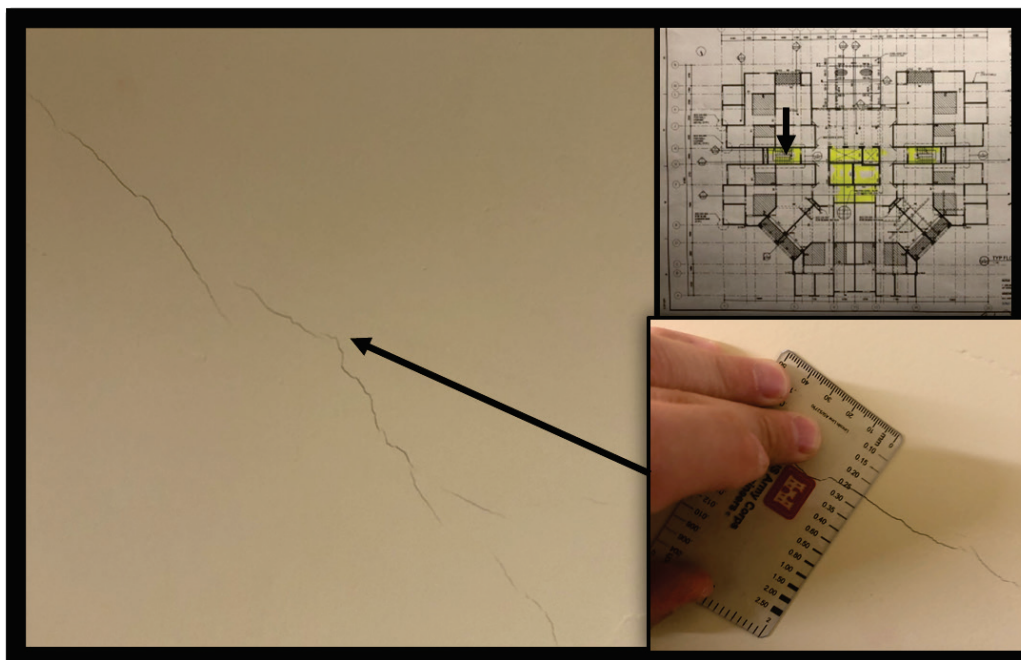


Figure 26. Observed cracking within Tower 3, 14th Floor stairwell (Stairway #2 of the floorplan insert). The widest area of the observed crack less than 0.25 mm. The crack did not intersect the ceilings, floors, or wall edges.



The cracking observed in all areas of Tower 3 was less than comparable areas of Towers 1 and 2. It was unclear from observation whether this difference was due to changes in materials, construction practices, age of the structure, or a different cause.

2.1.5 Tower 4 observations

Apartment Tower 4, also known as Kaya (Bldg. 830), was the last tower constructed. Construction began in December 2020 and, at the time of inspection, concrete for the basement through floor 14 had been cast and formwork on floor 15 was being installed. A thin (~1 mm) surface coating of mud had been applied to the walls of the basement and several floors above. However, the majority of the walls and slabs above the basement level were exposed (bare) concrete.

Overall, the walls and slabs of Tower 4 appeared to be homogeneous and well-consolidated, but some instances of cracking, cold joints, and areas of poor consolidation were observed throughout the structure. The most noticeable cracks were primarily located in the walls of the basement.

2.1.5.1 Diagonal cracks

Diagonal cracks were observed in the basement walls and were consistent with those observed in the basements of Towers 1, 2, and 3. Figure 27 shows diagonal cracks typical of those found in Tower 4. This type of cracking was not observed in the walls on floors above the basement. All of the diagonal cracks were isolated to the walls and did not propagate to the ceiling or floor slabs.

Figure 27. Typical diagonal cracking observed in the basement of Tower 4 (floorplan insert). The cracking was covered post placement but before visual inspections (insert shows the inspected crack on bare concrete without patch).



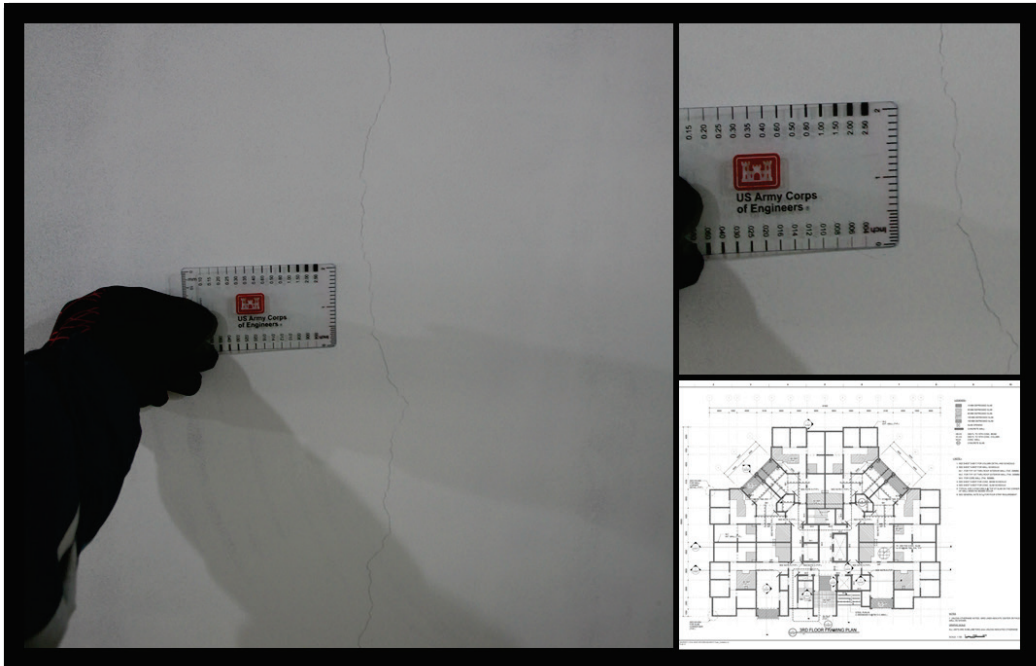
2.1.5.2 Vertical cracks

Vertical cracks were observed in basement walls and walls throughout the remaining floors and were consistent with those observed in the other towers. Crack widths ranged from hairline to approximately 0.25 mm. In the basement and other areas where the walls were thinly coated, many of the concrete cracks were manifest in the coating layer. Figure 28 shows an example of concrete cracking and the subsequent cracking of the surface coating in a basement wall. Figure 29 shows another vertical wall crack in a painted wall on an upper floor.

Figure 28. Vertical cracking observed in the basement of Tower 4 (floorplan insert). The cracking was covered post placement but before visual inspections (insert shows observable crack after patch/paint removed).



Figure 29. Observed vertical crack in Tower 4 (3rd Floor floorplan insert). The crack width was less than 0.20 mm (crack gauge insert).



2.1.5.3 Cracks in floor slabs

Cracks were observed in floor slabs throughout the tower, as shown in Figure 30. The sizes and multidirectional pattern of these cracks were consistent with those caused by plastic shrinkage that typically occur on slabs and other horizontal surfaces.

Figure 30. Observed slab cracking in Tower 4 (floorplan insert). The crack widths were less than 0.15 mm (crack gauge insert).



2.1.5.4 Cold joints

A number of cold joints were observed in walls throughout Tower 4. The majority of these were diagonal, but some were nearly horizontal. Diagonal cold joints indicate that the concrete was not properly consolidated but was instead allowed to accumulate in piles as the concrete dropped down the wall formwork. A diagonal cold joint on floor 2 is presented in Figure 31.

Figure 31. Observed cold joint in Tower 4 stairwell (floorplan insert).



2.1.5.5 Poor consolidation and nonuniformity

Some instances of poor consolidation and nonuniform concrete were observed throughout the tower. Poor consolidation and mortar patches were noted along the bottom of the walls of several balconies. Figure 32 shows one of these locations with additional consolidation issues in the adjacent columns.

Figure 32. Poor consolidation along bottom wall of Tower 4 balcony and adjacent columns (floorplan insert).



Surface voids, often referred to as bugholes, are another manifestation of poor concrete consolidation and were observed in some walls in Tower 4. Figure 33 shows a construction worker patching surface voids with mortar in an exterior concrete wall of Tower 4.

Figure 33. Patching of voids in exterior concrete of Tower 4 (floorplan insert).



Areas of nonuniformity, such as the one shown in Figure 34, were detected in some walls of Tower 4. In this case, the surface appears to be paste-rich with vertical flow patterns. This could be caused by the initial discharge of water in the pump line at the beginning or end of a concrete placement.

Figure 34. Nonuniformity in Tower 4 concrete wall (floorplan insert).



The types and extents of cracks, cold joints, and consolidation-related features were not significantly different in Tower 4 than in Towers 1–3. What was different was the ability to access a much larger proportion of the concrete surfaces in their bare state. This allowed for closer inspection of these features, particularly those associated with concrete placement practices.

2.2 Analysis and findings

The following sections give the results of the geotechnical, materials, and structural evaluations for the apartment towers. Each of these is based on the visual inspection, document review, and testing results.

2.2.1 Geotechnical evaluation

A detailed review of the foundation and in situ pile load test reports was conducted to determine whether potential foundation instability was the

cause of the observed concrete cracking at the four Camp Walker family housing towers. There was no evidence to suggest that the observed cracking was caused by foundational distress. However, a detailed review of the USACE Far East District supplied documentation for the Towers showed that there were errors in the initial foundation design calculations and subsurface exploration. Ultimately, specifications within the foundation reports for each tower indicated that the final foundation design was to be based on load test results that ultimately corrected any errors with the initial design calculations and subsurface exploration. Pile load test results, both dynamic and static, were performed according to industry standards and resulted in a conservative final foundation design.

2.2.1.1 Geotechnical observations from visual inspection

Based on visual inspection of Towers 1–4 there were no observable Service Limit State failure indicators. The building floors and corners were level and plumb with no differential displacement cracking. There were no reports or observations of mechanical or finish work, e.g., doors or pipes, being out of true, thereby prohibiting use. The one tenant complaint of gaps around a balcony door was investigated and observed to be due to door adjustment issues.

The ground outside Towers 1–4 showed no indications of upheaval, punching, or general shear associated with Ultimate Limit State failures. No displacement cracking in the surrounding infrastructure, e.g., sidewalks, architectural retaining walls, or roads, was observed. All observed drainage systems were observed to be functioning as designed with no signs of erosion or hydraulic-induced ground failures.

2.2.1.2 Geotechnical observations from design review

Four observations were made based on the design review. First, site investigation soil borings should have reached below the weathered rock zone or a minimum of 6 m below the anticipated pile tip. Second, unconfined compression (UC) testing should have been conducted for each of the towers; it was only conducted for Tower 4. This would have allowed for a good check of the point load test (PLT) and allowed for better calibration at the lower UC strengths (as recommended in Goodman 1989). Third, discrepancies and errors were found in the initial design calculations for Towers 1 and 2. Fourth, good construction QA and final design (i.e., based on the more extensive pile-

driving test results and static load tests) ensured that the construction of these pile foundations resulted in an adequate foundation.

A more detailed discussion of the geotechnical review is presented in Appendix A. The conclusions from this review are that the foundations for Towers 1–4 and associated parking structures were conservative. Through the review and inspection, the cracking identified in the concrete is not due to poor design or foundational distress.

2.2.2 Materials and construction evaluation

The concrete materials and construction methods used were evaluated based on the visual inspection, review of the design and construction documents, and discussion with USACE-POF personnel in charge of construction oversight. The following sections focus on the concrete mix design, review of construction practices, observations related to reinforcement, and petrographic evaluation of concrete samples cored from Towers 1–3.

2.2.2.1 Concrete mix designs and proportions

Concrete mixture design submittals and QA/QC reports for Towers 1, 2, and 3 were reviewed by the ERDC team. These documents were not made available for concrete used in Tower 4. The materials and mixture proportions used to produce concrete for Towers 1, 2, and 3 were nearly the same, with minor variations in aggregate size, water-to-cement ratio (w/cm), and overall proportions. These materials were developed in alignment with requirements provided in project specifications 03 30 00, including a design compressive strength (f'_c) of 27 MPa at 28 days, maximum water-to-cementitious materials ratio of 0.45, minimum air content of 5 to 6% depending on exposure, with slump of up to 100 mm (4 in.) at the point of discharge.

Based on an analysis of the approved mixture proportions, the materials used included an ASTM C150 Type I portland cement, crushed coarse aggregate, a combination of equal parts natural and crushed fine aggregates, and a chemical admixture that functioned as both a high-range water-reducing and air-entraining admixture. No supplementary cementitious materials such as fly ash or slag were reported in the approved mixture proportions. Concretes for Towers 1 and 2 used the same coarse and fine aggregates at the same proportions. Concrete for Tower 3 used the same fine aggregate as the previous towers, but the

coarse aggregate was different. Concretes for all three towers were produced by the same company, Suseong Co. Ltd., but different prime contractors were used. The Tower 1 contractor was Yo Jin Construction & Engineering Co. Ltd., and the contractor for Towers 2 and 3 was DAEBO Construction & Engineering Co. Ltd. A summary of the mixture proportions is provided below in Table 1.

Table 1. Mixture proportions used for Towers 1, 2, and 3.

	Tower 1	Tower 2	Tower 3
Concrete Manufacturer	Suseong	Suseong	Suseong
Contractor	Yo Jin	DAEBO	DAEBO
f'_c	28 MPa	27 MPa	27 MPa
w/cm	0.370	0.379	0.379
NMSA	25 mm	25 mm	19 mm
Air Content	6%	4.5–7.5%	4.5–7.5%
Admixture (MFG)	TC-AEV (Korea AD)	TC-AEV (Korea AD) FLOMIX 3000S (Dongnam)	TC-AEV (Korea AD)

The concrete mixture design for Tower 1 specified a w/cm of 0.37 and 6% air content. The f'_c used for proportioning of 28 MPa appeared to differ from the 27 MPa design strength used for the structural design of Tower 1. The High Range Water Reducing Admixture (HRWA) used was lignosulfonate-based. The 28-MPa mixture was designed to use a nominal maximum size aggregate (NMSA) of 25 or 20 mm; based on observation of the cores taken from Tower 1, it appears that the NMSA used in the wall concrete was 25 mm. In all cases, the 28-day compressive strengths achieved during trial batching and reported in approved mixture design documentation were in excess of f'_c , with compressive strengths of 37 to 40 MPa reported.

The concrete mixture design for Tower 2 included a w/cm of 0.379 and 4.5 to 7.5% air content. Two high-range water-reducing admixtures with air entrainment were employed; one was the same lignosulfonate-based admixture used in concrete for Tower 1, and the other was a polycarboxylate admixture. The NMSA for Tower 2 concrete was 25 mm.

The concrete mixture design for Tower 3 used a w/cm of 0.379 and 4.5 to 7.5% air content. The same HRWA with air entrainment that was used in Tower 1 was the only admixture used in the concrete of Tower 3. The NMSA was reduced from 25 mm to 19 mm, and a different coarse aggregate was used to meet this change. During the inspection of the towers, the ERDC team met with the quality assurance representative (QAR) and learned from him that the change in NMSA for Towers 3 and 4 was made to achieve better concrete consolidation and flow between reinforcing bars.

Using drilled cores of hardened concrete from Towers 1–3, the ERDC team conducted a more detailed analysis of the materials and proportions used for each of the towers. The paste fraction of the concrete, which is often an indicator of shrinkage and cracking susceptibility, was nearly identical among the towers and ranged between 25.6 and 27.1% by mass. According to the construction documents, the Blaine fineness of the cement also did not vary significantly, ranging from 3,420 to 3,790 cm²/g for the cements used.

2.2.2.2 Construction methods and curing

The project specifications for cast-in-place concrete 03 30 00 do provide basic requirements regarding means and methods for concrete placement, consolidation, finishing, and curing. Most of these are in conformance with guidance provided by the American Concrete Institute and, in particular, ACI 301 (2012), Specifications for Structural Concrete.

Specification section 03 30 00 provides specific requirements regarding joint placement and concrete placement and consolidation methods. In many cases, these do not appear to have been adhered to. Pictures provided by USACE-POF during construction included cold/construction joints located randomly within slabs and walls where concrete placements were terminated. Pictures reviewed along with field observations by the ERDC team indicated that this concrete had hardened prior to additional concrete being placed (see Figure 35 below). These do not conform with requirements in the specification 03 30 00 section 3.5 regarding the required position of construction joints during concrete placements.

Figure 35. Concrete placement terminated within a slab. The person standing on the concrete indicates that this concrete has hardened.



In addition, the methods that were reported for concrete placement in the towers and their monolithic slab/wall construction do not conform with typical means and methods for quality concrete placement. It was reported that typical procedures for construction consisted of erection of wall and slab formwork with concrete being placed by pumping concrete onto the slab and allowing it to flow and free-fall over the edge of the slab to infill the wall formwork. Congested reinforcing steel combined with the large NMSA and limited access to consolidate concrete in the walls via vibration is a likely cause of many of the honeycombs, laminations and layering in concrete placements, and poor consolidation around reinforcement that was observed by the USACE-POF and ERDC team in the field. This approach for concrete placement is also not in conformance with the recommendations of ACI 304.2 (2017) Guide to Placing Concrete by Pumping Methods which recommends the maximum free-fall height of concrete of 1.5 m (5 ft). On-site evaluation of ongoing construction of

Tower 4 indicated that some of the best practices for concrete placement were not possible with the current designs. Specifically, the tight spacing of rebar and thin walls precluded placing the concrete from directly above the wall (i.e., not on the slab) or reducing the drop height. Rebar congestion is discussed in more detail in the following section, 2.2.2.3.

The QA/QC documents available to the ERDC team do not thoroughly describe construction methods, i.e., placement, consolidation, and finishing methods, nor do they provide details on the curing regime of the concrete cast in the towers. The daily QA/QC reports do mention some of these activities, but the timing of the operations and the consistency with which they were performed is unclear. Dozens of reported instances of improperly placed cold joints, honeycombing, and debris present in form work prior to concrete placement were noted in summaries of QA reporting related to concrete placements. In all cases, the QAR noted that these concerns were fixed. However, it was unclear what that meant and, based on observations by the ERDC team, many of these “fixes” appear to consist of coating the deficient areas with mortar rather than a more extensive removal and replacement of the deficient concrete.

Curing of concrete following removal of formwork was also reported to be haphazard. The specification 03 39 00 provides requirements for moist curing or the use of curing compound/membranes. The ERDC team during its field inspections and discussion with USACE-POF staff reported that curing compound was applied inconsistently to the concrete, which in many cases may have also exacerbated issues with shrinkage and cracking in the highly restrained structure.

2.2.2.3 Reinforcement observations

Because many of the issues observed with concrete placement (cold joints, honeycombing, segregation, etc.) were attributed to reinforcement congestion, special attention was paid to observing rebar details (spacing, placement precision, etc.) in the ongoing construction of Tower 4 and associated parking structure. Analysis of the design documents and conversations with the Far East District construction representatives indicated that the details observed in these two structures were typical of the other six.

The rebar construction practices showed highly uniform rebar placement and good quality installation as seen in Figure 36 and Figure 37.

However, the observed rebar spacing was extremely congested. Figure 38 shows the congestion where a slab and beam come together. The congestion was even more severe where beams and columns intersected as seen in Figure 39. Examples from the parking garage are used here due to having more access to placed rebar; however, significant congestion was seen in the towers as well. Figure 40 shows the tight rebar spacing around an HVAC duct passthrough. This congestion created problems, noted in the QA/QC reports and in conversations with the Far East District inspectors, with the post-placement vibration wherein standard vibrational techniques were not practical or feasible. Importantly, this degree of rebar congestion would contribute to the poor consolidation and nonuniformity observed in the bare concrete.

Figure 36. Reinforcement in Parking Garage 4 roof. The rebar placement was very precise in all areas observed.

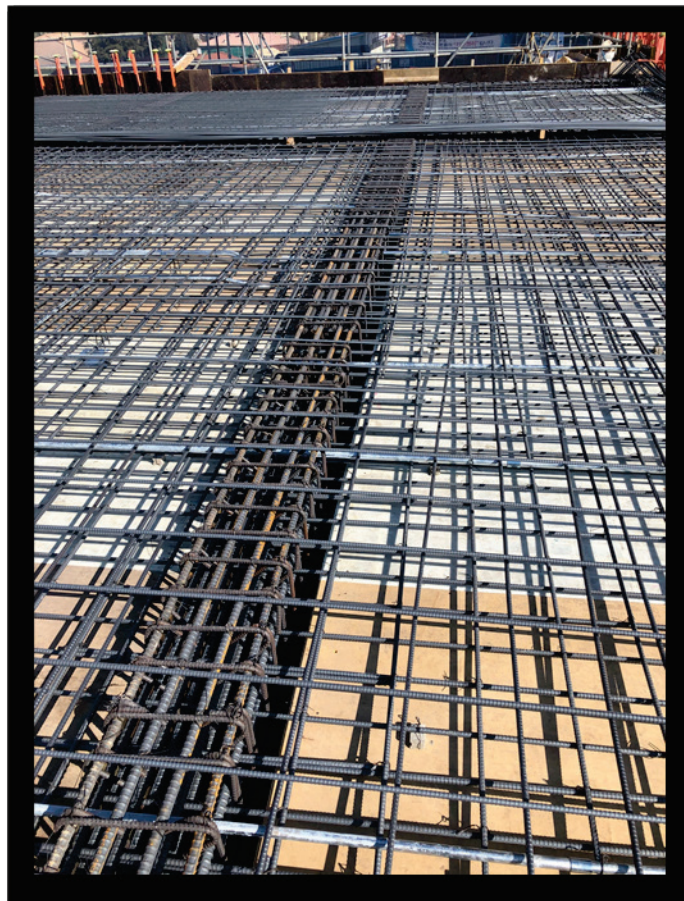


Figure 37. Typical rebar placement showing intersection between slab and beam (Parking Garage 4).

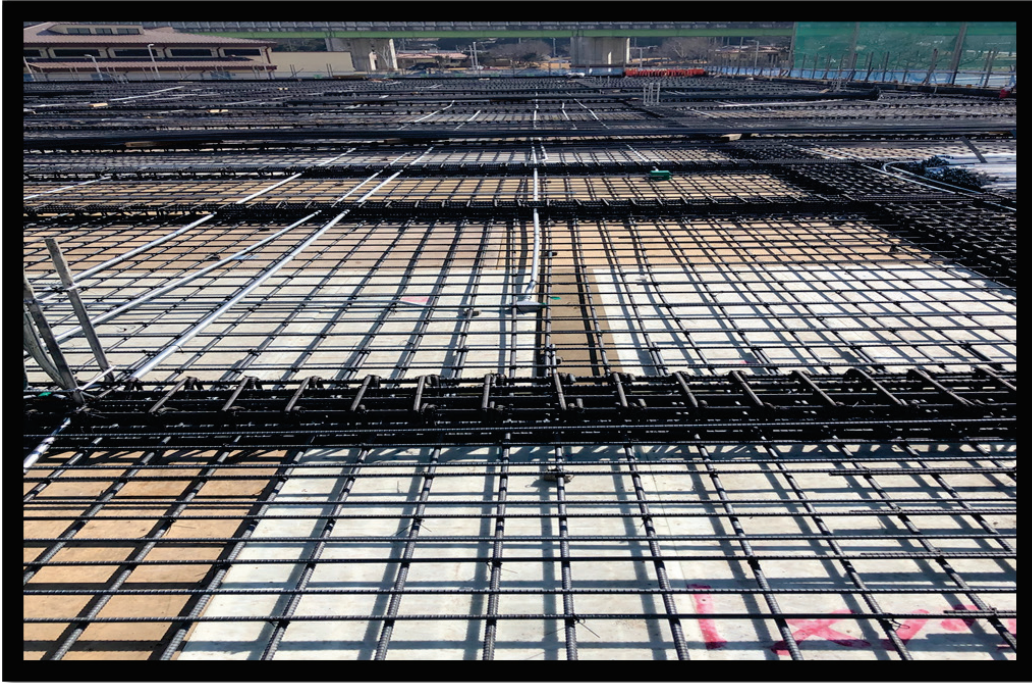


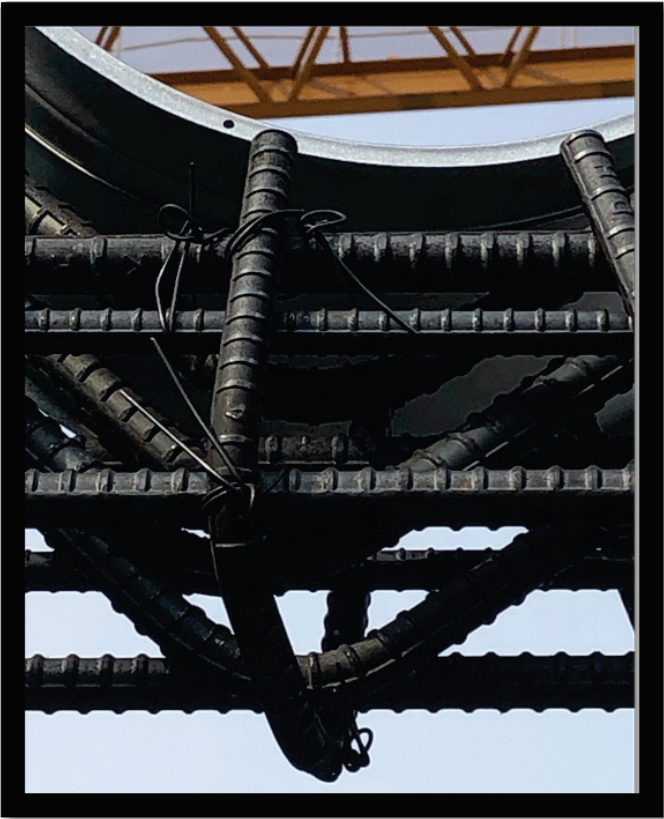
Figure 38. Rebar congestion in slab-beam intersection in Parking Garage 4.



Figure 39. Rebar congestion at intersection between beams and column in Parking Garage 4.



Figure 40. Congested rebar around HVAC duct passthrough in Tower 4.



2.2.2.4 Strength and petrographic analysis of concrete cores

Compressive strength measurements of concrete cores collected from Towers 1 and 2 are reported in Appendix E. The collection of these cores and their measurement was performed in conformance with ASTM C42 (2012) Standard Test Method for Obtaining and Testing Drilled Cores and Sawed Beams of Concrete. The measured compressive strengths ranged from 31.0 to 44.6 MPa, all of which well exceeded f'_c and were consistent with the anticipated long-term strengths based on the approved mixture proportion reports. These indicate that the in-place concrete mixture proportion, overall, is very similar to the mixture proportion that was approved for the projects.

Petrographic analysis was conducted on five cores obtained from Towers 1, 2, and 3. These results are reported in Appendix C. The concrete in total appeared similar in composition to what was reported in the mixture proportion, with the concrete being an air-entrained, straight portland cement (no supplementary cementitious materials) mixture. Concrete from Towers 1 and 2 appeared to vary significantly in proportion particularly across construction joints and concrete lifts with the coarse aggregate vs. mortar fraction shifting above and below joints and lifts. In many cases the coarse aggregate gradation also appeared to be gap-graded with large and small aggregate sizes. The increased paste fraction resulting from segregation and termination of concrete placements within the walls likely exacerbated the shrinkage cracking that was also observed, as the increased paste fraction would result in a higher local level of shrinkage. In limited cases, cracking present in the cores also appeared to result in fracture through aggregates, rather than solely through the paste and along aggregate interfaces. This indicates, along with the lack of other structural drivers observed, that the cracking occurred at later ages as a result of drying shrinkage cracking after the concrete had gained sufficient strength. An example of this cracking in a core obtained from Tower 2 is shown below in Figure 41.

Figure 41. Polished cross section of core T2-3 with locations of cracking through aggregates indicated.



2.2.2.5 Mechanisms causing cracking and distress

Based on the field observations made by the ERDC team, documentation reviewed, and strength and petrographic analysis conducted on cored concrete samples, it appears that the primary driver for the cracking is shrinkage along with defects in the concrete such as honeycombing and improperly placed cold joints due to random terminations in concrete placement. These issues are exacerbated in many areas by highly congested reinforcement details. The ERDC team did not observe structural drivers for the type of cracking observed, which appeared to be related largely to the sequence of placement and restraint in the structure that impacts the severity and orientation of shrinkage cracking.

There are three types of moisture-related shrinkage cracks that can occur in concrete – plastic shrinkage, drying shrinkage, and autogenous shrinkage cracks. Plastic shrinkage cracks occur before and during finishing operations and are caused by rapid evaporation of moisture from the surface of the concrete. These cracks are typically observed in slabs and other horizontal concrete surfaces. Drying shrinkage cracks are similar to plastic shrinkage cracks in that they are caused by a loss of moisture from the concrete, but drying shrinkage is generally considered to occur after finishing operations are completed and can continue to occur over several months after the concrete is placed. Autogenous shrinkage is caused by self-desiccation in the concrete as the cementitious materials hydrate and is typically observed in concretes with high cementitious materials contents, especially supplementary cementitious materials (SCMs), and w/cm less than 0.40. Based on the mixture designs and proportions, it is unlikely that the concretes used in these towers experienced autogenous shrinkage. Plastic shrinkage may have occurred on exposed surfaces of slabs/horizontal concrete placements. Based on the observed morphology of cracking in the walls, their limited exposure given they are in formwork at early ages, and the presence of cracking through aggregates in wall concrete, it appears that wall cracking is largely caused by drying shrinkage.

These crack sizes and defects in the concrete appear to be largely a durability concern for the concrete particularly in areas where the concrete is exposed to the elements (freezing and thawing, moisture, and potentially de-icing salts). Cracks larger than approximately 0.2 mm in width and exposed to the elements should be sealed to prevent moisture ingress and the potential for corrosion and other modes of deterioration such as accelerated freeze/thaw damage.

2.2.3 Structural evaluation

Although the overall structural designs and details vary among the four towers, all fundamentally consist of monolithic reinforced concrete walls and slabs throughout all stories. The resulting structures are very robust and stable. An inherent characteristic of the monolithic construction is that the edges of the walls and slabs are significantly restrained against movement, particularly volumetric movements. During the process of the described monolithic construction, the amount of restraint will vary, until eventually all edges of most of the walls are restrained.

Common causes of movement in reinforced concrete members include differential settlement, shrinkage, thermal effects, and creep. Creep is time-dependent and continues for years as the concrete member carries its self-weight and varying live loads. Thermal effects are the expansion and contraction movements of the structural member due to environmental temperature changes throughout the life of the structure. Shrinkage refers to the volumetric or length change of the member due to moisture content changes or the material chemical reactions. Of particular interest in this study are the volumetric changes associated with shrinkage effects. When the edges of the reinforced concrete member are restrained against movement, the volumetric changes induce internal stresses, and subsequent cracks.

As opposed to a multistory building of primarily beam/column frame construction, the robustness of the load-bearing wall structure results in relatively low service-load stresses. However, cracks can form as the tensile strength of the concrete is exceeded when structural members are heavily constrained (without contraction joints), and the conditions are prone to volumetric movement. Experimental and numerical studies based on restrained reinforced concrete walls concluded that the length-to-height (L/H) ratio is one of the main parameters influencing the crack's width due to drying shrinkage effects (Al Rawi and Kheder 1990, Kheder et al. 1994 and Kheder 1997). Parametric studies performed by Hooshmand and Kianoush (2018) showed that crack width increases with higher L/H ratios. This study also revealed that the crack width is not a function of the wall thickness but is significantly affected by dry environments and high temperature gradients.

A typical practice to avoid or control cracking in reinforced concrete structures is to include joints in the design. The three types of joints considered in design to control shrinkage effects are contraction, expansion, and construction joints. The contraction joint spacing recommendations vary depending on the type and use of the wall. ACI 224.3R recommends that contraction joints be located at a spacing equal to the wall height for walls taller than 3.6 m, and three times the wall height for walls less than 2.4 m. ACI 332R (1999) recommends a maximum 9.1 m contraction joint spacing in residential basement walls. PCA (1982) recommends that the joint spacing on walls with openings not exceed 7.6 m. It is desirable to have contraction joints within 3 to 4.5 m of a wall corner.

A common parameter within the subject towers is the height of the walls being 4.2 m for the basement and 3.6 m for other floors. Additional images of tower wall cracking are presented in Appendix B: Additional Photographs from Visual Inspection of Towers and Parking Garages. Wall lengths in these images varied from 4 m to 16 m giving L/H's varying from about 1 to 4. At the time of the inspection, contraction joints were not visible to the inspection team. According to Hooshmand and Kianoush (2018), crack width can vary from 0.2 mm to 0.9 mm for L/H of 1.5 to 4, respectively, for base-restrained walls without joints.

Considering the structural type (monolithic wall/floor-slab) that imposes significant restraint at the wall edges and the known volumetric effects of shrinkage and temperature changes, the observed cracks are the results of these factors, as opposed to the response to structural dead and live loads. This is further corroborated by observations that the severity of cracking may not correlate with the structural loading. If cracking were caused by dead and live loads, more severe cracking would be expected on the lower levels, which carry comparatively greater loads.

2.3 Conclusions and recommendations

Based on visual inspection, review of design and construction documentation, and the results of materials testing, the following conclusions and recommendations are made regarding Towers 1–4.

- Cracking, poor consolidation, and improper cold joints were observed throughout all four towers, but do not pose a life-safety concern.
- Restrained drying shrinkage is the primary cause of cracking observed throughout the towers.
- Until final report is provided by forensic AE firm, cracks in towers over 0.3 mm should be visually inspected every 12 months.
- Service life of the structures may be affected by cracking but can be mitigated by proper repair and sealing of cracks.

3 Parking Garage Evaluation

As with the apartment towers, the parking garages were evaluated using a combination of visual inspection, particular design and construction document review, and materials testing. The following sections detail those observations and analyses and provide conclusions and recommendations for the parking garages.

3.1 Observations from visual inspections of parking garages

The parking garages associated with each of the towers were inspected to determine if there was any concern about structural performance from either a life-safety or durability perspective. Parking Garages 1–3 were complete at the time of inspection, while Parking Garage 4 was still under construction. These four structures share similar concrete moment frame construction composed of traditional columns and beams cast monolithically with slabs. Concrete walls are used in stairways and as earth-retaining components but are not the main load-bearing components of these structures. Visual inspection was conducted on all four of the parking garages to determine the extent and severity of cracking in the structures and what mitigation and repair measures, if any, are necessary.

3.1.1 General garage observations

All visible concrete in the three completed garages was mudded and painted in a manner like that described in 2.1.1. Initially there was concern that the crack widths observed on the surface of the mud and paint would differ from those on the concrete. To ensure that the crack width measurements were accurate, a large section was cleared of mud and paint; the crack widths above and below the coating were then compared to ensure accuracy of surface measurements. Figure 42 shows the girder on Column Line E between Column Lines 3.5 and 4 on the upper floor of Parking Garage 1. The crack patterns and extents were observed to be the same above and below the surface coating. Likewise, the crack widths were measured to be the same within 0.05 mm.

Figure 42. Comparison of crack pattern and width above and below coating in Garage 1. The crack patterns did not change when the surface coating was removed, and the widths were all within 0.05 mm of those measured on top of the coating.



The types of cracking observed in Parking Garages 1–3 were similar across all three structures with only the prevalence and extents of cracking varying. Most of the cracking observed was vertical and diagonal cracking in the beams and girders of the garages. The diagonal cracks were oriented at approximately 45 deg and did not usually change orientation depending on where they were in the beam. In other words, the cracks near the centers of the beams were often at the same 45-deg angle as those cracks near the ends of the beams. Figure 43 shows this type of cracking in a beam in Garage 1.

None of the cracks observed showed any signs of differential movement along the length of the crack (i.e., slipping between the sides of the cracks). The cracks also tended to decrease in width near the top and bottom of the beam as seen in Figure 44.

Figure 43. Parallel diagonal cracks in beam on Column Line E between Column Lines 5 and 6 of upper floor of Garage 1.

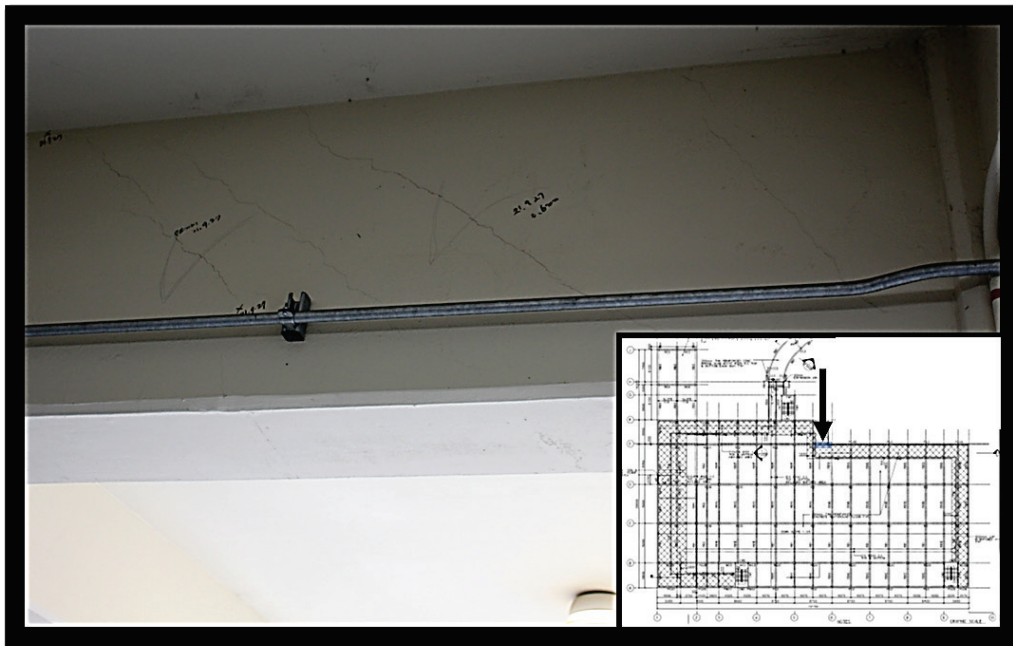
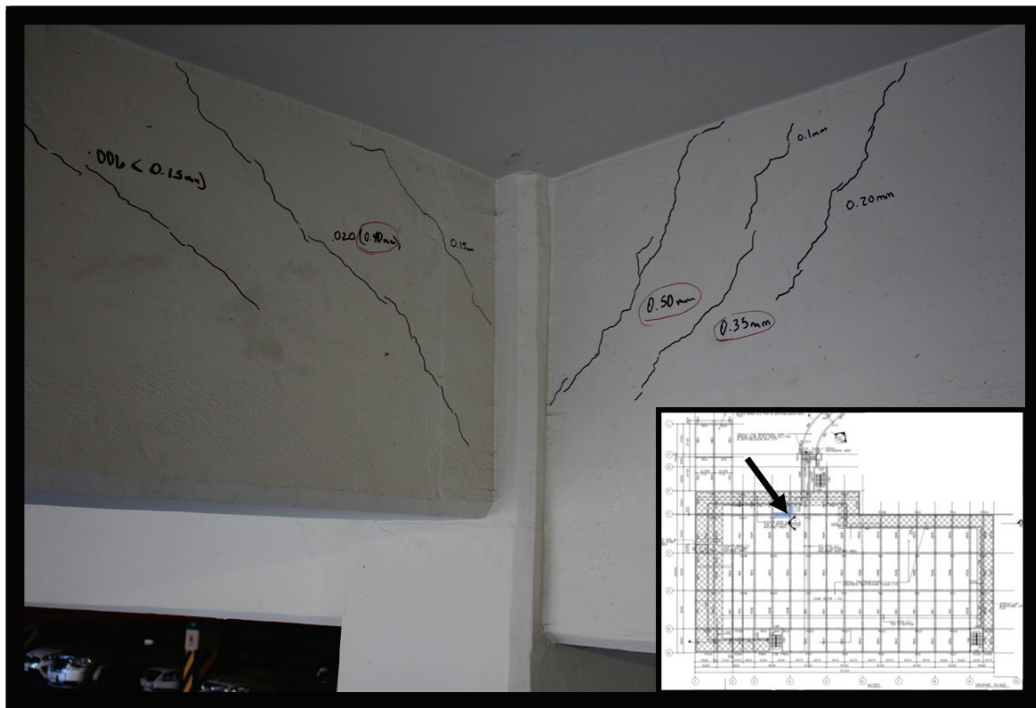


Figure 44. Typical diagonal crack in beam showing decrease in crack width at bottom and top of beam.



Within each structure, there was not a discernable pattern as to where cracks were more prevalent or wider. The cracks were not more pronounced in beams vs. girders as is seen in Figure 45. Adjacent beams would often exhibit differing levels of cracking despite similar geometry, location in the structure, and load demand. Cracking also seemed to be of similar severity in both directions (i.e., both girders and beams). The one consistent variation that was observed was that upper floor beams seemed to exhibit more cracking than lower floor beams. This was unexpected due to the fact that the upper floor beams carry very little load (playground and recreation area) in comparison to the lower floor beams (vehicular loads). The most likely explanation for this difference is the difference in exposure of these floors. The upper floors are more exposed to wind, which, particularly early-on, is a large contributor to drying shrinkage. The following sections will describe specific observations from the four garages.

Figure 45. Diagonal cracks in beam and girder at the intersection of Column Lines E and 4 on the upper floor of Garage 1.



3.1.2 Garage 1 observations

Garage 1 (Bldg. 801) is composed of three levels—the basement and ground levels provide parking, while the top level contains a playground and outdoor recreation area with grills and a small gazebo. Figure 46 shows the ground level entrance to Parking Garage 1. For both Garage 1 and 2, the USACE-POF

had already created a report detailing the locations and sizes of cracks throughout the structures*. This document was used as the basis for further evaluation by the ERDC.

Figure 46. Ground level entrance to Parking Garage 1.



For Garage 1, the USACE-POF report showed diagonal cracking in most of the beams and girders of the upper floor. These areas had the most numerous and widest cracks observed in any of the parking garages.

The lower, below-ground floor showed significantly less cracking in beams and girders but did display cracking in the walls. The cracks in the walls tended to be primarily diagonal in orientation with some of the cracks being vertical. The angle on the diagonal cracks tended to be much steeper (closer to vertical) than cracking observed in the garage beams or tower walls (see Figure 47). The largest cracks observed in walls were approximately 0.5 mm with most of the cracks being less than 0.2 mm.

* Site Visit for Crack Inspection of Family Housing Tower Parking Lot #1 and #2, Camp Walker, Korea. Memorandum to USACE-POF-ED-D from USACE-POF-EDD-C, U.S. Army Corps of Engineers, Far East District, 19 January 2022.

Even though these walls served as retaining walls, no significant water intrusion through the cracks or staining was observed.

Figure 47. Diagonal cracks in first floor (basement) of Parking Garage 1.



The largest crack observed was found in the roof beam of the ramp going down to the basement of Garage 1 and is shown in Figure 48. This crack was approximated to have a maximum width of 1.2 mm, although the bottom of the crack was significantly narrower at the location of the longitudinal reinforcing steel and the crack did not show any differential movement along its length. The crack also had a relatively steep angle, which reduces the effectiveness of any shear stirrups present. This beam was under very minimal loading due to it only supporting a thin sheet of metal roofing. At the time of this visual inspection, USACE-POF had already let a contract to repair this particular beam.

The report by the engineers of the USACE-POF provided a very extensive and detailed accounting of the cracks in Parking Garage 1 including mapping of approximate locations and widths. Visual inspection by ERDC corroborated this detailed report.

Figure 48. Crack in roof beam over Parking Garage 1 ramp. Crack width was approximately 1.2 mm.



3.1.3 Garage 2 observations

Parking Garage 2 (Bldg. 811) is composed of three levels—a ground-level lower parking floor, a second-story level with additional parking, and a third-story level with basketball courts and other recreational spaces. A two-level walkway connects the second and third levels of the parking garage with the second and third floors of Tower 2. Parking Garage 2 exhibited similar cracking to Parking Garage 1 in both the beams and girders. Also, like Parking Garage 1, these cracks seemed to be more prevalent and of larger width in the upper floor. These cracks are well-documented in the USACE-POF memorandum.

Figure 49 shows typical diagonal cracking in a girder of Parking Garage 2. Like in Parking Garage 1, these cracks did not change angle depending on their location on the beam. This would not be typical of cracks induced by shear loads. This figure also shows some slab cracking in the ceiling with staining indicating that water is ingressing. This can be a concern for long-term durability of the structure. There were very few areas where this kind of water ingress was seen, but none would be expected in such a new structure. Figure 50 shows the largest crack observed during visual inspection of Parking Garage 2. This crack

was 0.7 mm in width at its widest but was closed near the bottom of the beam and much narrower at the top of the beam.

Figure 49. Typical diagonal cracking in girder of Parking Garage 2. Note the staining near a crack on the ceiling indicating water coming through from the upper floor.



Figure 50. Most severe diagonal crack noted in Parking Garage 2 (0.7 mm).



Figure 51 shows multidirectional cracking in the beams and ceiling of the roof over the ramp into the upper floor of Parking Garage 2. This was unusual, because this portion of the structure only serves to cover the rampway and holds no significant loads. In this way, it is similar to the largest crack found in Parking Garage 1. It is unclear why these two areas of the structures exhibited some of the most severe cracking observed in Parking Garages 1 or 2.

Figure 51. Multidirectional cracking extending from beams into ceiling slab of roof over ramp to floor 2.



Parking Garage 2 did not exhibit any cracking or other distress that was significantly different from Parking Garage 1. The report by USACE-POF provides recommendations for remediation of the larger cracks in this structure. The visual inspection by the ERDC supports this course of action. For both Parking Garages 1 and 2, it is recommended that cracks over 0.2 mm be monitored for growth every 6 months until final AE report is provided.

3.1.4 Garage 3 observations

Parking Garage 3 (Bldg. 821) is composed of three levels—a ground-level lower parking floor, a second-story level with additional parking, and a third-story level with a playground and outdoor gathering areas. Observation of cracking in the stairwell walls of Parking Garage 3 was the initial impetus for further evaluation of cracking in the Camp Walker towers

and parking garages. By the time the ERDC visual inspection was performed, those particular cracks had been epoxy-injected and refinished as specified in the contract documents. Figure 52 shows a picture of this repaired wall. The diagonal repairs can be very faintly seen in the painted surface. Figure 53 shows similar repairs on the exterior of Parking Garage 3. Due to the different surface coating, these repairs are much more visible. In both cases, the repairs appear to have been performed properly.

Figure 52. Repaired wall of cracked stairwell in Parking Garage 3.



Figure 53. Repaired diagonal concrete cracks visible beneath exterior coating on Parking Garage 3.



Despite being the structure that initiated the current investigation, Parking Garage 3 showed significantly less cracking in its beams and girders. No cracks of repairable size (>0.2 mm) were observed in any of these major structural members. It was unclear why this structure exhibited so much less cracking. Since this structure is the newest of the three occupied parking garages, it is recommended to perform annual

inspections over the next two to three years to ensure that cracks like those in Parking Garages 1 and 2 are not manifesting.

3.1.5 Garage 4 observations

Unlike Parking Garages 1–3, Parking Garage 4 was still under construction at the time of visual inspection. This section of the report will focus on the lower finished floor. Some photographs and discussion of the top of Parking Garage 4 are presented in section 2.2.2.3 where rebar placement and congestion are discussed.

Due to Parking Garage 4 still being under construction, observations should not be directly compared with Garages 1–3. Features noted in Garage 4 may also have been present in Garages 1–3 in their unfinished states. Observations from Parking Garage 4 do indicate that many types of cracking were manifest at a very early age. Figure 54 shows vertical cracking in the wall of a stairwell in Parking Garage 4. These cracks have occurred very early and prior to any significant load being applied to the structure. Figure 55 shows ongoing crack monitoring that was initiated more than a month prior to the photograph being taken. This is further evidence of the early-age nature of these cracks. Figure 56 depicts a crack in the ceiling slab of the first floor of the parking garage. The white staining suggests that water was able to penetrate through the slab and that the crack is through the entire depth of the slab.

Figure 57 shows vertical cracking in a beam within the first floor of Parking Garage 4. This cracking is of particular interest, because it is immediately adjacent to a piece of shoring that has been in place since the concrete was cast. Since this is the case, it is very unlikely that the crack was caused by external loading. Rather, the location, orientation, and age of the crack all suggest plastic shrinkage.

Figure 54. Vertical cracking in stairwell wall of Parking Garage 4.



Figure 55. Crack monitoring in Parking Garage 4.



Figure 56. Crack in slab of Parking Garage 4 showing staining at location of water ingress.



Figure 57. Vertical crack in beam immediately adjacent to shoring. This shoring was in place continuously since concrete was cast.



In addition to cracking, the same types of cold joints were observed in Parking Garage 4 that were observed in the other structures. Figure 58 shows one of these cold joints beneath a staircase.

Figure 58. Diagonal cold joint under staircase in Parking Garage 4.



Parking Garage 4 did not exhibit different types of cracking than the other parking garages, but the unfinished concrete provided an opportunity for closer observation of these cracks. Also, due to the very new age of the concrete, Parking Garage 4 gave significant insights into the age at which the concrete may have begun to crack. While it is not certain that cracks occurred in the other structures at the same relative age, it is reasonable to assume that they also experienced cracking very early on. It is not possible to give definitive recommendations on how to manage cracking in Parking Garage 4 since the structure is not complete. Based on the issues seen in Parking Garages 1 and 2, it would be prudent to inspect the structure periodically (every 6 months) for the appearance of new cracks or the growth of existing cracks.

3.2 Analysis and findings

The following sections give the results of the geotechnical, materials, and structural evaluations for the parking garages. Each of these is based on the visual inspection, document review, and testing results.

3.2.1 Geotechnical evaluation

The design of the parking structure foundation was similar to the tower structures described in section 2.2.1. Minor discrepancies in the exploration and design calculations were overcome through in situ testing in the form of static and dynamic pile load tests. The results of this design were conservative and met industry standards. A more detailed discussion of the design review is provided in Appendix A.

Three key observations were made from the on-site investigation of the parking garages. First, in Parking Garage 1, cracking was observed in the subsurface retention walls; however, there was no observed lateral or shear displacement that would accompany a retaining structure failure. Additionally, there was no observed rotational movement of the walls, and the structure was still plumb and level. Therefore, the observed cracks were not attributed to lateral earth pressures or hydraulic loads.

Second, in all the parking structures, the ground floor parking slab exhibited no signs of foundational distress. There was no observed separation or cracking between the floor slab and the columns or walls. The corners of all parking garage structures were level and plumb with no signs of upheaval, punching or general shear, differential settlement, down-drag, or structural failure of individual piles or the pile system. Slab-on-grade connections with the pile-supported ground floor slab did not show any signs of separation or differential movement.

Third, all observed drainage systems appeared to be functioning as designed with no signs of erosion or hydraulic-induced ground failures.

3.2.2 Materials and construction evaluation

3.2.2.1 Concrete mix design and proportions

The same mixture proportions used in the towers was used for the appurtenant parking garage construction. These are described in section 2.2.2.1.

3.2.2.2 Construction methods and curing

The same cast-in-place concrete specification 03 30 00 was used for the parking garages as was used for the towers. The configuration of the concrete placements in the parking deck minimized many of the challenges

with concrete placement and consolidation that were observed in the slab and wall structures in the towers. There were limited reports of concrete consolidation issues around dense reinforcement in the parking structures, but minimal bare concrete was accessible to make further observations.

3.2.2.3 Mechanisms causing cracking and distress

The cracking observed in beam and slab systems in the parking garage structures is also likely the result of shrinkage. There does not appear to be any structural drivers for the cracking observed. The observed cracks are primarily durability concerns, especially given the exposure of the parking garage concrete to the elements and potential for freeze/thaw events and the use of de-icing salts.

3.2.3 Structural evaluation

As with the towers, the structural designs vary somewhat among the four parking garages, but all four garages share the same fundamental design characteristics. The parking garages are cast-in-place, reinforced concrete structures with monolithic slabs. Vertical loads are resisted by reinforced concrete walls and columns. The seismic load resisting system is an ordinary reinforced concrete moment frame. During the inspection, the field team did not observe any expansion/contraction joints. As discussed previously, it is often desirable to incorporate contraction joints to control cracking in reinforced concrete structures. Cracking in concrete structures can have many causes, including shrinkage.

The design analysis for Parking Garage 1 (DA 2015, pp. 7B–87 through 7B–90) refers to National Academy of Sciences (NAS) Report 65 (National Research Council 1974) to determine the permissible length for a building without expansion joints. The use of NAS Report 65 for this purpose is in accordance with UFC 3-301-01 (NAVFAC 2013)*. However, NAS Report 65 considers only thermal effects, and shrinkage of concrete is specifically outside its scope. Therefore, following the provisions of NAS Report 65 does not guarantee good control of concrete cracks arising from shrinkage. Shrinkage is addressed under construction joints in the UFC 3-301-01 (NAVFAC 2013) Section 1901.5, which references

* UFC 3-301-01, dated 1 June 2013, was in effect at the time of the design. It has since been superseded by UFC 3-301-01, dated 1 October 2019 with Change 1 of 4 February 2022 (NAVFAC 2022). The provisions relating to NAS Report 65 have not changed.

the American Concrete Institute (ACI) 224.3R (ACI 2001) and ACI 318 (ACI 2011) for more robust concrete volumetric changes. Crack control due to shrinkage is also addressed in ACI 362.1R (ACI 2012), Guide for the Design and Construction of Durable Concrete Parking Structures. However, this was not a required specification for these structures.

As discussed in Section 3.1.1, diagonal cracks in Parking Garages 1 and 2 were narrower at the bottom of the beam. Further, no differential movement was observed across the diagonal cracks. Thus, the observed cracks are not an indication of shear cracking due to overload. Instead, these observations are consistent with cracking due to restrained volume change. The beams are restrained by the columns at either end and by the slab above. The volume change is likely caused by concrete drying shrinkage. In addition, observations indicated that cracking in Parking Garages 1 and 2 was greater on the upper floors. The upper floors are loaded less heavily than the lower floors, but the upper floors could be exposed to larger fluctuations in temperature. This provides further evidence that the cracking was not due to overload.

Structural engineering research literature is not definitive in the correlation of specific crack widths to the degradation of shear capacity. Aggregate interlock is a known factor that contributes to shear strength along a crack in a reinforced concrete beam. At some crack width (not well-defined), the effects of aggregate interlock will diminish. The large vertical and horizontal reinforcement ratios in these beams provide clamping forces across the cracks, which allow the concrete to continue to carry shear even after cracking.

As stated and documented in the USACE-POF Memorandum, "Site Visit for Crack Inspection of Family Housing Tower Parking Lot #1 and #2, Camp Walker, Korea," dated 19 January 2022: "A few diagonal cracks and many hair line vertical cracks were observed on the 1st floor concrete beams of parking lot #1 and 2nd floor concrete beams of parking lot #2. The width of cracks ranges from hair line to 0.6 mm." By far, most of the cracks are in the range of 0.2 mm to 0.3 mm in width.

In addition to the shear strength of the concrete (which includes the effects of aggregate interlock), a major contribution to the shear strength of a beam comes from the presence of reinforcing steel stirrups. Another often neglected contribution to shear resistance is dowel action of the longitudinal steel.

Considering the nature and width of the observed cracks and the various contributions to the shear capacity of the beams, the cracks do not pose a safety concern. However, the widths of many of the cracks exceed 0.2 mm, the threshold for long-term durability concerns. Further deterioration of the cracks due to environmental factors could eventually lead to unsafe conditions. To ensure the continued performance of the structure as designed, it is prudent to perform crack repair and CFRP beam strengthening as described in the Far East District's site visit memorandum dated 19 January 2022.

3.3 Conclusions and recommendations

Based on visual inspection, review of particular design and construction documentation, and the results of materials testing, the following conclusions and recommendations are made regarding Parking Garages 1–4.

- Diagonal cracking observed throughout the beams and girders of Parking Garages 1–4 is primarily the result of restrained drying shrinkage.
- No cracks were observed that cause any concern for life safety in their current state.
- Beams with diagonal cracks can continue to carry significant shear loads through shear reinforcement, aggregate interlock, and dowel action; however, to ensure that Parking Garages 1 and 2 continue to perform as designed, the repair recommendations outlined by USACE-POF should be followed.
- Until the more detailed report is provided by the forensic AE firm, it is recommended that the cracks over 0.2 mm be visually inspected every 6 months.
- Cracks observed in the basement walls of Parking Garage 1 do not pose a life safety risk but could create durability issues. This is particularly true since they function as retaining walls.
- Cracks greater than 0.2 mm (or 0.1 mm in direct weather or contact with soil) should be sealed to prevent water ingress even if they are determined to not need structural repair.
- Fewer cracks were observed in Parking Garages 3 and 4. This may be because these structures are newer than Parking Garages 1 and 2. While Parking Garages 3 and 4 do not currently need repair, it is recommended that they also be inspected every 6 months to monitor cracking and determine if repair has become necessary.

4 Conclusions and Overall Recommendations

Based on the inspection and evaluation of Towers 1–4 and Parking Garages 1–4, the following conclusions and recommendations are made:

- Observed cracking was attributed to restrained drying shrinkage as a primary cause. This cracking may have been exacerbated by concrete construction techniques. This finding is corroborated by visual inspection, review of structural design best practices, petrographic analysis, and evaluation of construction documentation.
- Improper cold joints, honeycombing, and other consolidation issues were a result of highly congested rebar, large aggregate (MSA = 1”), and poor placement techniques.
- Neither the observed cracking nor concrete placement-related features pose a life safety concern in the towers or parking garages.
- Parking garage cracks should be analyzed and repaired as recommended by USACE-POF in order to ensure the structures continue to perform as designed.
- Cracks greater than 0.2 mm (or 0.1 mm in direct weather or contact with soil) should be sealed to prevent water ingress and resulting deterioration, which could lead to decreased service life or safety concerns.
- Until the final report is provided by the forensic AE firm, cracks over 0.2 mm in parking garages should be visually inspected every 6 months and cracks over 0.3 mm in towers should be inspected every 12 months to ensure cracks remain unchanged.

References

- ACI (American Concrete Institute) Committee 224. 2001. *Control of cracking in concrete structures*. ACI 224.3R-95 Joints in Concrete Construction. Farmington Hills, MI: ACI.
- ACI Committee 301. 2012. *Specifications for structural concrete*. ACI 301-12. Farmington Hills, MI: ACI.
- ACI Committee 304. 2017. *Guide to placing concrete by pumping methods*. ACI 304.2R-17. Farmington Hills, MI: ACI.
- ACI Committee 318. 2011. *Building code requirements for structural concrete*. ACI 318-11. Farmington Hills, MI: ACI.
- ACI Committee 332. 1999. *Guide to residential cast-in-place concrete construction*. ACI 332R-99. Farmington Hills, MI: ACI.
- ACI Committee 362. 2012. *Guide for the design and construction of durable concrete parking structures*. ACI 362.1R-12. Farmington Hills, MI: ACI.
- American Society for Testing and Materials (ASTM) International. 2012. *Standard test method for obtaining and testing drilled cores and sawed beams of concrete*. ASTM C42-12. West Conshohocken, PA: ASTM.
- _____. 2012. *Standard test method for obtaining and testing drilled cores and sawed beams of concrete*. ASTM C42-12. West Conshohocken, PA: ASTM.
- _____. 2017. *Standard test method for high-strain dynamic testing of deep foundations*. ASTM D4945-17. West Conshohocken, PA: ASTM.
- _____. 2018. *Standard test method for rebound number on hardened concrete*. ASTM C805/C805M-18. West Conshohocken, PA: ASTM.
- _____. 2020. *Standard test method for deep foundation elements under static axial compressive load*. ASTM D1143-20. West Conshohocken, PA: ASTM.
- _____. 2020. *Standard test method for determination of the point load strength index of rock and application to rock strength classifications*. ASTM D5731-16. West Conshohocken, PA: ASTM.
- _____. 2021. *Standard test method for compressive strength of cylindrical concrete specimens*. ASTM C39/C39M-21. West Conshohocken, PA: ASTM.
- Al Rawi, R. S., and G. F. Kheder. 1990. Control of cracking due to volume change in base restrained concrete members. *ACI Structural Journal* 87(4):397-405.
- Brown, E. 1981. *Rock characterization testing and monitoring*. Oxford: Pergamon Press.
- Deere, D. U., and Deere, D. W. 1988. *The rock quality designation (RQD) index in practice*. In *Rock Classification Systems for Engineering Purposes*, ed. Louis Kirkaldie. ASTM STP 984, 91-101. Philadelphia: American Society for Testing and Materials.

- Department of the Army (DA). 2015. *Design analysis for FY15 MCA, PN81230, family housing new construction, Camp Walker, Korea*. Pyeongtaek, Korea: U.S. Army Corps of Engineers, Far East District.
- Federal Highway Administration (FHWA). 2006a. *Design and construction of driven pile foundations, reference manual volume I*. Publication no. FHWA NHI-05-042. Washington, DC: FHWA.
- _____. 2006b. *Design and construction of driven pile foundations, reference manual volume II*. Publication no. FHWA NHI-05-042. Washington, DC: FHWA.
- Goodman, R. E. 1989. *Introduction to rock mechanics*. 2nd ed. Hoboken, NJ: John Wiley and Sons.
- Hooshmand, A., and M. R. Kianoush. 2018. Cracking behavior of restrained reinforced concrete walls under temperature and shrinkage strains. In *Proceedings, Building Tomorrow's Society, 13-16 June, Fredericton, Canada, ST100:1-10*. Surrey, Canada: Canadian Society for Civil Engineering.
- Kheder, G. F. 1997. A new look at the control of volume change cracking of base restrained concrete walls. *ACI Structural Journal* 94(3):262-71.
- Kheder, G. F., R. S. Al Rawi, and J. K. Al Dhahi. 1994. Study of the behavior of volume change cracking in base-restraint concrete walls. *ACI Materials Journal* 91(2):150-7.
- National Research Council. 1974. *Expansion joints in buildings*. Technical Report No. 65. Washington, DC: The National Academies Press. <https://doi.org/10.17226/9801>.
- Naval Facilities Engineering Command (NAVFAC) (Preparing Activity). 2013. *Structural engineering*. Unified Facilities Criteria (UFC) 3-301-01. Washington, DC: U.S. Army Corps of Engineers (USACE), NAVFAC, and U.S. Air Force Civil Engineer Center (AFCEC).
https://www.wbdg.org/FFC/DOD/UFC/ARCHIVES/ufc_3_301_01_2013.pdf.
- _____. 2022. *Structural engineering*. Unified Facilities Criteria (UFC) 3-301-01. Washington, DC: U.S. Army Corps of Engineers (USACE), NAVFAC, and U.S. Air Force Civil Engineer Center (AFCEC).
https://www.wbdg.org/FFC/DOD/UFC/ufc_3_301_01_2019_c1.pdf.
- Portland Cement Association (PCA). 1982. *Building movements and joints*. Skokie, IL: PCA.
- Teng, W. C. 1962. *Foundation design*. Englewood Cliffs, N.Y.: Prentice Hall Inc.
- USACE. 1991. *Engineering and design -- design of pile foundations*. EM 1110-2-2906. Washington, DC: U.S. Army Corps of Engineers (USACE), Department of the Army.
- Zhang, L., and H. H. Einstein. 1998. End bearing capacity of drilled shafts in rock. *Journal of Geotechnical and Geoenvironmental Engineering* 124(7):574-584.

Appendix A: Geotechnical Evaluation Report

On-site foundation investigation

An on-site foundation inspection was completed between 19 JAN 22 and 1 FEB 22 as part of the U.S. Army Engineer Research and Development Center (ERDC) Camp Walker Family Housing Investigation. The ERDC Camp Walker Family Housing Investigation identified extensive concrete cracking throughout all four housing structures (Towers 1–4) and the associated parking structures. The goal of the on-site geotechnical investigation was to ascertain if these cracks were the result of foundational distress, hydraulic instability associated with improper drainage, or subsurface subsidence. The visual inspection criteria, per standard geotechnical practice, used for this are as follows:

- Assess site factors that may impact foundation design and/or performance to include areal topography, geology, past/current construction activities.
- Discuss construction sequence and Quality Assurance/Quality Control (QA/QC) with Far East District personnel to understand construction details.
- Visually inspect the structures for signs of vertical movement indicative of excessive, uniform, or differential settlement.
- Visually inspect the structures for horizontal movement indicative of excess lateral forces.
- Visually inspect the surrounding exterior area for any signs of punching or general shear indicative of Ultimate Limit State failure of the foundation system.
- Assess the drainage system for signs of hydraulic instability.

In all of the above inspection criteria, the investigation was looking for signs of the following:

- Bulging of walls connected to the ground floor slab or pile foundation system.
- Leaning of walls connected to the ground floor slab or pile foundation system.
- Shape, pattern, and frequency of the cracking.
- Upheaval or separation of the exterior soil and the structure.

- Shift in vertical and horizontal members causing them to be out of level or plumb alignment.
- Signs of surface or subsurface erosion or improper drainage.
- Signs of distress to finish work, operation of doorway, windows and other openings, cracked or stressed pipes, or mechanical systems.

The Towers 1–4 and associated parking structures were known to have extensive cracking; therefore, specific attention was placed on ascertaining if the observed cracking exhibited any of the following high-risk indicators for foundational distress or settlement:

- The diagonal or stair-step cracking from corner to adjacent opening is wider at the top than at the bottom.
- Vertical cracks that are wider at the bottom than at the top.

Additionally, Towers 1–4 and associated parking structures were evaluated for the following low-risk indicators for poured concrete foundations, typically associated with shrinkage cracking patterns, and not associated with settlement or foundational distress:

- Vertical, diagonal, or stair-step cracking that is straight or wandering of uniform in width.
- Cracking that tapers to an irregular hairline or discontinuous crack.

For the observed structures, the cracking pattern was consistent with that of the low-risk indicators suggesting that the cracking was most likely not a product of foundation distress or settlement. Thus, the aforementioned inspection criteria were critically investigated to support or contradict the crack pattern observations.

For Towers 1–4 there were no observable Service Limit State failure indicators. The building floors and corners were level and plumb with no differential displacement cracking. There were no reports or observations of mechanical or finish work, e.g., doors or pipes, being out of true, thereby prohibiting use. The ground outside Towers 1–4 showed no indications of upheaval, punching or general shear associated with Ultimate Limit State failures. No displacement cracking in the surrounding infrastructure, e.g., sidewalks, architectural retaining walls, or roads, was observed.

In Tower 1 parking structure, cracking was observed in the subsurface retention walls. However, there was no observed bulging, leaning, lateral or shear displacement that would accompany a retaining structure failure. Additionally, there was no observed rotational movement of the walls, and the structure was still plumb and level. Therefore, the observed cracks were not attributed to lateral earth pressures, freeze-thaw cyclic loading, or hydraulic pressures.

In all the parking structures, the ground floor parking slab exhibited no signs of foundational distress. There was no observed separation or cracking between the floor slab and the columns or walls. The corners of all parking garage structures were level and plumb with no signs of upheaval, punching or general shear, differential settlement, down-drag or structural failure of individual piles or the pile system. Slab-on-grade connections with the pile supported ground floor slab did not show any signs of separation or differential movement.

All observed drainage systems were observed to be functioning as designed with no signs of erosion or hydraulic-induced ground failures. Discussions with the Far East District Construction QA/QC personnel did not reveal any improper construction sequences or shortcomings that would suggest any cause for foundational distress.

Foundation design review

Geotechnical engineers from the Engineer Research and Development Center were asked to review the foundation design and perform an inspection of the four family housing towers and associated parking structures at Camp Walker, South Korea. As part of this effort, a detailed review of the site characterization, foundation reports, and load tests was conducted. Separately, a senior geotechnical engineer was deployed to perform visual inspections of the structures. This appendix will focus on the design documentation review. Table A1 contains a list of documents reviewed during this effort; documents will be referenced throughout this appendix by reference number located in column 1. Current status of the family housing towers is that Towers 1 and 2 are completed and occupied. Towers 3 and 4 are under construction. Figure A1 shows the tower locations at Camp Walker, Daegu, South Korea, as of March 2021.

Figure A1. Tower locations on Camp Walker, Daegu, South Korea (courtesy Google Earth).



The foundation design review was particularly focused on the static analysis for the reason that the cracking identified in the structure occurred between the construction of these structures and the present, which is within the past 5 yr. During this time no seismic events have occurred or other loading that would cause the cracking. Therefore, focus was paid to the static stability and in particular the pile design, static and dynamic load tests, and field and laboratory investigations. The primary objective of the design review was to identify whether the concrete cracking was due to foundation instability.

Table A1. Documents reviewed.

Ref. #	Project	Document	Date	Structure	Designer
1	FY15 MCA PN81230 Family Housing New Construction (G&EE 13-048G/G14-069)	Foundation and Pavement Design Analysis	10/28/2014	Tower 1 and Parking Structure	Mr. Pak, Ki-Hong
2	FY16 AFH MILCON PN 81427, Construct a 15 Story AFH Tower	Foundation and Pavement Design Analyses Report (G&EE Project 15-036G/Report G2016-09)	1/15/2016	Tower 2 and Parking Structure	Steve H. Kim
3	FY17 MILCON PN 81428 Family Housing New Construction	Foundation and Pavement Design Analyses Report (G&EE Project 16-021G/Report G2016-023)	9/1/2016	Tower 3 and Parking Structure	Yon-chun Yu
4	FY19 AFHC PN 81429 Family Housing New Construction, Tower #4	Foundation and Pavement Design Analyses Report (G&EE Project 18-009G/Report G2019-003)	11/2/2018	Tower 4 and Parking Structure	Yon-chun Yu
5	FY15 MCA PN81230, FAMILY HOUSING CONSTRUCTION	Report of Dynamic Pile Load Test	6/1/2016	Tower 1 Parking Structure	Korea Institute of Construction
6	FY15 MCA PN81230, FAMILY HOUSING CONSTRUCTION	Report of Static Load Test	4/1/2016	Tower 1	Korea Institute of Construction
7	FY15 MCA PN81230, FAMILY HOUSING CONSTRUCTION	Report of Dynamic Pile Load Test	5/1/2016	Tower 1	Korea Institute of Construction
8	G&EE Project 17-015C/Report C2017-017	Memorandum for Test Pile Inspection and Driving Quality Assurance, FY16 AFH MILCON PN81427 Family Housing New Construction (Tower 2), Camp Walker, Korea	9/27/2017	Tower 2 and Parking Structure	Jay H. Pak
9	FY17 PN 81428 Family Housing New Construction Project, Tower#3	Quality Assurance (QA) Report for Test Pile Driving (G&EE Project 18-016C/Report C2018-017)	7/26/2018	Tower 3 and Parking Structure	Yon-chun Yu
10	CONTRACT NO. W912UM-20-C-0001	FY19 AFHC, PN81429 Family Housing Tower #4 Camp Walker, Korea, Indicator Pile Report	5/1/2020	Tower 4 Parking Structure	Daehan Foundation ENG Co., Ltd.
11	CONTRACT NO. W912UM-20-C-0001	FY19 AFHC, PN81429 Family Housing Tower #4 Camp Walker, Korea, Indicator Pile Report	5/2/2020	Tower 4	Daehan Foundation ENG Co., Ltd.
12	CONTRACT NO. W912UM-20-C-0001	FY19 AFHC, PN81429 Family Housing Tower #4 Camp Walker, Korea, Production Pile Report	7/1/2020	Tower 4	Daehan Foundation ENG Co., Ltd.

The results of the design review are presented in the following sections and are organized by topic. These topics are site investigation, laboratory investigation, foundation design, pile load tests, and summary and conclusions.

Site investigation

Site investigation for the family housing towers and parking structures consisted of performing soil borings. The soil borings were conducted by the U.S. Army Corps of Engineers Far East District (USACE-POF) drill crew with a USACE-POF geologist logging the boreholes (Table A2). Review of the borings showed that appropriate means and methods were followed during this process. However, the depths of the borings were terminated prematurely and failed to fully capture the bearing capacity zone for this foundation system.

Table A2. USACE-POF soil borings per structure.

Structure	Borings	Depths (m)	Bottom Elevation (m)	Quantity of Borings
Tower 1 (and Parking Structure)	B14-530 to B14-540	16.5 to 25.5	60.9 to 71.7	11
Tower 2 (and Parking Structure)	B16-011 to B16-023	10.1 to 19.5	68.0 to 79.7	13
Tower 3 (and Parking Structure)	B16-191 to B16-204	16.8 to 24.1	67.3 to 74.5	14
Tower 4 (and Parking Structure)	B18-156 to B18-169	20.5 to 26.2	77.6 to 87.8	14

Additional soil borings were specified in each of the foundation reports (Table A1, Ref # 1–4); these were to be performed by the piling contractor for validation of the USACE-POF borings and to identify pile predrilling depths. The piles were to be drilled and cased through the overburden and primarily intended to be end bearing and founded on competent rock.

The foundation of the site consists of fill material, colluvial soil, residual soil, and bedrock. Some soil contamination was identified, this was determined to be petroleum-based. The fill material extends to a depth of 1.5 m and consists of mainly coarse-grained materials. The colluvial soils consists of clayey gravel with sand (GC), clayey sand (SC), clayey sand with gravel (SC), gravelly lean clay (CL), poorly graded gravel with silt and sand (GP-GM), poorly graded sand with gravel (SP), poorly graded sand with silt (SP-SM), poorly graded sand with silt and gravel (SP-SM), silty gravel with sand (GM), silty sand (SM), and silty sand with gravel (SM). Residual soils are more fine-grained and consist of fat clay (CH), lean clay (CL), silt (ML), clayey sand (SC), clayey sand with gravel (SC), and silty sand (SM).

Bedrock below the site consists of slightly to highly weathered shale and andesite. The rock quality designation (RQD) ranged from 0 to 100% across the site. The RQD is a modified core recovery percentage in

which unrecovered core, fragments and small pieces of rock, and altered rock are not counted so as to downgrade the quality designation of rock containing these features (Deere and Deere 1988). The RQD serves as a tool to identify zones where greater scrutiny or further investigation may be needed. The higher the RQD the higher the quality of the rock. Table A3 shows the range of RQDs calculated at the site. Very low RQDs were found, indicating a weathered and fractured rock foundation. The pile foundation was primarily intended to carry the load through end bearing. The RQD calculated for the cores taken from the bottom of the boreholes are shown in the last column of Table 3. This shows that there is limited variation in RQD at the bottom borehole elevation and indicates the soil borings did not extend beyond the weathered rock zone as required for bearing on competent rock.

Table A3. Rock Quality Designation (RQD) range per tower.

Tower	RQD (%)	RQD (%) at Depth Drilled
1	0-25	0-25
2	0-100	0-100
3	0-33	0-33
4	0-84	13-84

Laboratory investigation

Soil and rock samples collected from the site during the site investigation phases were used to perform soil classification and acquire shear strength of the bedrock. No shear strength testing was performed on the overburden soil samples. Shear strength for the soils was assigned based on soil type. The unconfined compressive strength of the rock cores was attained through the point load test and unconfined compressive testing. The laboratory investigation for Tower 4 was the only investigation that performed unconfined compressive testing while point load tests (PLT) were performed for all of the tower exploration (Towers 1-4).

Figure A2 and Figure A3 show the results of the PLT for each tower. Preliminary predrilling depths and pile lengths were estimated based on the results of the PLT. These are shown in each of the figures as dashed lines.

Review of these results show that for Towers 1 and 2 the borings extend 4 m below the estimated pile tip. U.S. Army Corps of Engineers guidance recommends extending 6 m below the longest pile (USACE 1991). FHWA (2006a) recommends extending borings through unsuitable strata to reach hard or dense materials. As the piles were intended to be primarily end-bearing the borings were terminated prematurely, especially for Tower 3.

It was clearly stated in each of the foundation reports that a minimum unconfined compressive strength of 15 MPa was assumed for design. This (15 MPa) is the minimum strength for which the PLT is applicable, ASTM D-5731 (2020). Brown (1981) reports that results below 25 MPa may yield ambiguous results. The design value is the minimum for which the PLT is applicable; lower unconfined strengths may have been encountered. Performing unconfined testing for each tower may have helped identify a correlation between PLT and actual unconfined strengths.

The foundation reports stated that during construction, dynamic load tests would be performed on all test piles by the contractor to verify maximum service loads. Therefore, to ensure that the piles were embedded to the proper depth a performance criterion was included (Table 1, Ref #1–4). Additional borings were also required of the contractor for each Tower, but records of these borings were only provided for Towers 3 and 4. Tower 3 contractor borings also included PLT and are shown in Figure A3(A.)

Observational comments on the PLT results are as follows:

- PLT variability increases from Tower 1 to Tower 4,
- Preliminary embedment elevations were reasonable,
- Due to shallow boring depths, inclusion of a performance criterion was appropriate.

Figure A2. Results of point load tests, reported as unconfined compression for A. Tower 1 and B. Tower 2.

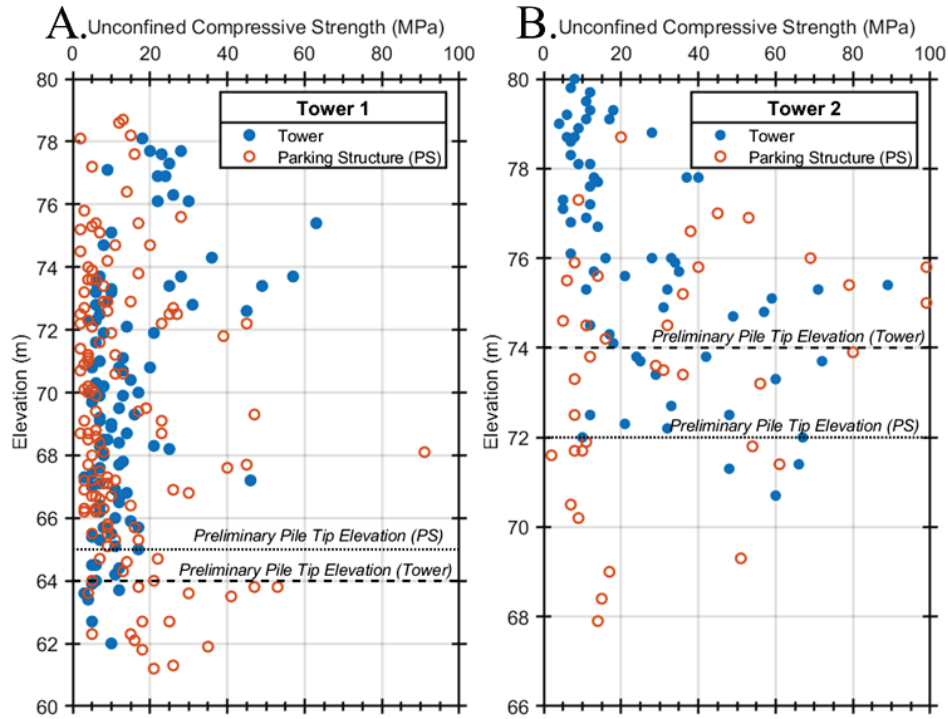
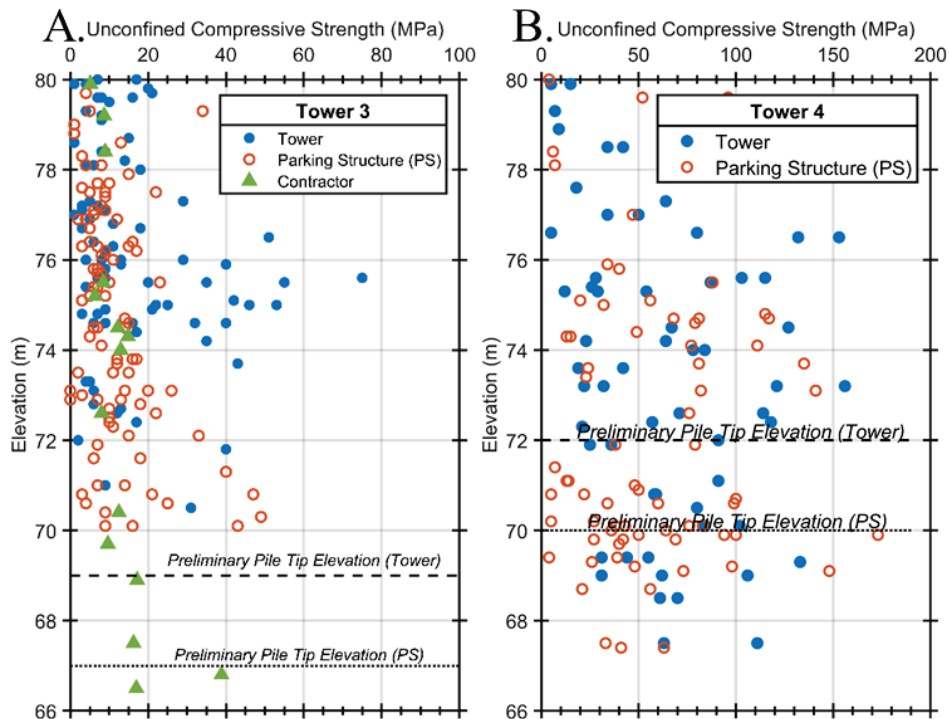
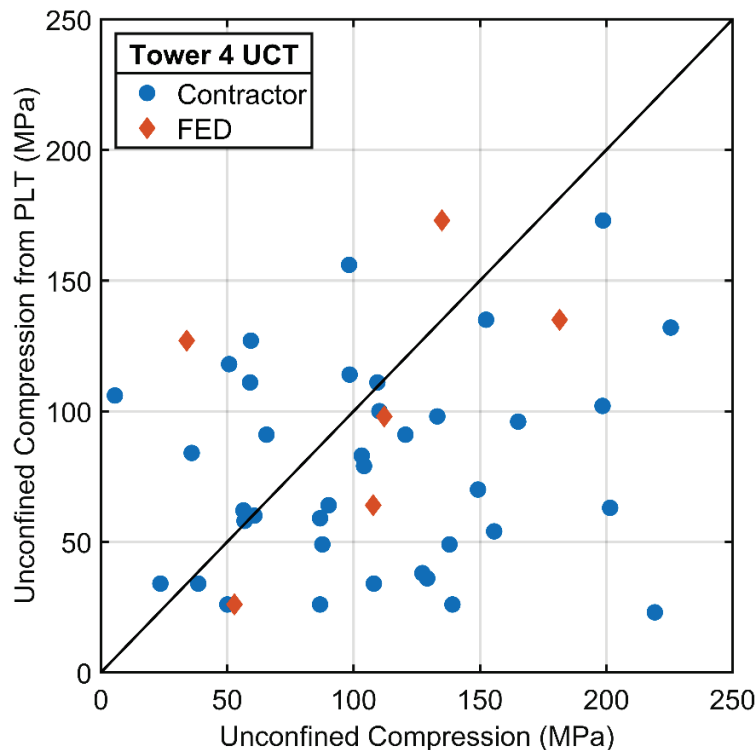


Figure A3. Results of point load tests, reported as unconfined compression for A. Tower 3 and B. Tower 4.



Laboratory testing of bedrock samples from Tower 4 included unconfined compression testing (UCT) performed by the Far East District (FED) geotechnical laboratory as well as a commercial laboratory. The UCT results allow for a direct comparison of the PLT correlation directly to UCT results. Figure A4 shows this comparison. Most of the tests were conducted on samples with a UC strength greater than 50 MPa. Figure A4 shows that, typically, the directly measured UC strengths are greater than the PLT derived strengths. Therefore, the PLT results are considered conservative with the caveat that the comparison was performed on samples with strengths much greater than those assumed for design.

Figure A4. Tower 4 laboratory testing results comparing unconfined compression test results to PLT derived unconfined compression.



Pile foundation design

A pile foundation was selected for the family housing towers and parking structures due to the large structural loads. The piles were to be founded on competent bedrock. Pretensioned spun high strength concrete piles were selected: 500-mm and 600-mm diameters were considered, and 500-mm-diam piles were selected for construction. The maximum allowable loads for each of the towers are shown in Table A4. The foundation reports specified that the overburden soils may contain adverse pile-driving conditions such

that pile-installation holes would be pre-drilled and cased and socketed into the bedrock. The casing was to be withdrawn after the pile was socketed into bedrock and the annular space grouted.

Table A4. Maximum allowable axial loads for 500-mm-diam piles.

Structure	Maximum Allowable Axial Load (kN)
Tower 1 (and Parking Structure)	1,300
Tower 2 (and Parking Structure)	1,200
Tower 3 (and Parking Structure)	1,003
Tower 4 (and Parking Structure)	1,003

Preliminary unconfined compressive strengths of 15 MPa and embedment depths were provided for bidding purposes (Table 1, Refs #1–4). The final pre-drilling depths were specified to be determined after completion of the test pile installation, which included pile load testing, both static and dynamic. The contractor was also specified to perform additional soil borings and provide verification of the unconfined compressive strengths. These borings were specified to have a depth greater than the specified preliminary pile embedment elevations. These boring logs and UC verifications were not fully provided but were provided for Tower 3, as shown in Figure A2(A.)

The allowable axial loads were calculated using an assumed UC strength of 15 MPa. The results of the allowable axial capacity calculations are shown in Table A5. The UC strength was reported to be the same for each calculation but from inspection there are five changes in the calculated values. The first change is the side resistance, which decreased from 314 kN to 126 kN due to an increased factor of safety (FS). For Tower 1 a FS of 4 was assigned while in Towers 2–4 a FS of 10 was selected. The increase in the factor of safety was associated with the uncertainty of the side resistance due to the piles being pre-drilled. This does represent an inconsistency between the towers.

Table A5. Results of allowable axial capacity design calculations from each foundation report.

Structure	Side Resistance (kN)	End Bearing Capacity (kN)			Allowable Axial Capacity (kN)
		Teng (1962)	Goodman (1980)	Zhang and Einstein (1998)	
Tower 1 (and Parking Structure)	314	785	1047	1460	1300
Tower 2 (and Parking Structure)	126	785	1047	1460	1200
Tower 3 (and Parking Structure)	126	589	785	1256	1003
Tower 4 (and Parking Structure)	126	589	785	1256	1003

A mathematical error was found in the end-bearing calculations for the initial designs of Towers 1 and 2. The stated design unconfined compressive strength was 15 MPa; however, within the design calculations an unconfined compressive strength of 20 MPa was used throughout. This error was not noticed/corrected by any internal review of the foundation design of Towers 1 and 2, nor was a reassessment documentation of Towers 1 and 2 provided after this was corrected for the initial design calculations in Towers 3 and 4. The allowable capacity was decreased from Tower 1 to Tower 2, it would seem that the results of the dynamic load tests from Tower 1 were taken into account when selecting the allowable capacity for Tower 2. In summary, the pile design specifications were appropriate but discrepancies in the allowable axial capacity calculations were made.

Pile load test

Static, dynamic, and lateral pile load tests were conducted (Table A1, Ref #5–10). For this evaluation only the static and dynamic load tests were reviewed. An indicator pile-driving program was specified in the foundation report (Table A1, Ref #1–4), the results of which were used to determine ordering lengths for production piles. As part of the indicator pile program, dynamic load tests were conducted using a pile driving analyzer (PDA) at end of driving and after concrete curing (7–14 days). The re-strike tests give valuable information about final pile capacity (FHWA 2006a, 2006b). The dynamic testing was specified and performed to adhere to ASTM D-4945 (2017). The results of the dynamic pile load testing are presented in Table A6. Results show that the minimum allowable working load fell below the design axial capacity in a single pile

of Tower 1. The change in allowable capacity from end of active driving to re-strike is positive indicating a gain in strength as the grout set-up.

Table A6. Results of the dynamic pile load test, allowable working loads presented from restrike testing.

Structure	Allowable Working Load w/ FS = 2.0 (kN)			Change in Allowable			# of Piles Tested
	Min.	Median	Max.	Min.	Median	Max.	
Tower 1	1259	1557	1876	20	206	742	33
Tower 1 PS	1606	2144	2442	107	431	1192	9
Tower 2	2060	2489	2851	59	490	1223	39
Tower 2 PS	2062	2146	2362	525	747	872	9
Tower 3	1617	2423	3239	207	895	1758	67
Tower 3 PS	2098	2408	2623	585	937	1392	28
Tower 4	1392	1690	1913	107	276	743	28
Tower 4 PS	1481	1668	1926	255	525	792	7

Two static load tests were performed for each of the towers. The maximum applied axial loads were 2400 kN, 2452.6 kN, 1900 kN, and 2060.1 kN for Towers 1–4 respectively, and were more than the design loads. The static load tests were performed to meet ASTM 1143 (2020) using Procedure A: Quick Test. Results are shown in Figure A5 in the form of load-settlement curves. Pile failure load was found using Davisson's method and the allowable load was found using a factor of safety of 2.0. The tabular results of the static load tests for Towers 1–4 are shown in Table A7. The stated allowable structural settlements from the foundation reports (Table A1, Ref #1–4) were stated to be 25 mm total and 12.5 mm differential settlement. The results shown in Table A7 and Figure A5 show that the settlements at the maximum loads are well below the differential settlement threshold, which indicates that the pile foundations have sufficient capacity to carry the design structural loads without excessive foundation settlement.

Figure A5. Load settlement curves from static load tests: A. Tower 1, B. Tower 2, C. Tower 3, and D. Tower 4.

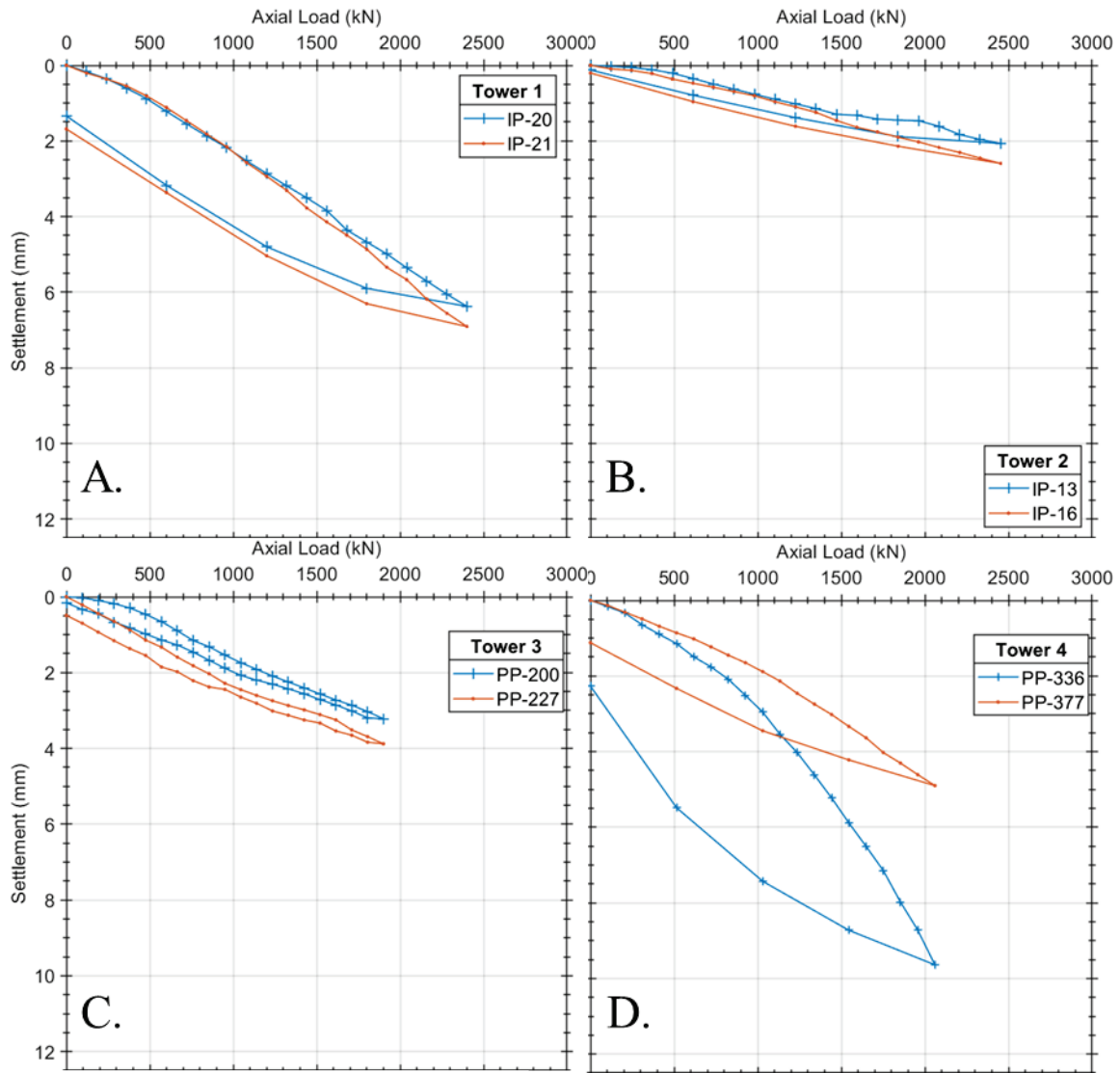


Table A7. Results of static load tests for Towers 1-4.

Structure	Pile #	Pile Size (diameter, mm)	Pile Penetration Depth (m)	Δt (days)	SLT Max. Load (kN)	Settlement @ Max. Load (mm)	FS	Design Load (kN)	Final Allowable Capacity (kN)
Tower 1	IP-20	500	18.7	9	2400	6.9	2.0	1150	1200
	IP-21		18.7	10	2400	6.9		1150	1200
Tower 2	IP-13		6.6	15	2453	2.1		1226	1200
	IP-16		6.7	14	2453	2.6		1226	1200
Tower 3	PP-200		21.7	19	1900	3.2		950	950
	PP-227		21.6	19	1900	3.9		950	950
Tower 4	PP-336		10.3	19	2060	9.6		1003	1031
	PP-377		10.2	20	2060	4.9		1003	1031

Summary and conclusions

On-site investigations did not reveal any signs of foundational distress or crack patterns associated with excessive settlement. Performing a design review after construction has taken place affords the reviewer the luxury of not only reviewing the design but also construction and post-construction inspection data. During design most of this information is not available unless similar construction was performed in the near vicinity. In this case for Towers 2 to 4 additional data were available and the design was improved upon from tower 1. Reports were more detailed and data collection was improved. Overall, the foundation design for these towers and parking structures proved to be conservative. With that said, a few comments are appropriate; these are provided such that future designs can be improved.

- Borings should have been conducted below the weathered zone or a minimum of 6 m from the anticipated pile tip.
- Unconfined compression testing should have been conducted for each of the towers. It was only conducted for Tower 4. This would have allowed for a good check of the PLT and allowed for better calibration at the lower UC strengths (as recommended in Goodman 1989).

- Better quality assurance of design calculations, as discrepancies were found in the design calculations for Towers 1 and 2. Fortunately this error had little impact on the design due to *in situ* testing.
- It was through good QA and design recommendations that the construction of these pile foundations resulted in an adequate foundation.

Team conclusions from this review are that the foundations for the Camp Walker Family Housing Towers and associated parking structures were conservative. Through the review and inspection, the cracking identified in the concrete is not due to poor foundation performance.

Appendix B: Additional Pictures from Visual Inspection of Towers and Parking Garages

Tower 1 Photos

Figure B1. Cracking in walls of Tower 1.

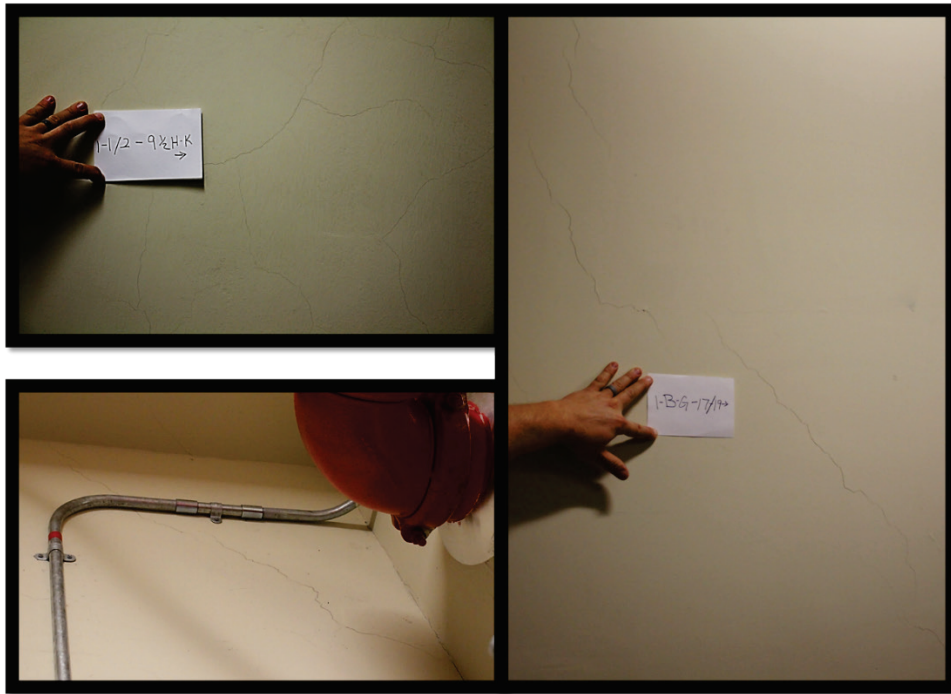


Figure B2. Honeycombing and cold joint in cored shaft of Tower 1.



Figure B3. Cracking in mapped wall of elevator mechanical room in Tower 1.



Figure B4. Cracking in concrete and cementitious coating in wall of Tower 1.



Figure B5. Rebound hammer test locations in Tower 1—Basement through Floor 3.



Figure B6. Rebound hammer test locations in Tower 1—Floor 4.



Figure B7. Rebound hammer test locations in Tower 1—Floor 5.



Figure B8. Rebound hammer test locations in Tower 1—Floors 6 through 9.



Figure B9. Rebound hammer test locations in Tower 1—Floors 10 through 13.

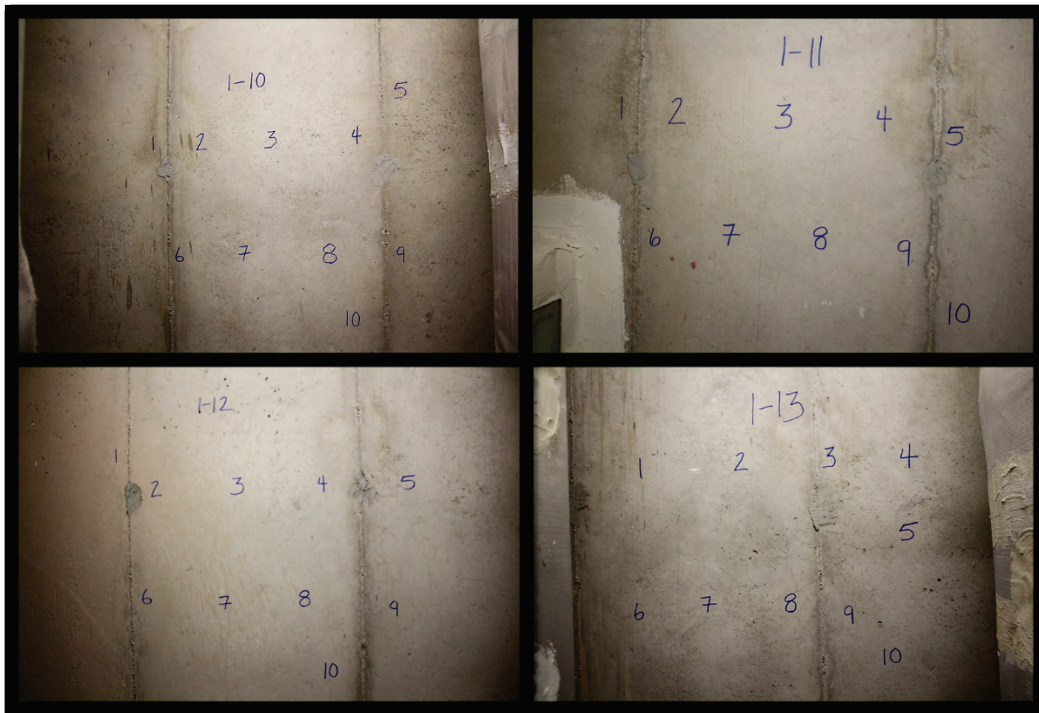


Figure B10. Rebound hammer test locations in Tower 1—Floors 14 and 15.

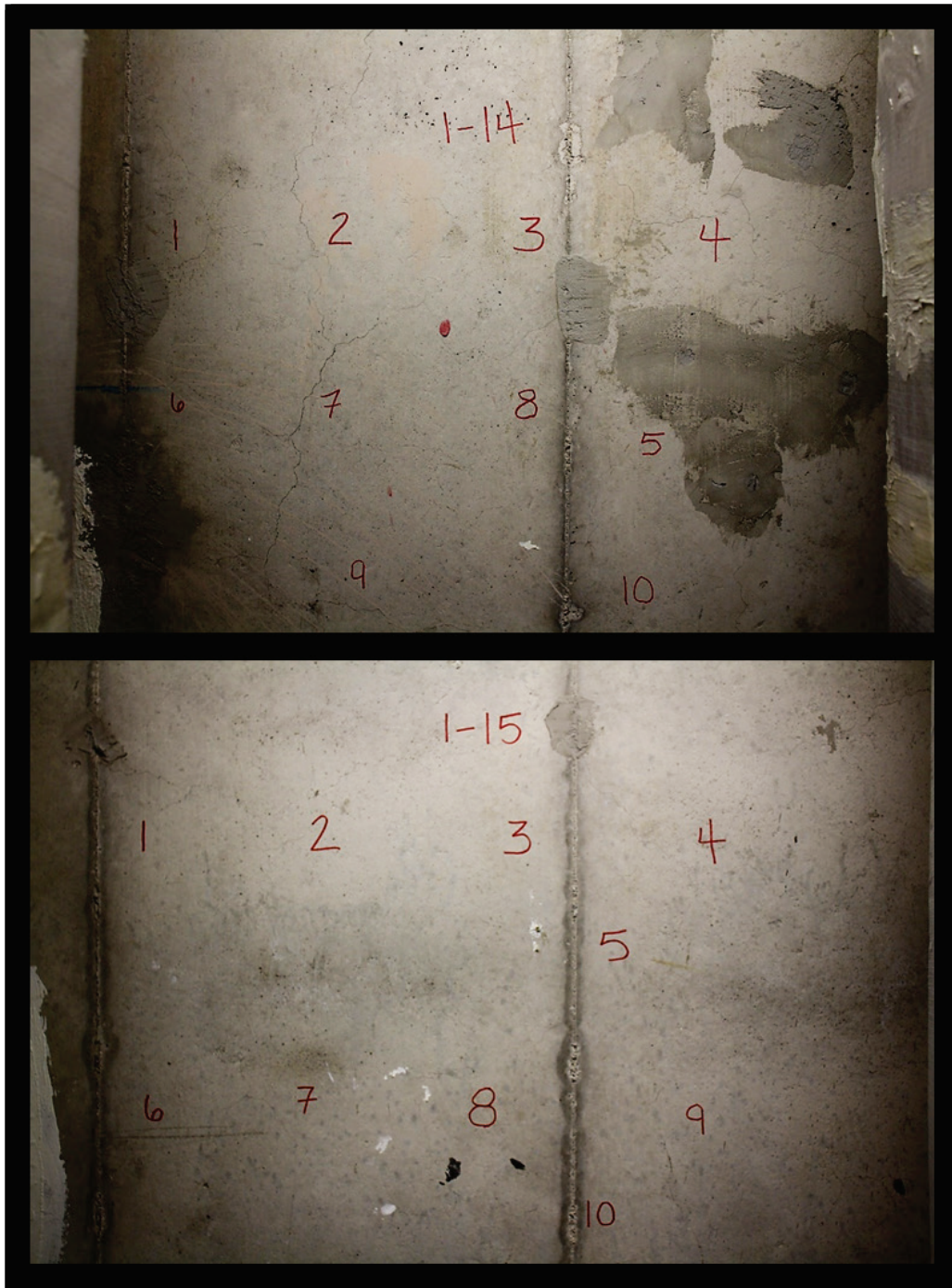


Figure B11. Coring activities in Tower 1.



Tower 2 Photos

Figure B12. Wall cracks with gauges in Tower 2 basement.

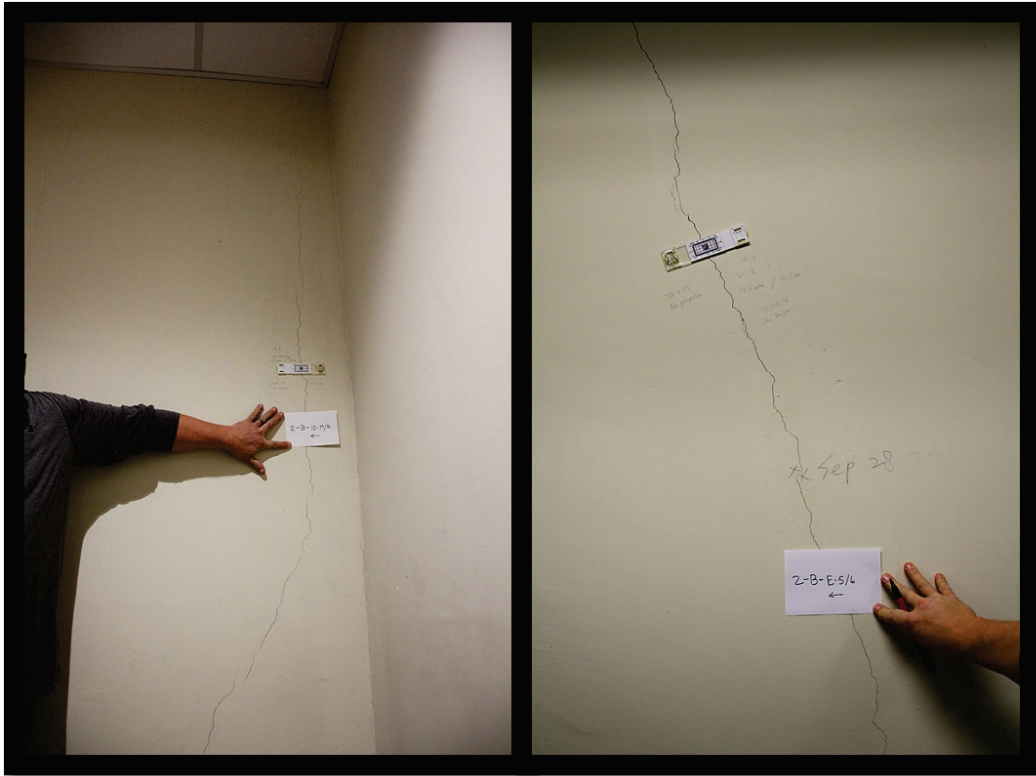


Figure B13. Wall crack with gauge in Tower 2 basement.



Figure B14. Wall cracks with gauges in Tower 2 basement.

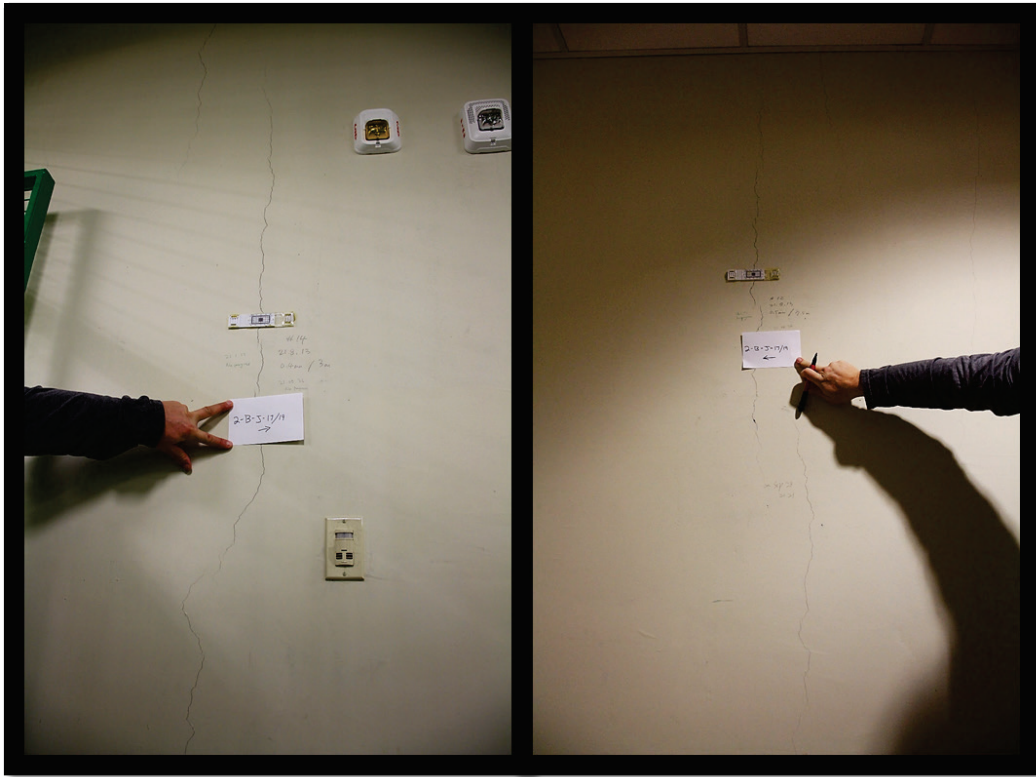


Figure B15. Wall cracks with gauges in Tower 2 basement.



Figure B16. Wall cracks with gauges in Tower 2 basement.

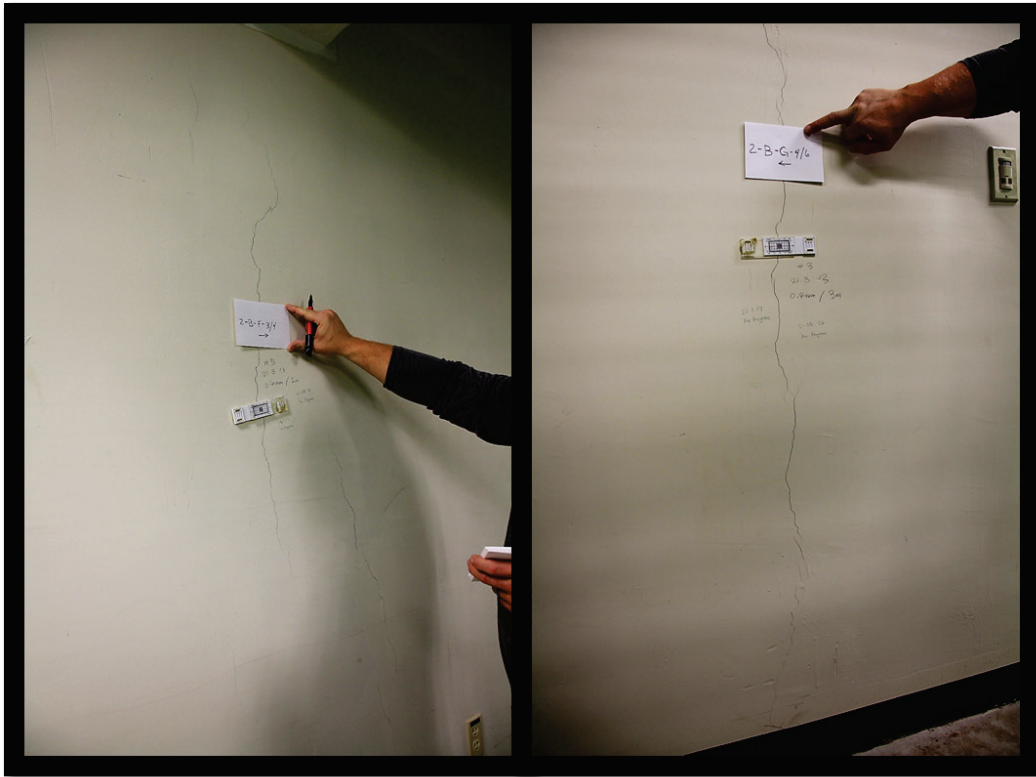


Figure B17. Wall crack with gauge in Tower 2 basement.

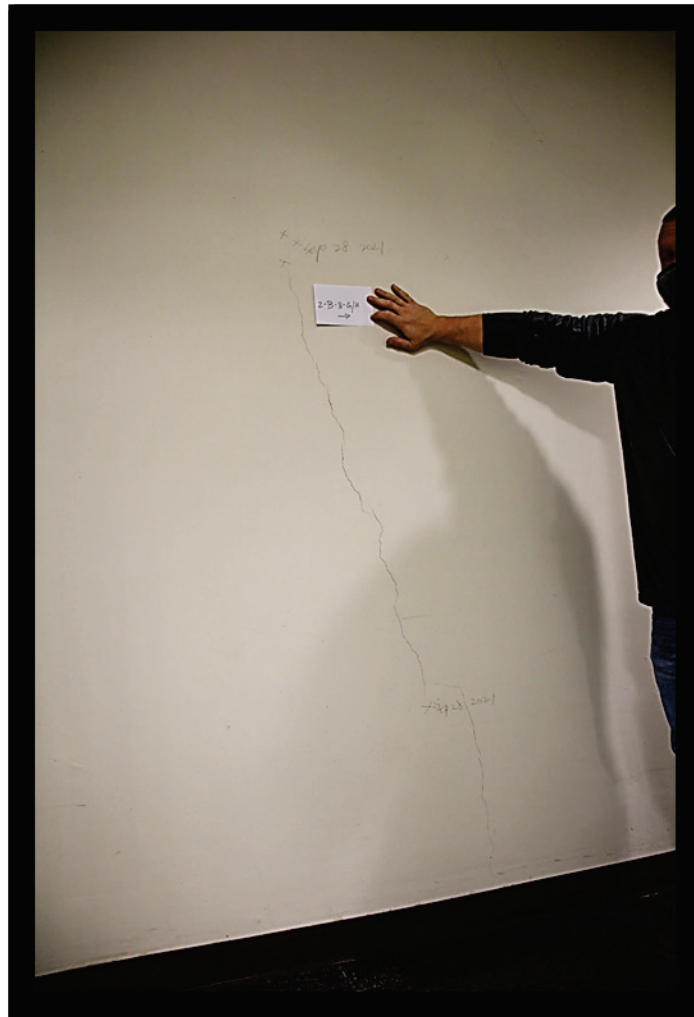


Figure B18. Sealed cracks in Tower 2 basement.



Figure B19. Mapped diagonal cracks in basement storage area of Tower 2.



Figure B20. Vertical and horizontal cracks in stairwell wall of Tower 2.



Figure B21. Cracks in basement mechanical room of Tower 2.



Figure B22. Wall cracks in shaft behind elevators in Tower 2.

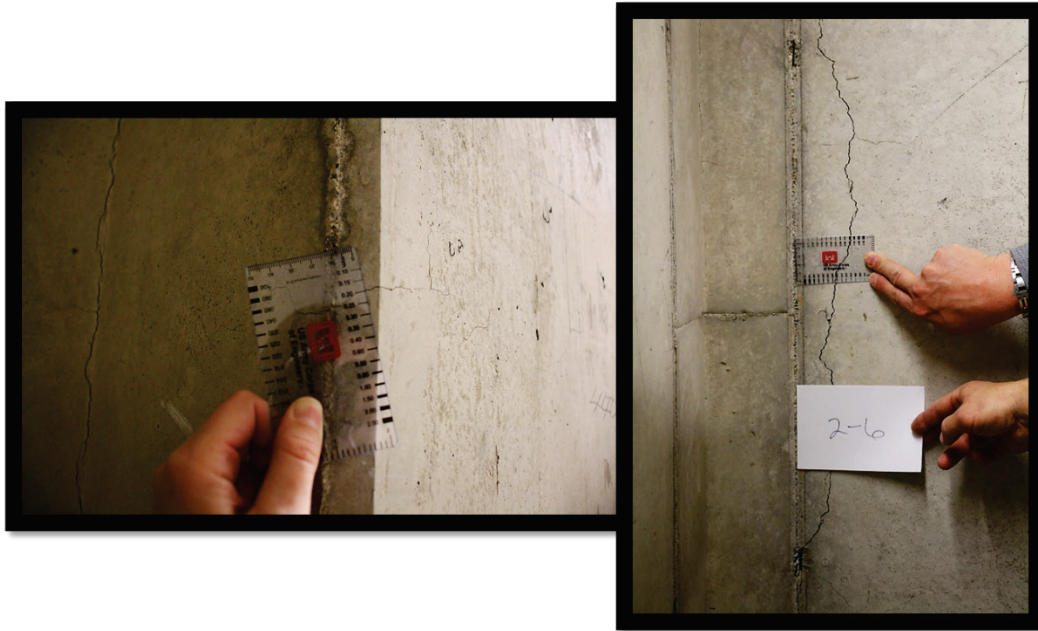


Figure B23. Cold joints in shafts behind elevators in Tower 2.



Figure B24. Embedded rebar support (top left) and honeycombing and poor consolidation in shafts behind elevators in Tower 2.



Figure B25. Mapped wall cracks (top) and floor slab shrinkage cracks in elevator mechanical room in Tower 2.

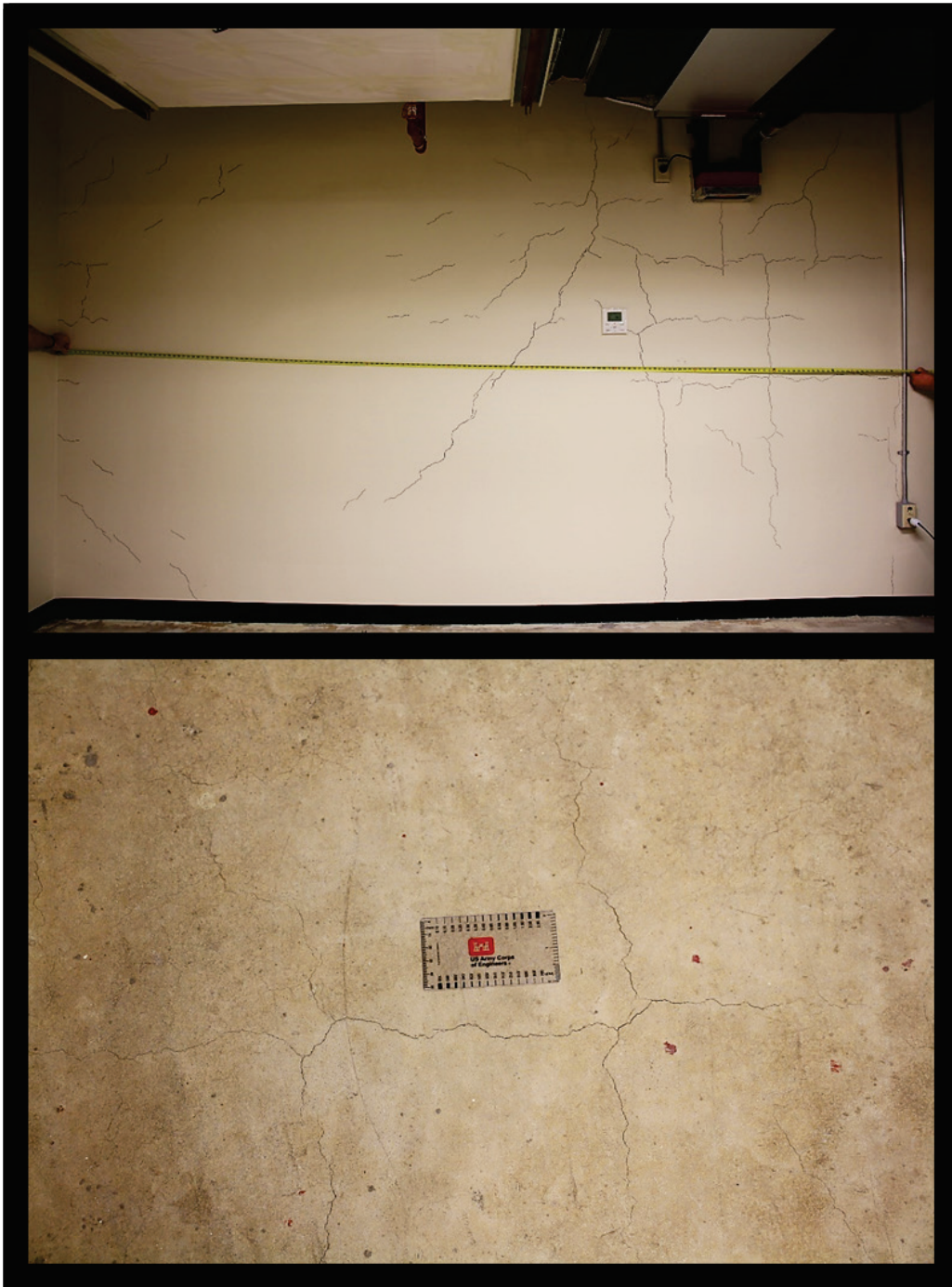


Figure B26. Diagonal cold joint in wall of attic in Tower 2.



Figure B27. Rebound hammer test locations in Tower 2—Basement through Floor 3.



Figure B28. Rebound hammer test locations in Tower 2—Floors 4, 5, and 7.



Figure B29. Rebound hammer test locations in Tower 2—Floors 8, 9, and 10.



Figure B30. Rebound hammer test locations in Tower 2—Floors 12 through 15.



Tower 3 Photos

Figure B31. Vertical and horizontal cracks in basement wall of Tower 3.



Figure B32. Diagonal cracks in basement walls of Tower 3.

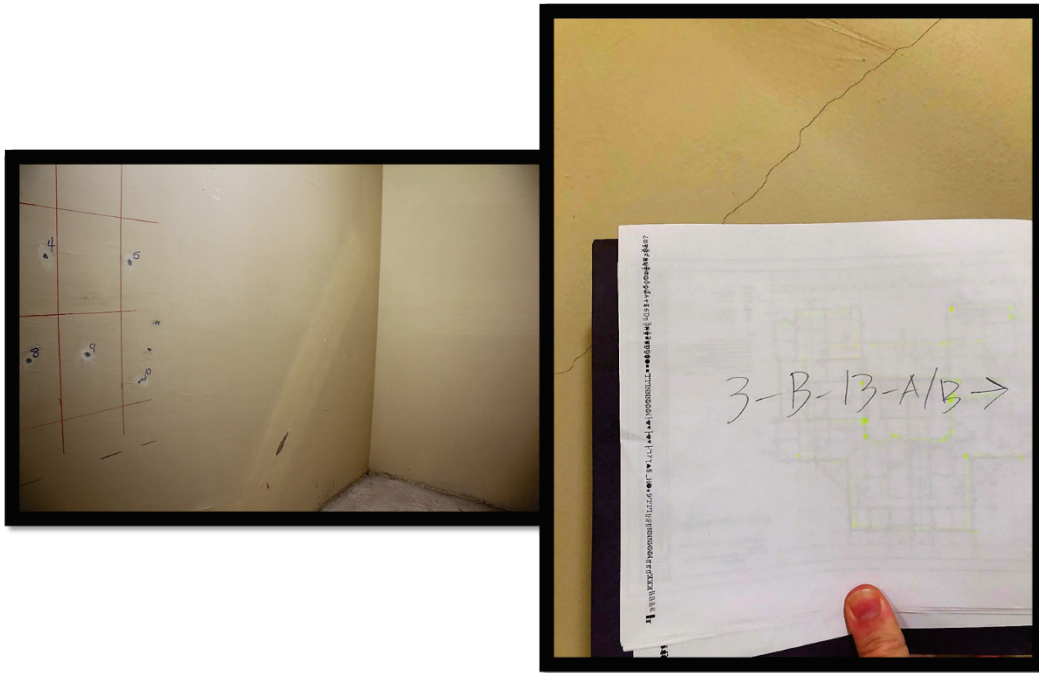


Figure B33. Cold joints in walls of shaft behind the elevators in Tower 3.



Figure B34. Rebound hammer test locations in Tower 3—Basement through Floor 3.



Figure B35. Rebound hammer test locations in Tower 3—Floors 5, 6, and 7.



Figure B36. Rebound hammer test locations in Tower 3—Floors 8 through 11.



Figure B37. Rebound hammer test locations in Tower 3—Floors 12, 14, and 15.



Figure B38. Coring activities in basement of Tower 3.



Tower 4 Photos

Figure B39. Diagonal cracks in basement walls of Tower 4.



Figure B40. Diagonal cracks in basement walls of Tower 4.



Figure B41. Cracks in walls of Tower 4.



Figure B42. Cold joints in walls of Tower 4.



Figure B43. Poor consolidation at balconies of Tower 4.



Figure B44. Nonuniformity (top) and staining (bottom) of concrete in Tower 4.



Figure B45. Rebound hammer test locations in Tower 4—Basement through Floor 3.



Figure B46. Rebound hammer test locations in Tower 4—Floors 4 through 7.

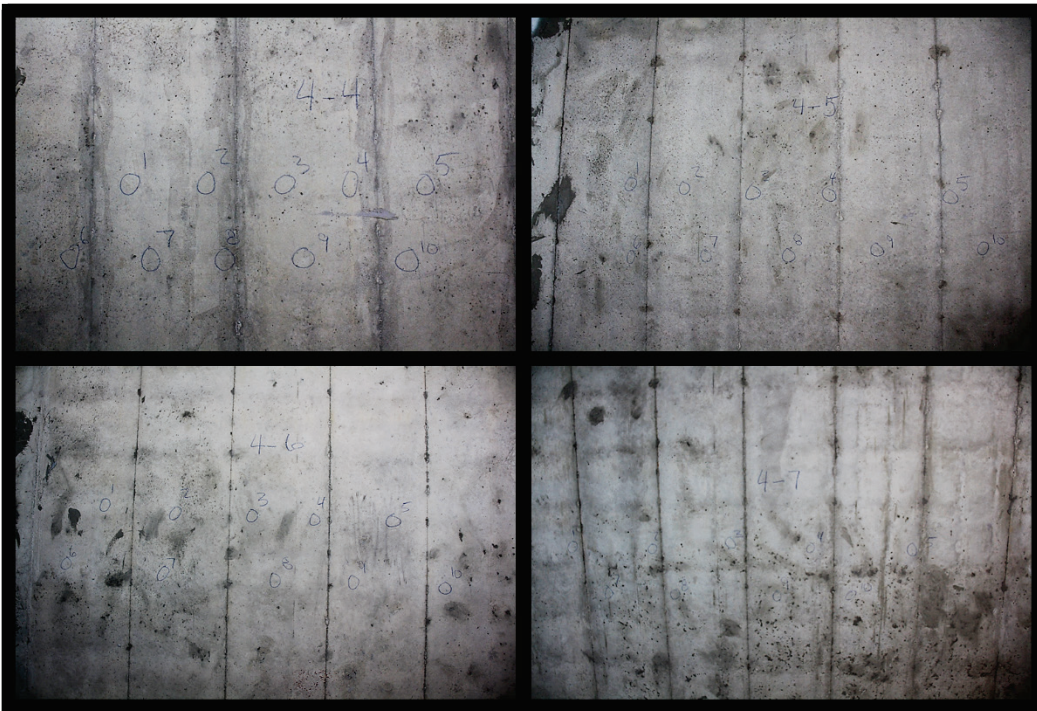


Figure B47. Rebound hammer test locations in Tower 4—Floors 8 through 11.



Figure B48. Rebound hammer test locations in Tower 4—Floors 12 through 14.



Figure B49. Wall reinforcement of Floor 15 in Tower 4.



Figure B50. Reinforcement on Floor 15 of Tower 4.



Parking Garage 1 Photos

Figure B51. Diagonal cracks in girders and beams in Parking Garage 1.

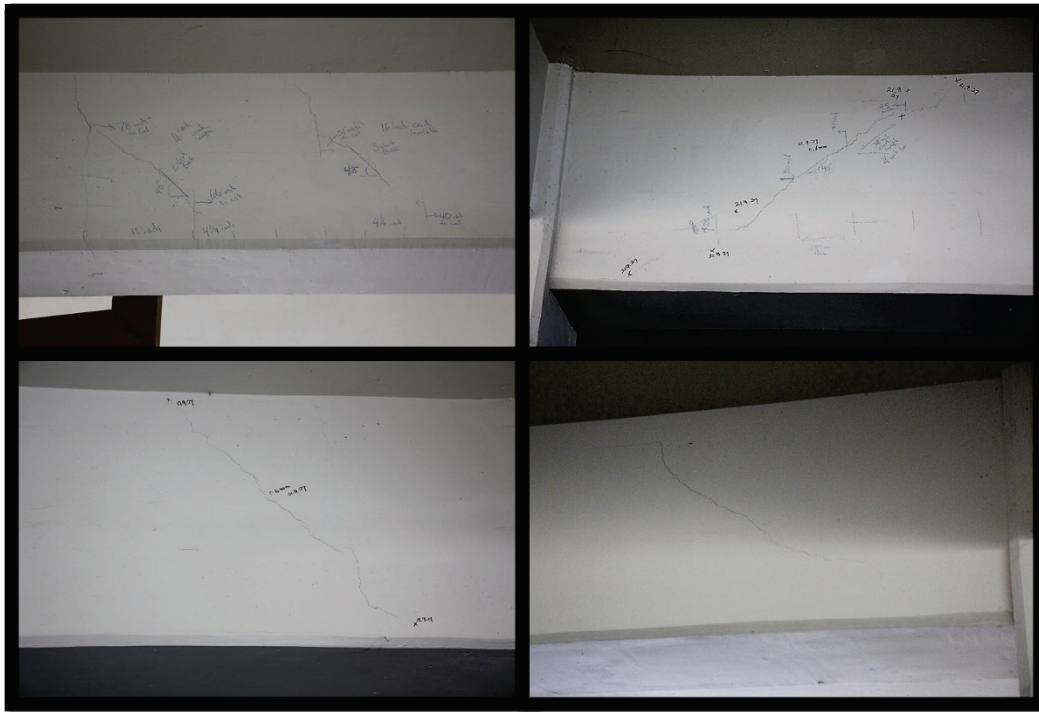


Figure B52. Diagonal cracks in girders in Parking Garage 1.

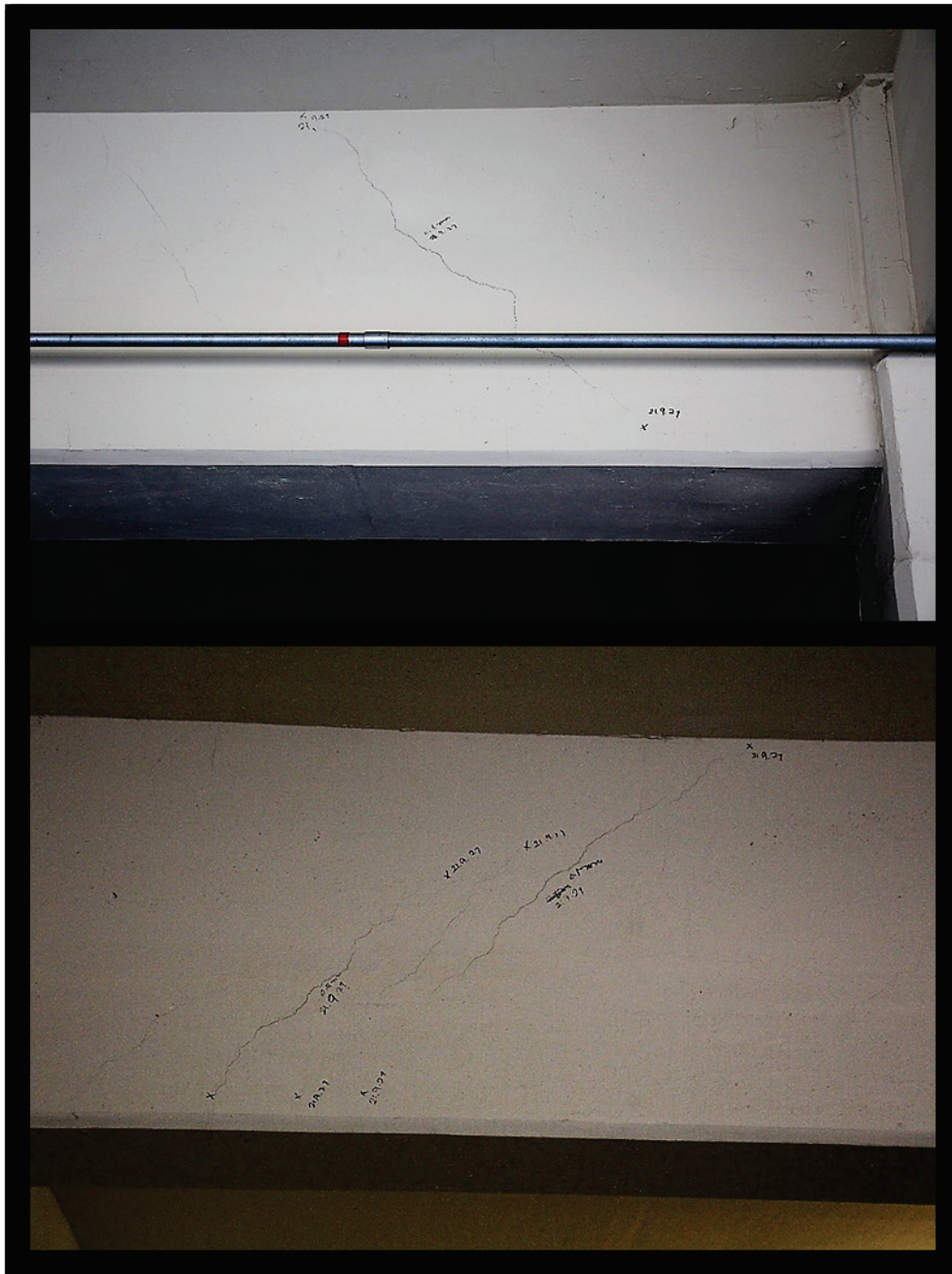


Figure B53. Diagonal cracks in walls in Parking Garage 1.



Figure B54. Cracks in ceiling, beams, and wall of entrance to basement of Parking Garage 1.



Figure B55. Mapped cracks in beam along column line 4 in Parking Garage 1.



Figure B56. Mapped cracks in girder along column line E in Parking Garage 1.

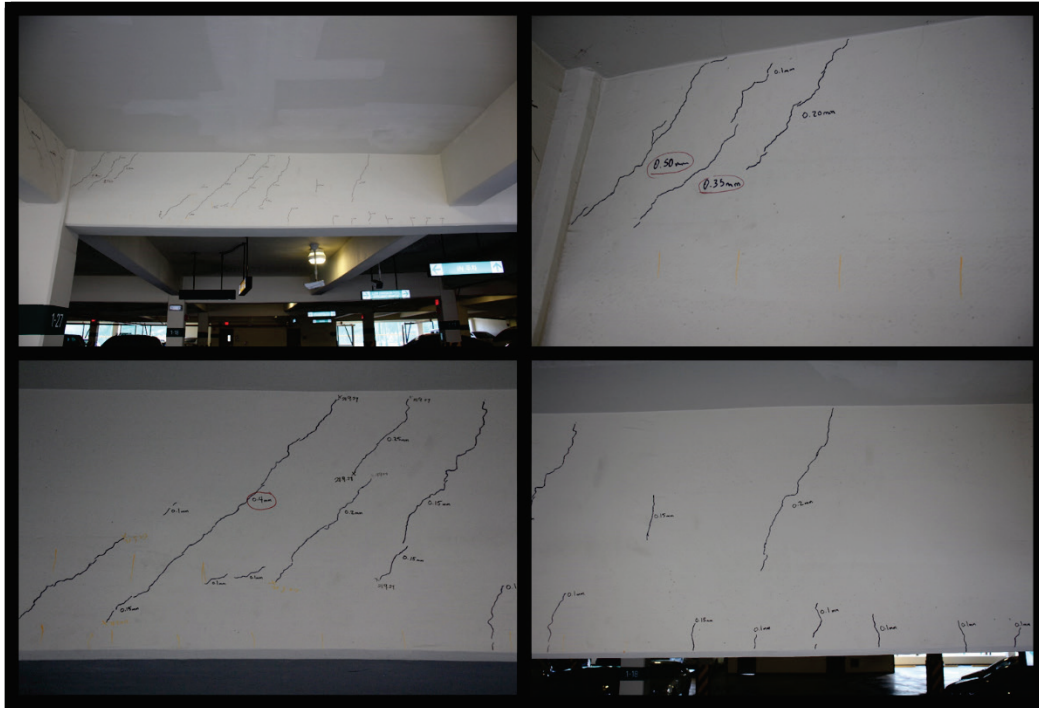


Figure B57. Removal of paint and top coating from girder and beam in Parking Garage 1. The girder is in line with column E, and the beam is in line with column 4 of the floor plan.

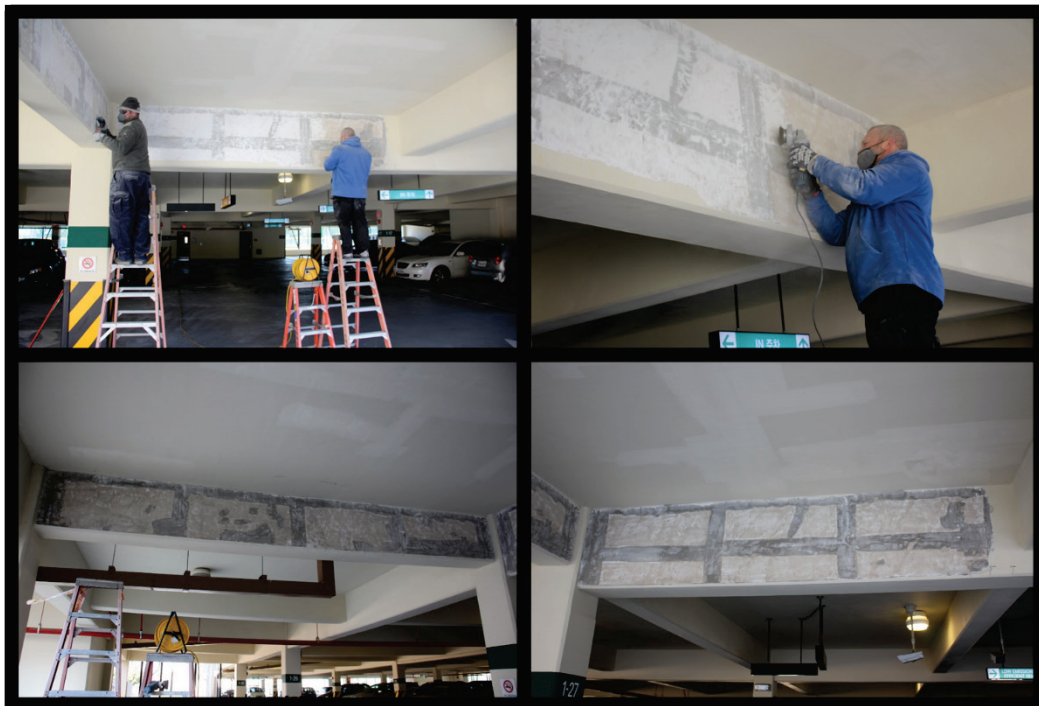


Figure B58. Cracks in bare concrete of beam along column line 4 in Parking Garage 1.

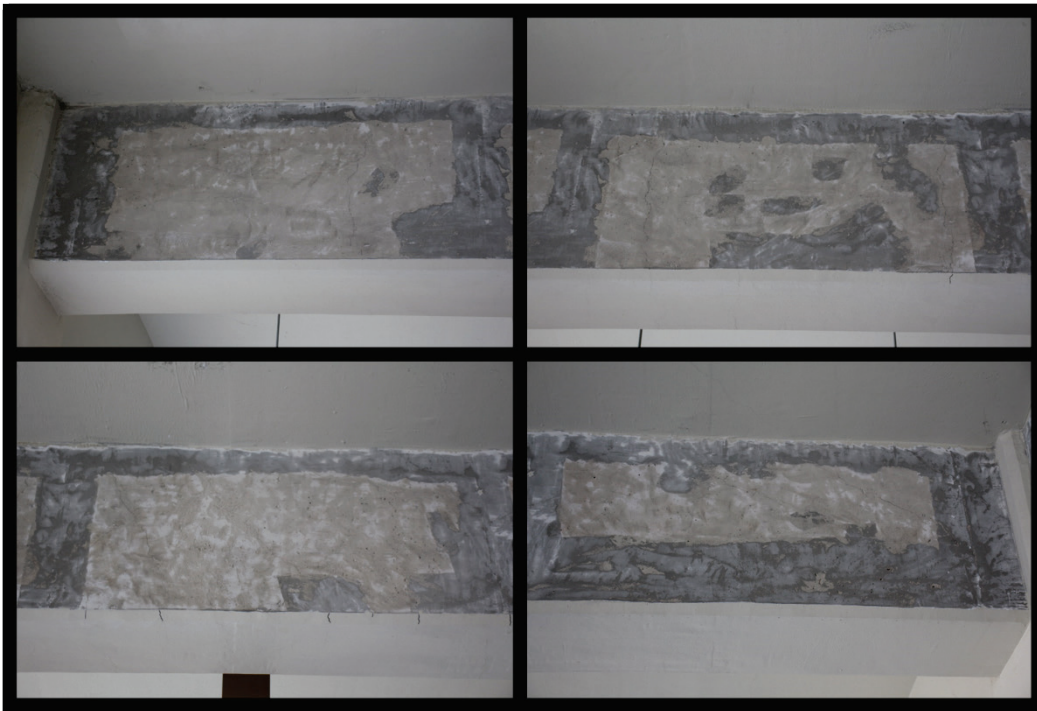


Figure B59. Cracks in bare concrete of girder along column line E in Parking Garage 1.

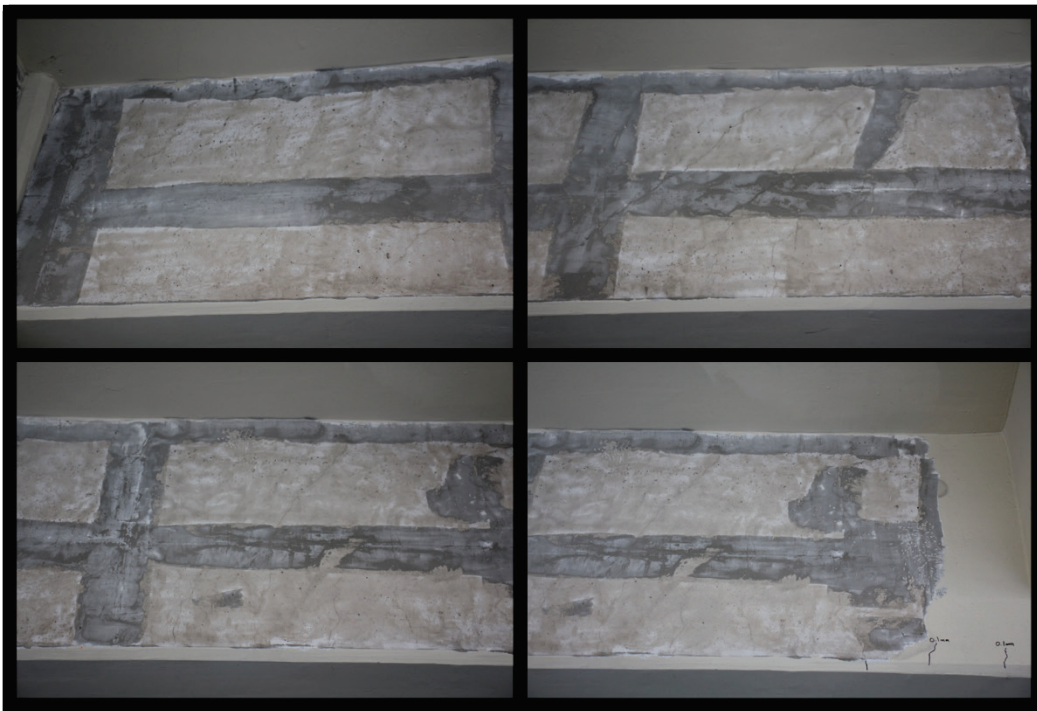


Figure B60. Mapped cracks in bare concrete of beam along column line 4 in Parking Garage 1.



Figure B61. Mapped cracks in bare concrete of girder along column line E in Parking Garage 1.



Parking Garage 2 Photos

Figure B62. Multidirectional cracks in ceiling and cracks in girder of entryway of Parking Garage 2.



Figure B63. Diagonal cracks in girders and beams in Parking Garage 2.



Figure B64. Diagonal cracks in girders and beams in Parking Garage 2.



Parking Garage 3 Photos

Figure B65. Vertical cracks manifest in surface architectural coating on exterior of Parking Garage 3.



Figure B66. Diagonal crack in wall of stairwell in Parking Garage 3.



Parking Garage 4 Photos

Figure B67. Shoring for girders and beams throughout Parking Garage 4.



Figure B68. Cold joints in walls in Parking Garage 4.



Figure B69. Cracks with gauges and bugholes in walls in Parking Garage 4.



Figure B70. Vertical cracks in beam in Parking Garage 4.



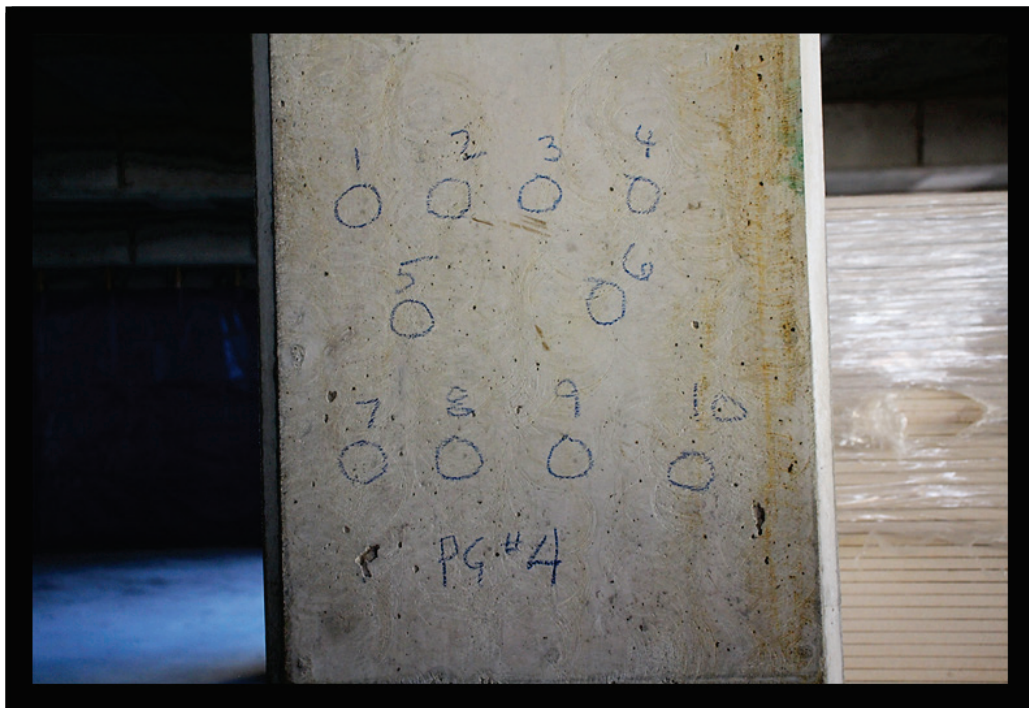
Figure B71. Vertical crack in wall in Parking Garage 4.



Figure B72. Cracks in exterior column and connected girder in Parking Garage 4.



Figure B73. Rebound hammer test location in column in Parking Garage 4.



Appendix C: Petrographic Analysis of Cores from Camp Walker, South Korea*

* Authored by Kyle L. Klaus, Cody M. Strack, Stephanie G. Wood, Jason A. Morson, C. Kennan Crane, and Robert D. Moser

Abstract

The Concrete and Materials Branch (CMB) of the Geotechnical and Structures Laboratory was requested to perform an analysis on concrete cores collected from the Camp Walker Army Family Housing Complex to determine the cause of structural cracking observed in service at relatively young age (1–3 yr from completion of construction). Five cores were extracted on site and delivered to the Engineer Research and Development Center for laboratory study. The samples were subjected to investigative procedures that included petrographic analysis (ASTM C856), modified point count analysis for evaluation of the air-void system (ASTM C457), and scanning electron microscopy (ASTM C1723). The concrete generally appeared to be similar in composition and proportions as what was noted in the approved mixture proportions for the project. The concrete is an air-entrained, straight portland cement concrete with no use of supplementary cementitious materials. The coarse aggregate varied from 25 to 19 mm in maximum size. The concrete samples exhibited no signs of internal disruption of the coarse and fine aggregate portions nor were other features associated with ASR expansion or freeze-thaw distress detected. Segregation of the coarse aggregate was observed in cores T1-1, T1-2, and T-3 causing potential durability issues and related cracking. The concrete appeared to be severely segregated with large variations in composition across cold joints, cracks, and likely interruptions in concrete placements. These variations may locally increase the paste content and propensity for shrinkage. The cracking observed appears to be caused by shrinkage, specifically drying shrinkage. This conclusion is made due to the observation that in many cases cracks extend through coarse aggregate, an indicator that cracking occurred at later ages following removal of formwork when concrete had gained sufficient strength to cause cracking to extend through aggregates.

Scope

The Concrete and Materials Branch (CMB), Geotechnical and Structures Laboratory (GSL), U.S. Army Engineer Research and Development Center (ERDC), was requested by the U.S. Army Corps of Engineers Far East District (USACE-POF) to perform an analysis of concrete core samples from structures exhibiting varying levels of deterioration and cracking located at Camp Walker in South Korea. Five cores were extracted on Towers 1–3 for analysis, delivered to CMB, and checked in under CMB Serial Numbers 220053-1 through 220053-3, 220054, 220055 (see Table C1).

The following sections provide an explanation of the methods utilized, results obtained, and a summary and recommendations regarding potential improvements on the site investigated.

Table C1. Summary of locations investigated, year constructed, corresponding CMB Serial No, and tests performed. T1, T2, and T3 sample identifiers correspond to Towers 1, 2, and 3, respectively.

Section ID	Core #	CMB Serial No.	Tests Performed
T1-S-1	1	220053-1	ASTM C856, SEM/EDS
T1-S-2	2	220053-2	ASTM C856, SEM/EDS
T1-3	3	220053-3	ASTM C856, ASTM C457, SEM/EDS
T2-3	4	220054	ASTM C856, ASTM C457, SEM/EDS
T3-3	5	220055	ASTM C856, ASTM C457, SEM/EDS

Methods

The methods below are those employed by this study to verify the quality of the concrete sampled from Camp Walker Army Family Housing Complex. They included standard petrographic analysis, air void analysis, and electron microscopy. The cores were set in hydrostone before further analysis to preserve their structure during cutting and polishing.

Petrographic analysis (ASTM C856)

First, visual examinations assessed modes of distress, such as physical distress and dimensional stability, of the as-received cores. Second, the polished cores were subject to petrographic analysis according to ASTM C856, *Standard Practice for Petrographic Examination of Hardened Concrete*. The cores were prepared for the petrographic analysis by bisection longitudinally through the length of the core. The section was polished using diamond-encrusted polishing pads for petrographic analysis. An overall image was obtained for the sample at low magnification using a flat-bed scanner, and at least three selected sites were also imaged at higher magnification with a stereomicroscope. The top section of the bisected cores was analyzed using a Zeiss Stereo Discovery V20 microscope at magnifications of 5X to 50X. Specific focus was given to microcracking, air void structure, aggregate deterioration, and any other possible modes of concrete deterioration.

Air void analysis (ASTM C457)

Air void content was determined according to the provisions outlined in ASTM C457—*Standard Test Method for Microscopical Determination of Parameters of the Air-Void System in Hardened Concrete*. Along with characterizing the hardened air void structure, additional information was gathered through point counting on the paste, aggregate, and other observed defects. The test method has multiple procedures. Procedure B, Modified Point-Count Method, was used for this study. Samples were cut and polished cross sections prepared according to ASTM C856—*Standard Practice for Petrographic Examination of Hardened Concrete*. The minimum length of traverse and minimum number of points for the point count method was determined based on the maximum size of aggregate found in each sample. Calculations for air content were determined on the total number of air voids (N), total number of stops (S_t), number of stops in air voids (S_a), number of stops on paste (S_p), and the E-W translation distance between stops (I). Results are reported as a percentage of total stops.

Scanning electron microscopy examination (ASTM C1723)

Specimens were examined from each sample using scanning electron microscopy (SEM) to obtain high-resolution images and examine the paste microstructure according to ASTM C1723—*Standard Guide for Examination of Hardened Concrete Using Scanning Electron Microscopy*. Fifteen-mm-diam cores were taken from each sample, mounted in epoxy, and polished to 0.3 μm in a 50:50 ethanol and ethylene glycol mixture prior to imaging. SEM imaging was performed using an FEI Nova NanoSEM 630, capable of high-resolution imaging on nonconductive materials. Imaging was performed in low-vacuum mode at pressures of 0.1–0.5 mbar and accelerating voltage of 15k V. All images were acquired using a backscattered electron detector to improve phase contrast. Imaging was performed at multiple random sites and at various levels of magnification to capture the overall microstructure along with specific regions of interest (e.g., aggregate interfaces, cracks, air voids).

Results and discussion

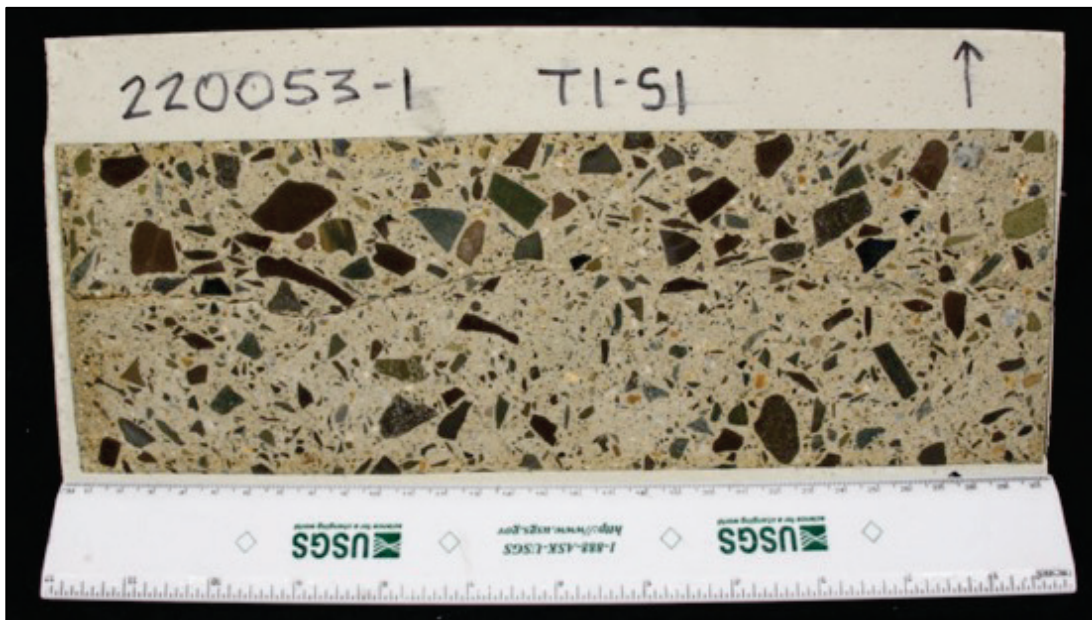
Tower 1, Shaft 1

The as-received core from Korea is shown in Figure C1 with the bisected half shown in Figure C2. The following provides a synopsis of the physical and durability related properties resulting from analysis of Tower 1, Shaft 1 (T1-S1) (CMB# 220053-1).

Figure C1. As-received core T1-S1.



Figure C2. Photo of bisected core T1-S1.



Petrographic analysis

A scanned image from a polished section of the top 4 in. of the core is provided in Figure C3. Detailed photomicrographs of the core's microstructure are shown in Figure C4. The core was 12 in. in length, approximately 4.0 in. in diameter, and was placed horizontally across a cold joint in the wall.

Examination of the core presented one crack on the core surface that extended with depth over the entire length of the core (Figure C5). The crack varied in width from 0.25 to 2.50 mm and represented the only macrocracking present in the sample. The coarse aggregate was a crushed stone and had a maximum nominal size of 1.0 in. It consisted primarily of granitic mineralogies with some sandstone particles present. The fine aggregate was a crushed stone and a quartz sand. The coarse aggregate was not uniformly dispersed, with some areas having a low concentration of coarse aggregate. These regions were concentrated on one side of the crack. Darkened rims were observed on some coarse aggregates, indicative of a reaction between the particles and paste; however, no disruption to the concrete was associated with this feature. Internal microfractures were observed in some coarse aggregates but are likely pre-existing features. No indicators of deleterious reactions, such as alkali-silica reaction (ASR), were observed within the sample. The paste was Yellowish Gray (5Y 8/1) in color and was air entrained. Entrapped air voids up to 0.5 in. in diameter were observed, but rare.

Figure C3. Scanned image of polished sections from core T1-S1. Lettered boxes refer to locations of micrographs in Figure 4.



Figure C4. Photomicrographs of T1-S1: (a) 5.0x photomicrograph of paste microstructure; (b) 10x photomicrograph showing crack extending from surface; (c) 15x photomicrograph showing crack along a coarse aggregate with changing width; (d) 30x photomicrograph of air voids within paste.

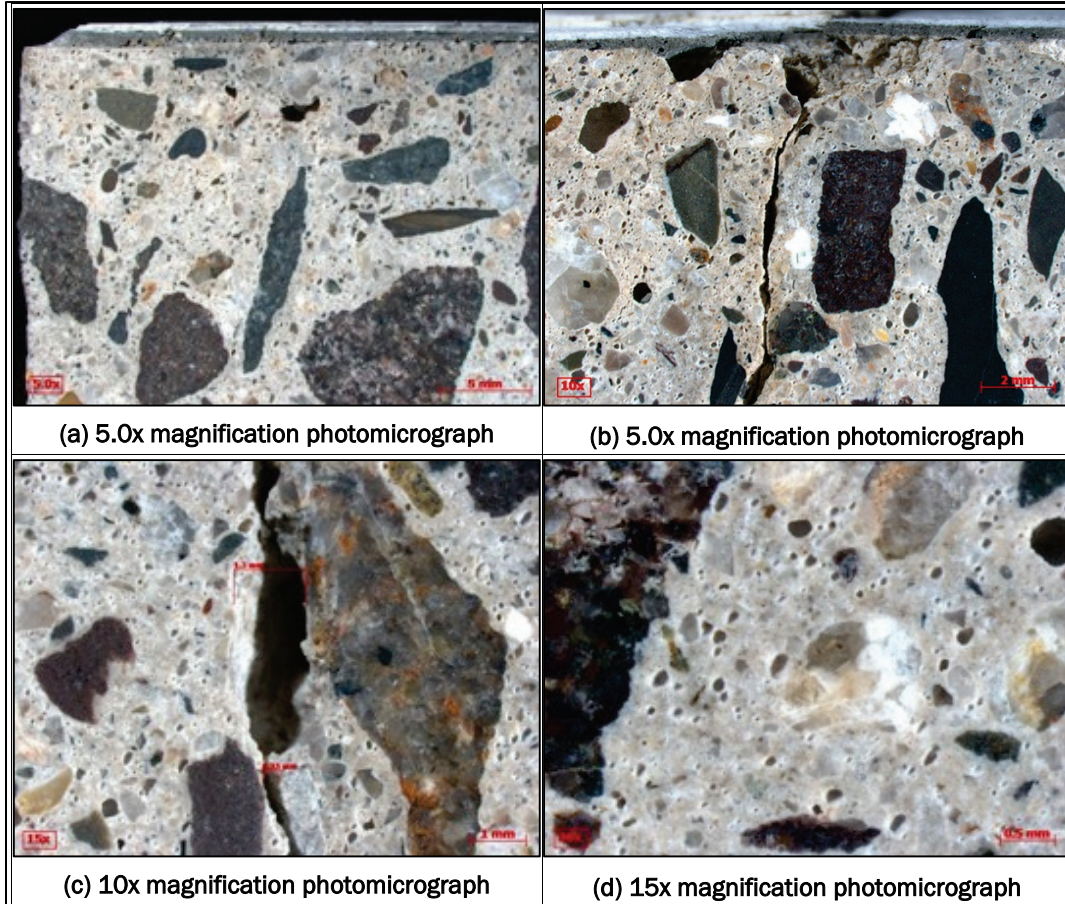
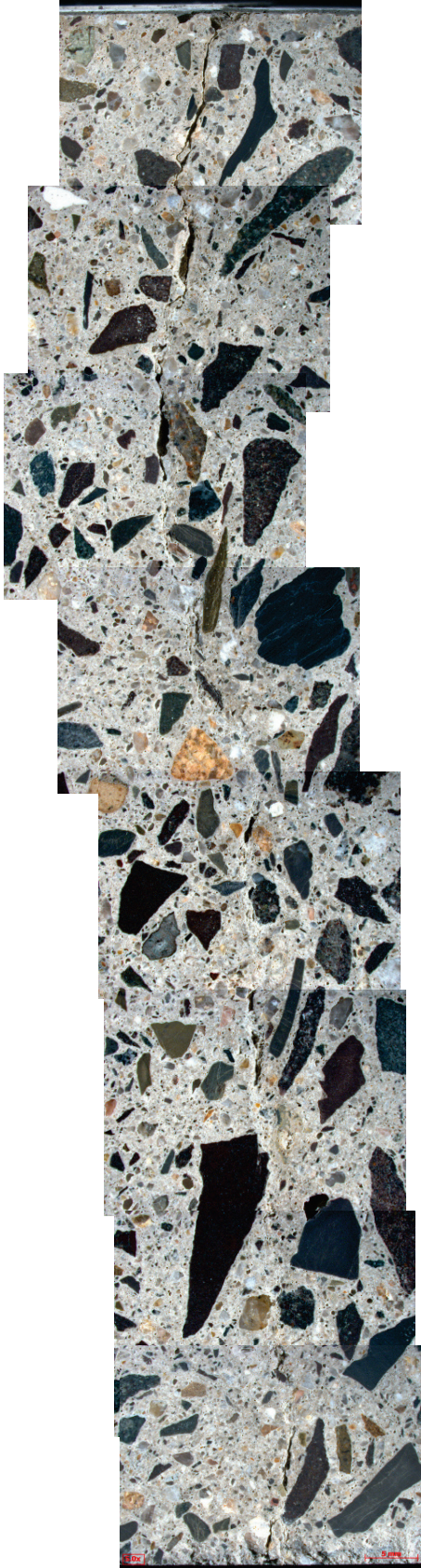


Figure C5. Map of crack observed in T1-1.



SEM analysis

Electron photomicrographs were obtained at different locations of Tower 1, Shaft 1 and are shown in Figures C6 and C7.

Figure C6. Low magnification montage electron photomicrograph of T1-S1 (200x magnification).

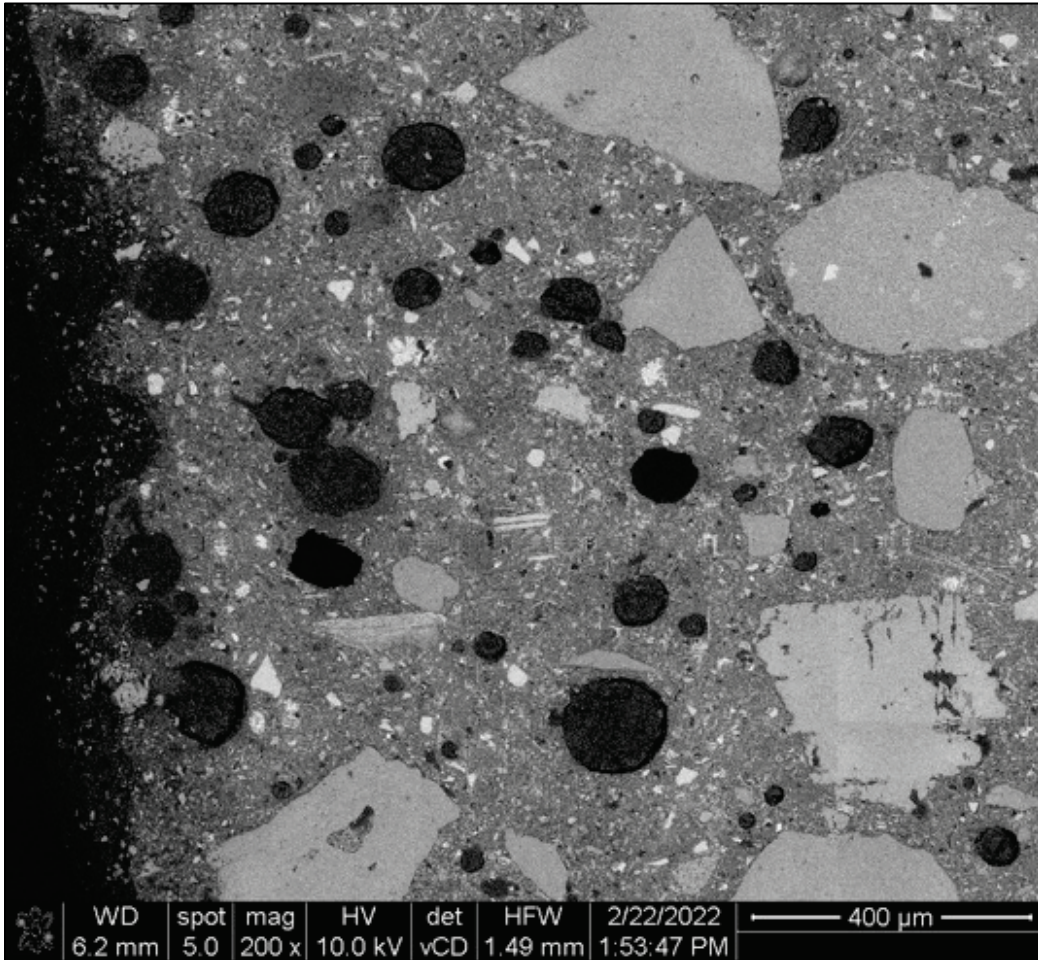
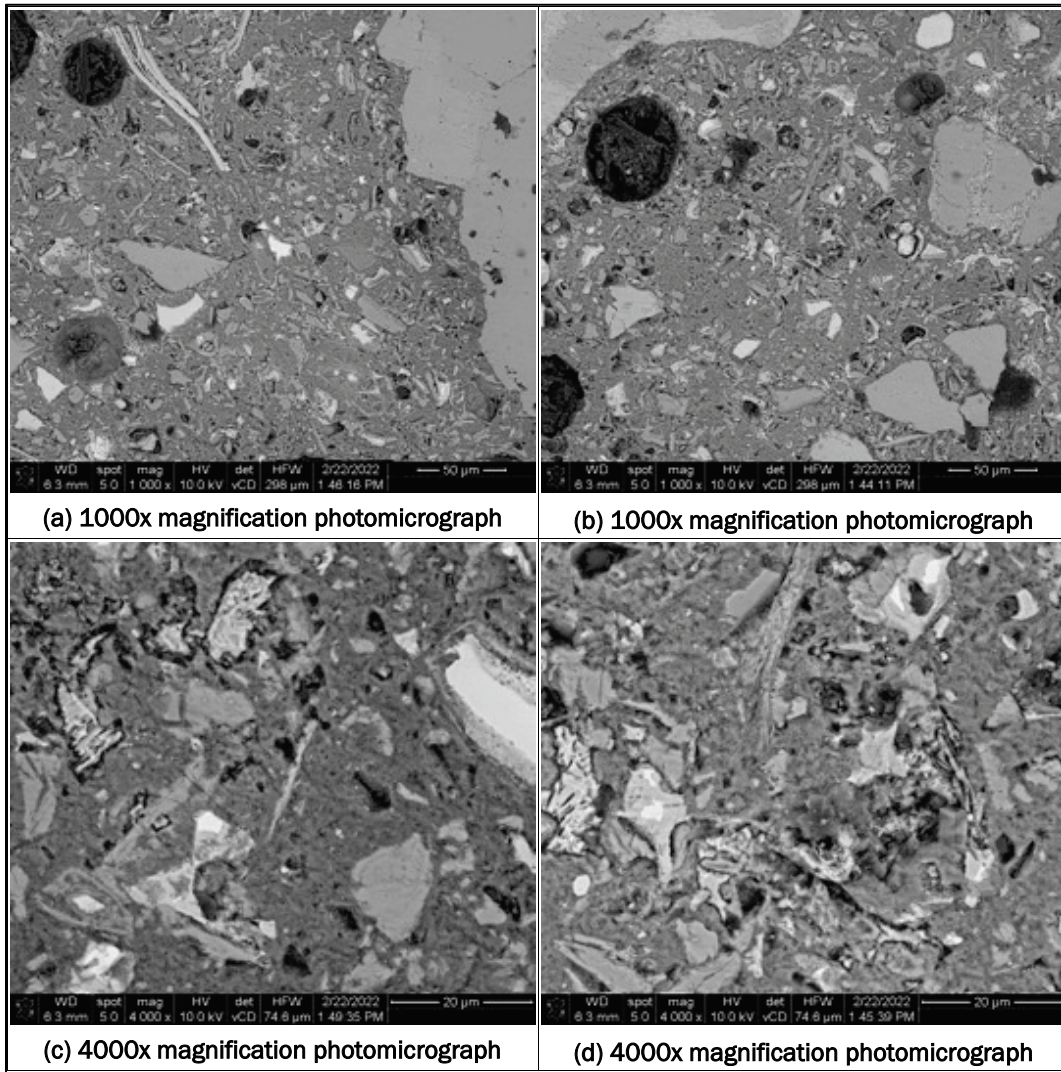


Figure C7. Electron photomicrographs of T1-S1: (a) 1000x photomicrograph of paste microstructure; (b) 1000x photomicrograph of paste; (c) 4000x photomicrograph of paste; (d) 4000x photomicrograph of paste.



Tower 1, Shaft 2

The as-received core from Korea is shown in Figure C8 with the bisected half shown in Figure C9. The following provides a synopsis of the physical and durability related properties resulting from analysis of Tower 1, Shaft 2 (T1-S2) (CMB# 220053-2).

Figure C8. As-received core T1-S2.

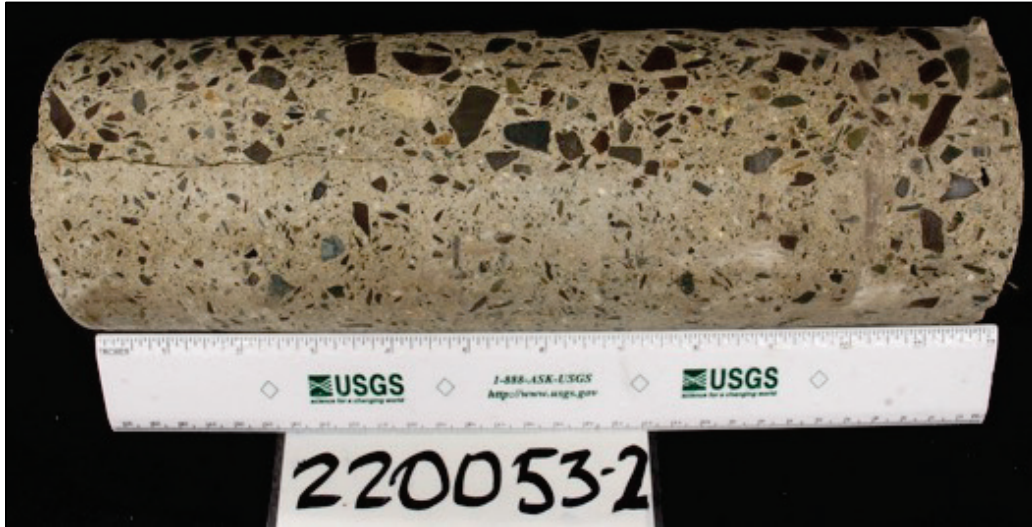
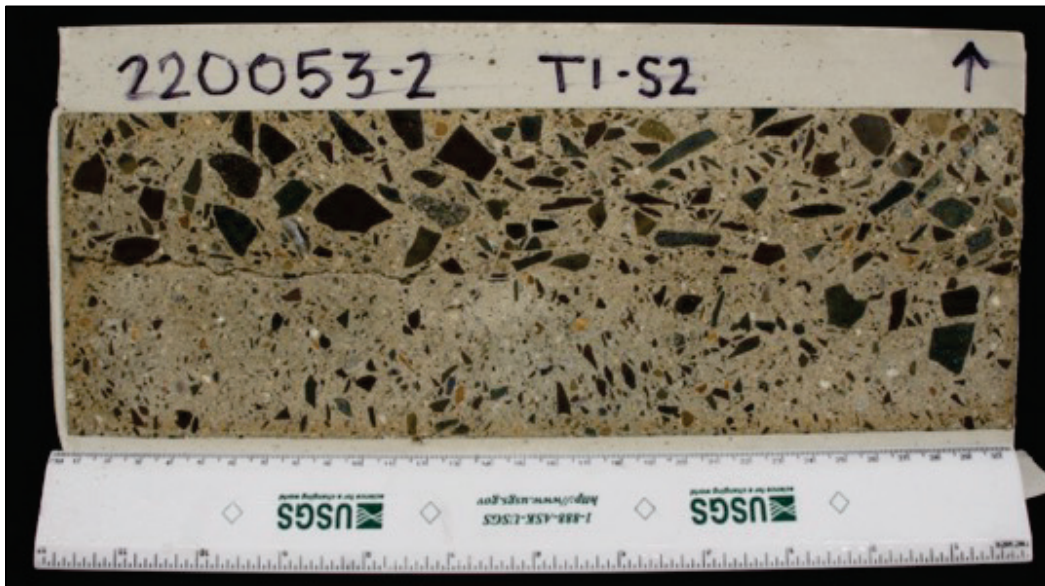


Figure C9. Photo of bisected core T1-S2.



Petrographic analysis

A scanned image from a polished section of the top 6 in. of the core is provided in Figure C10. Detailed photomicrographs of the core's microstructure are shown in Figure C11. The core was 12 in. in length and approximately 4.0 in. in diameter.

Examination of the core presented one extensive crack on the core surface that extended with depth up to 8 in. (Figure C12). The crack varied in width from 0.10 to 2.0 mm and represented the only cracking present in the sample. The coarse aggregate was a crushed stone and had a maximum nominal size of 1.0 in. It consisted primarily of granitic mineralogies with some sandstone particles present. The fine aggregate was a crushed stone and a quartz sand. The coarse aggregate was not uniformly dispersed, with some areas having a low concentration of coarse aggregate. These regions were concentrated on one side of the crack. Darkened rims were observed on some coarse aggregates, indicative of a reaction between the particles and paste; however, no disruption to the concrete was associated with this feature. Internal microfractures were observed in some coarse aggregates but are likely pre-existing features. No indicators of deleterious reactions, such as alkali-silica reaction (ASR), were observed within the sample. The paste was Yellowish Gray (5Y 8/1) in color and was air entrained. Entrapped air voids up to 0.2 in. in diameter were observed, but rare.

Figure C10. Scanned image of polished sections from core T1-S2. Lettered boxes refer to locations of micrographs in Figure C11.



Figure C11. Photomicrographs of T1-S2: (a) 5.0x photomicrograph of paste microstructure; (b) 5.0x photomicrograph of paste microstructure with clusters of voids near an entrapped void; (c) 10x magnification showing vertical cracking with varied width; (d) 15X photomicrograph of air voids.

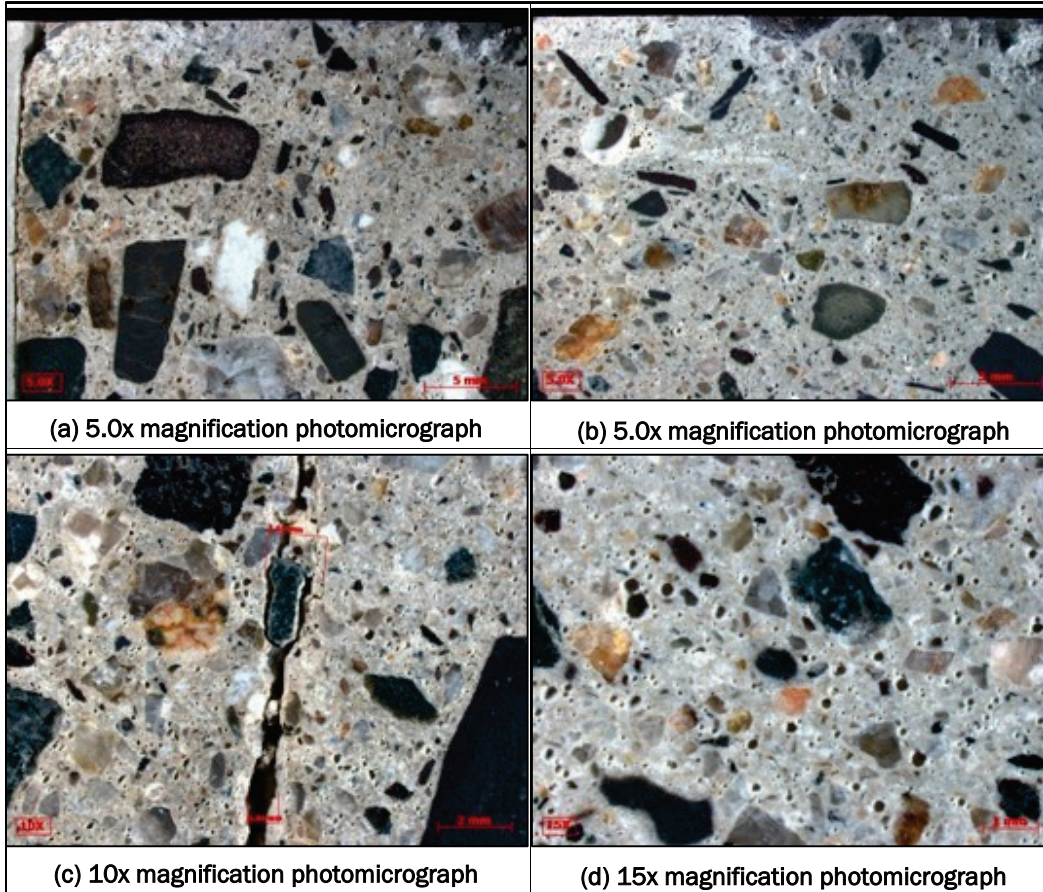
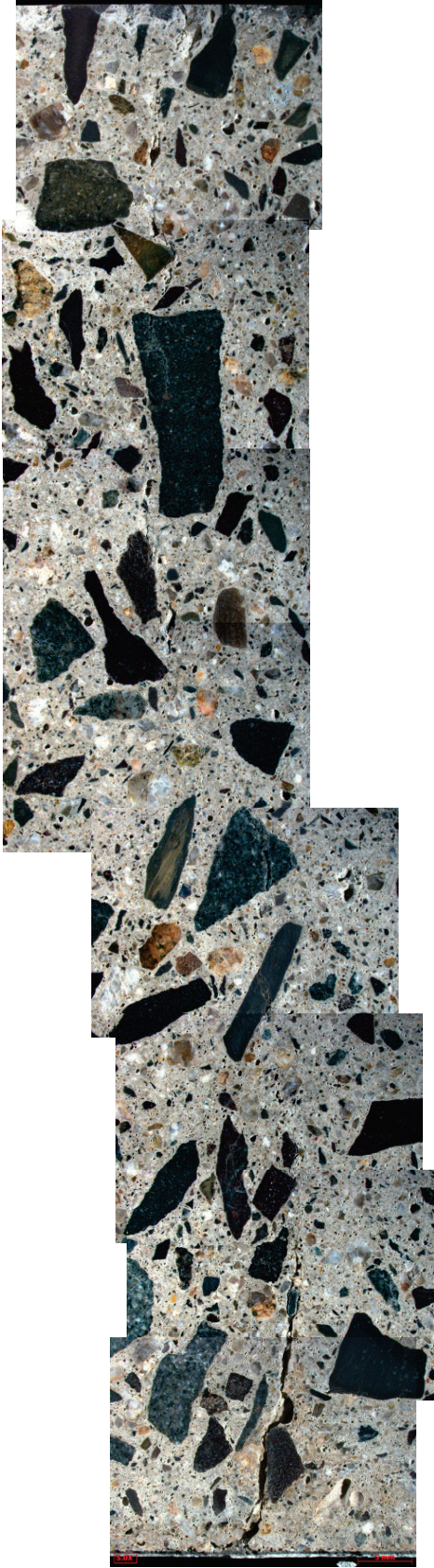


Figure C12. Map of crack observed in core T1-S2.



SEM analysis

Electron photomicrographs were obtained at different locations of Tower 1, Shaft 2 and are shown in Figures C13 and C14.

Figure C13. Low magnification montage electron photomicrograph of T1-S2 (200x magnification).

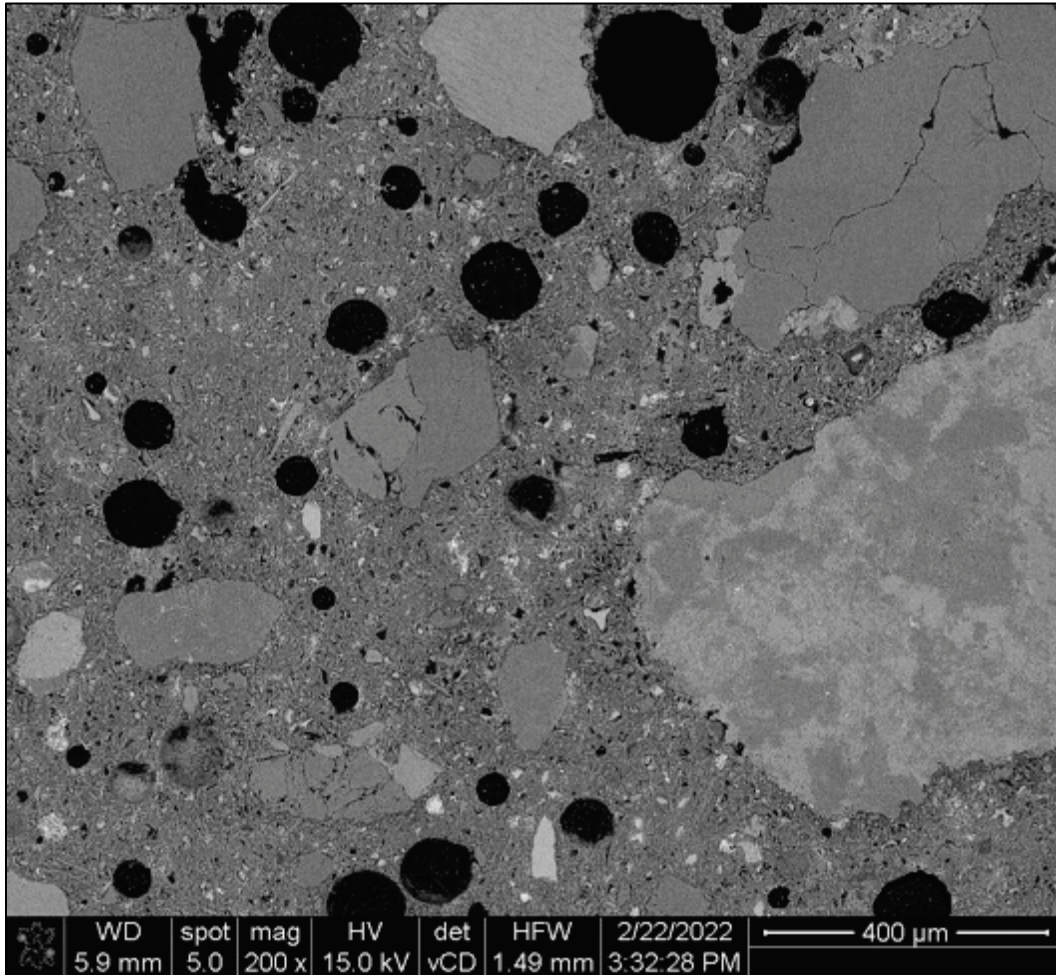
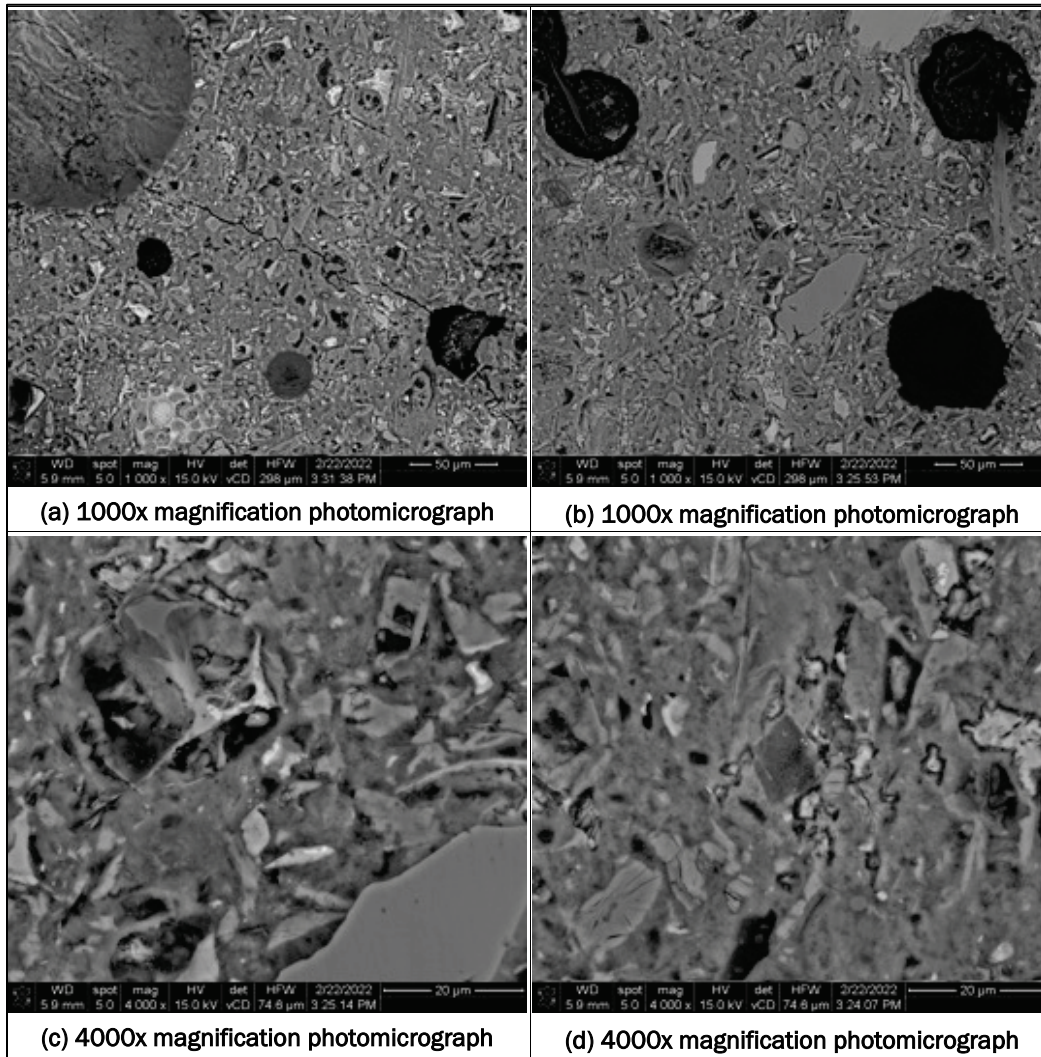


Figure C14. Electron photomicrographs of T1-S2: (a) 1000x photomicrograph of paste microstructure; (b) 1000x photomicrograph of paste; (c) 4000x photomicrograph of paste; (d) 4000x photomicrograph of paste.



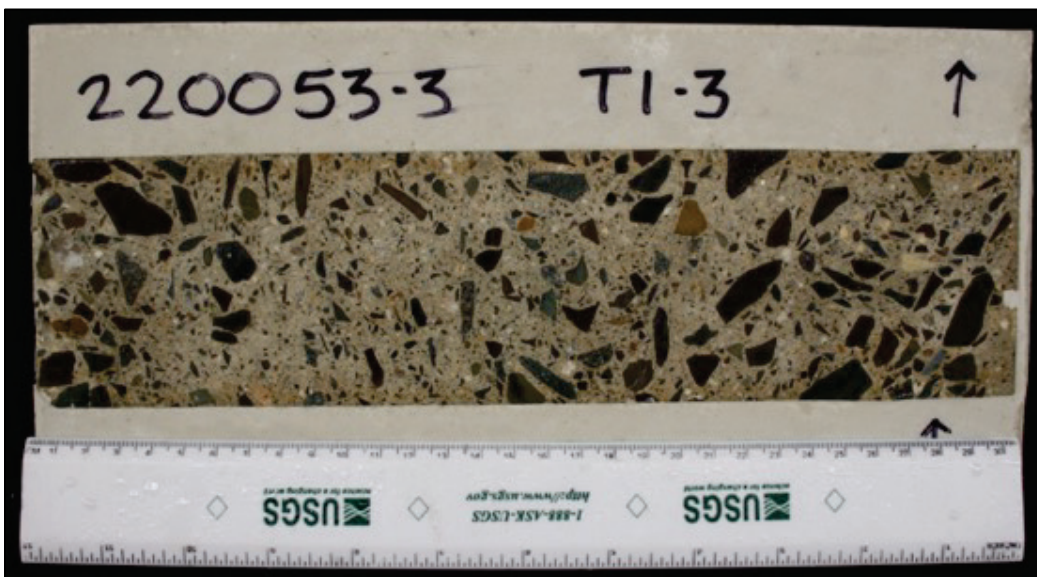
Tower 1, Core 3

The as-received core from Korea is shown in Figure C15 with the bisected half shown in Figure C16. The following provides a synopsis of the physical and durability related properties resulting from analysis of Tower 1, Core 3 (T1-3) (CMB# 220053-3).

Figure C15. As-received core T1-3.



Figure C16. Photo of bisected core T1-3.



Petrographic analysis

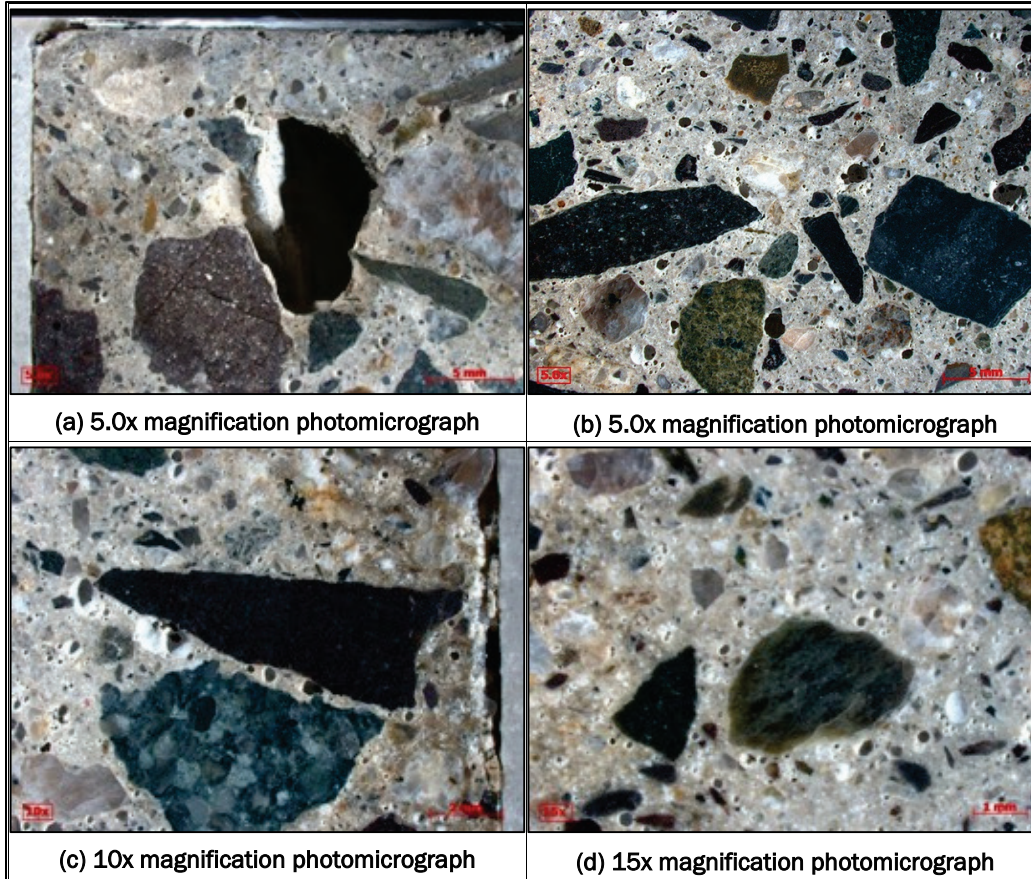
A scanned image from a polished section of the top 8 in. of the core is provided in Figure C17. Detailed photomicrographs of the core's microstructure are shown in Figure C18. The core was 12 in. in length, approximately 3 in. in diameter.

Examination of the core presented some hairline cracks on the surface, but none were observed with depth. The coarse aggregate was a crushed stone had a maximum nominal size of 1.25 in. It consisted primarily of granitic mineralogies with some sandstone particles present. The fine aggregate was a crushed stone and a quartz sand. The coarse aggregate was not uniformly dispersed, with some areas having a low concentration of coarse aggregate. Darkened rims were observed on some coarse aggregates, indicative of a reaction between the particles and paste; however, no disruption to the concrete was associated with this feature. Internal microfractures were observed in some coarse aggregates but are likely pre-existing features. No indicators of deleterious reactions, such as alkali-silica reaction (ASR), were observed within the sample. The paste was Yellowish Gray (5Y 8/1) in color and was air entrained. Entrapped air voids up to 0.5 in. in diameter were observed, but rare.

Figure C17. Scanned image of polished sections from core T1-3. Lettered boxes refer to locations of micrographs in Figure C18.



Figure C18. Photomicrographs of 220053-3: (a) 5.0x photomicrograph of paste microstructure showing large entrapped air void; (b) 5.0x photomicrograph showing paste microstructure; (c) 10x photomicrograph clusters of entrapped air along aggregate-paste boundary; (d) 15x photomicrograph of air voids within paste.



SEM analysis

Electron photomicrographs were obtained at different locations of Tower 1, Core 3 and are shown in Figures C19 and C20.

Figure C19. Low magnification montage electron photomicrograph of T1-3 (200x magnification).

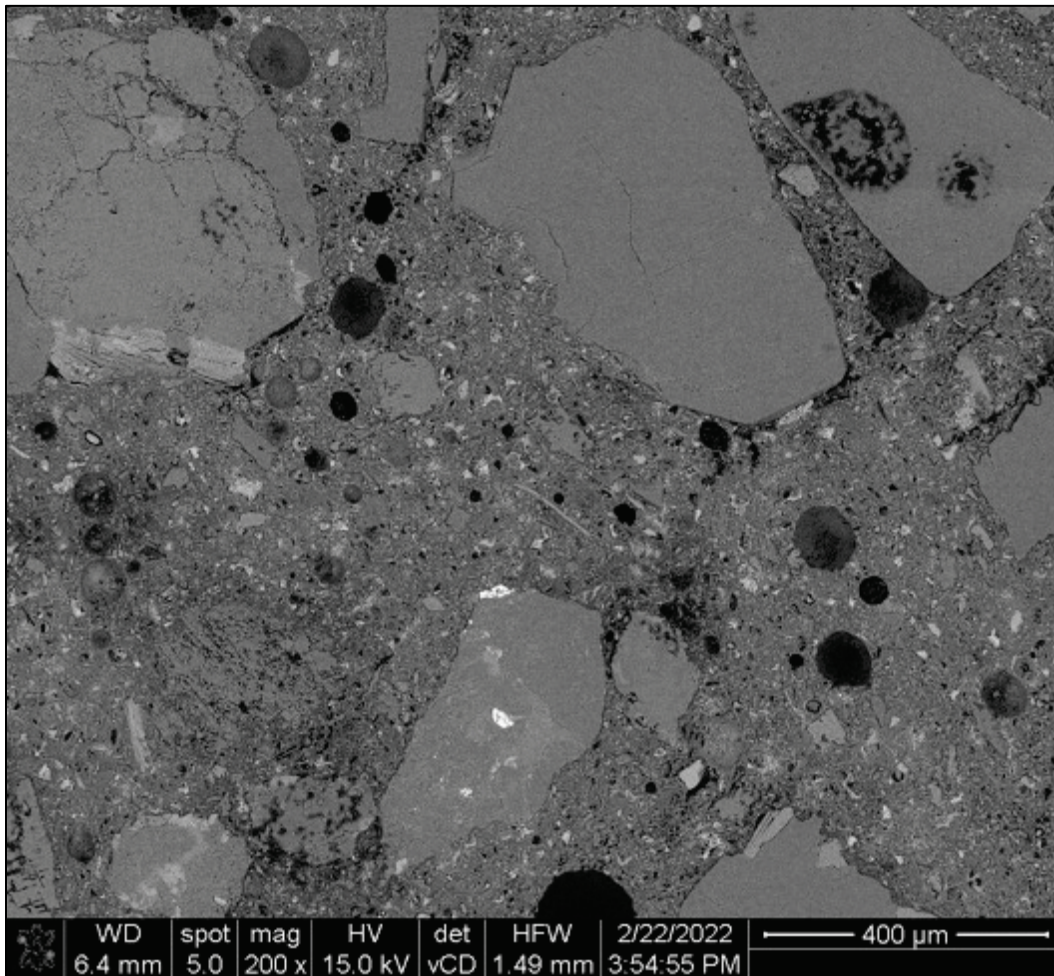
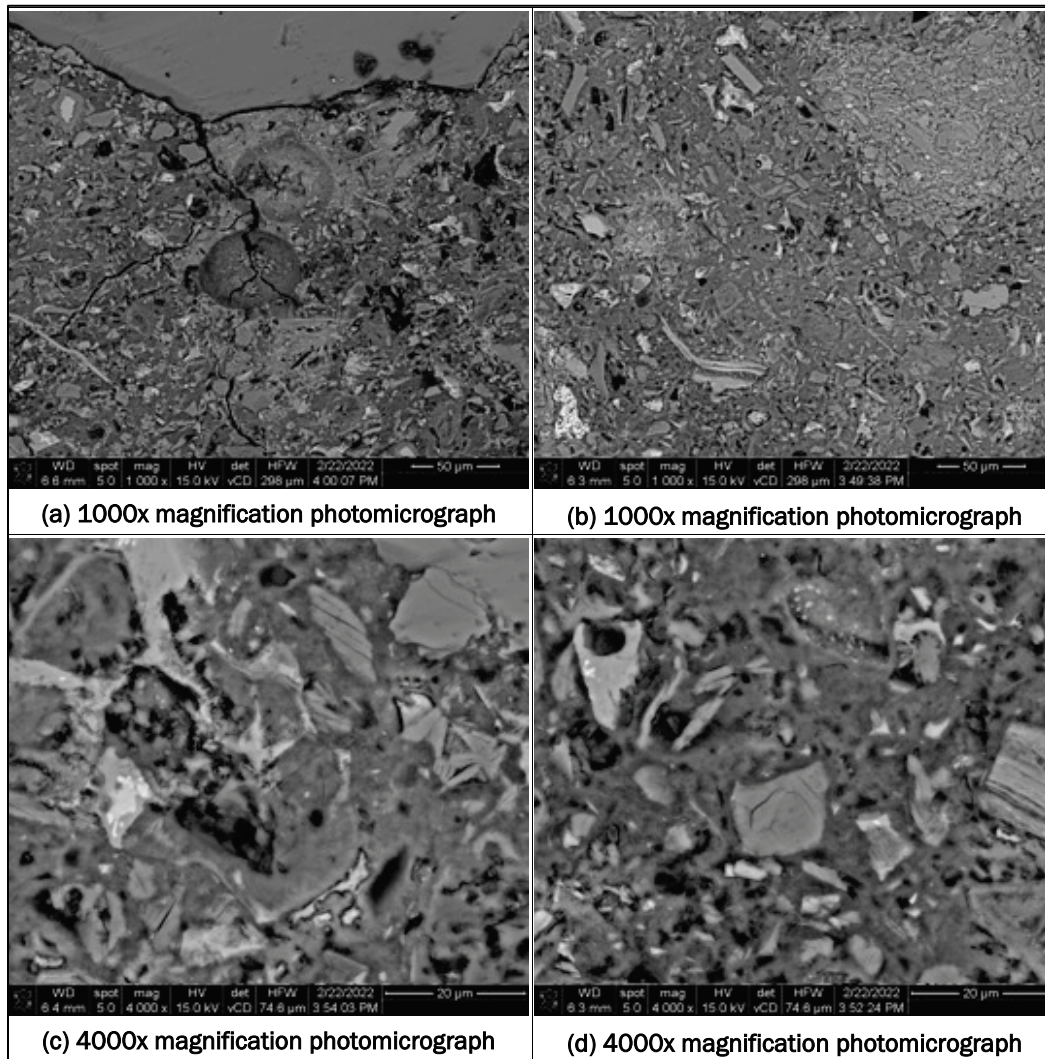


Figure C20. Electron photomicrographs of T1-3: (a) 1000x photomicrograph of paste microstructure; (b) 1000x photomicrograph of paste; (c) 4000x photomicrograph of paste; (d) 4000x photomicrograph of paste.



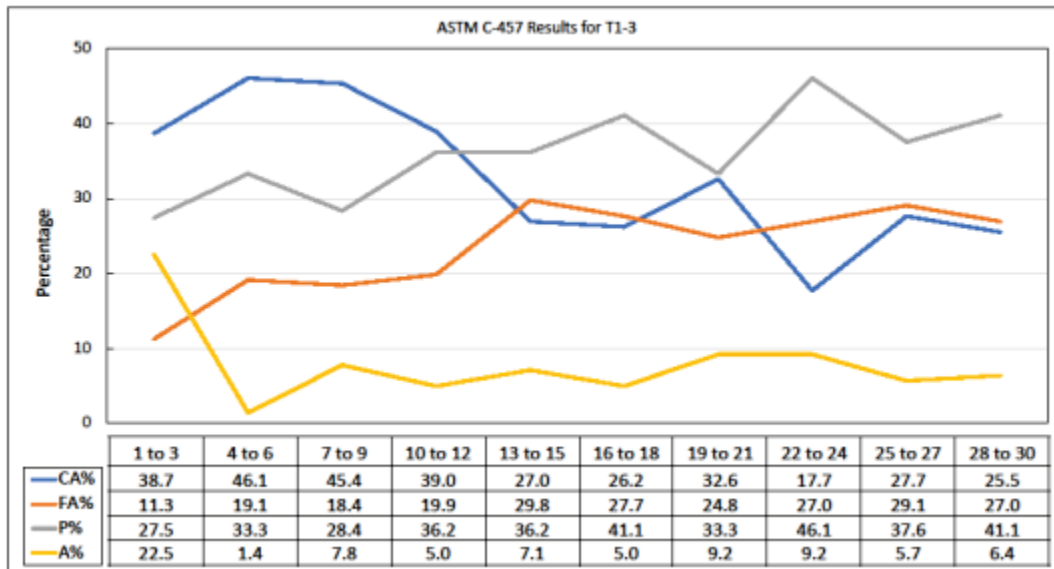
Air void / phase fraction analysis

Air void analysis was conducted on sample T1-3. To determine the minimum length of traverse and/or minimum number of points needed for accurate analysis, the nominal size of coarse aggregate used was 1.0 in. (as measured in initial petrographic analysis). The total traverse length needed was 95 in. or a minimum of 1425 points counted. Mixture proportions for each sample were calculated based on data gathered during from ASTM C-457.

The air content was 7.8% (entrained air was 3.4% and entrapped air was 4.4%), paste volume fraction was 36.0%, and the paste to air ratio was 4.6.

Figure C21 shows a comparison of the concrete constituents for every 1 cm, or 3 traverses into the sample. The phases do not have any discernible trend with depth. Entrained air voids were often concentrated in clusters while entrapped air voids were consistently found along aggregate boundaries. The largest entrapped air voids were found in the top several centimeters.

Figure C21. Comparison of concrete phases in sample T1-3 with depth acquired during ASTM C-457 analysis. The x-axis represents traverse lines across the core, 3 of which equal approximately a centimeter.



Tower 2, Core 3

The as-received core from Korea is shown in Figure C22 with the bisected half shown in Figure C23. The following provides a synopsis of the physical and durability related properties resulting from analysis of Tower 2, Core 3 (T2-3) (CMB# 220054).

Figure C22. As-received core T2-3.

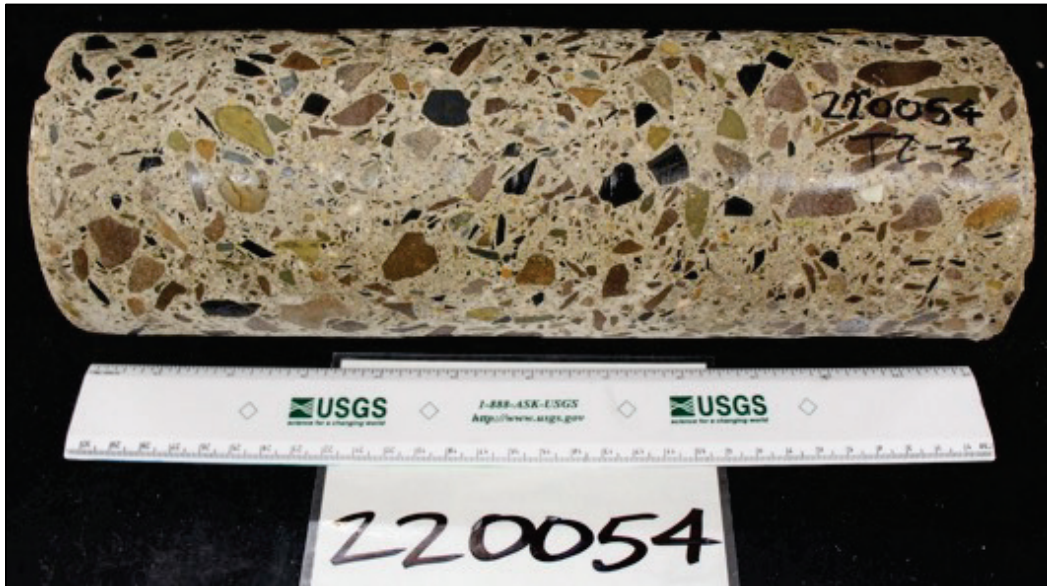


Figure C23. Photo of bisected core T2-3.



Petrographic analysis

A scanned image from a polished section of the top 4 in. of the core is provided in Figure C24. Detailed photomicrographs of the core's microstructure are shown in Figure C25. The core was 12 in. in length, approximately 4.0 in. in diameter.

Examination of the core presented one extensive crack on the core surface that extended with depth over the entire length of the core (Figure C26). The crack varied in width from 0.25 to 2.50 mm and represented the only cracking present in the sample. The white material infilled throughout the crack is hydrostone and not a product of ASR. The coarse aggregate was a crushed stone had a maximum nominal size of 1.0 in. It consisted primarily of granitic mineralogies with some sandstone particles present. The fine aggregate was a crushed stone and a quartz sand. The coarse aggregate was not uniformly dispersed, with some areas having a low concentration of coarse aggregate. These regions were concentrated on one side of the crack. Darkened rims were observed on some coarse aggregates, indicative of a reaction between the particles and paste; however, no disruption to the concrete was associated with this feature. Internal microfractures were observed in some coarse aggregates but are likely pre-existing features. Reinforcing bar was present within the sample. No indicators of deleterious reactions, such as alkali-silica reaction (ASR), were observed within the sample. The paste was air entrained. Entrapped air voids up to 0.5 in. in diameter were observed, but rare.

Figure C24. Scanned image of polished sections from core T2-3. Lettered boxes refer to locations of micrographs in Figure C4.

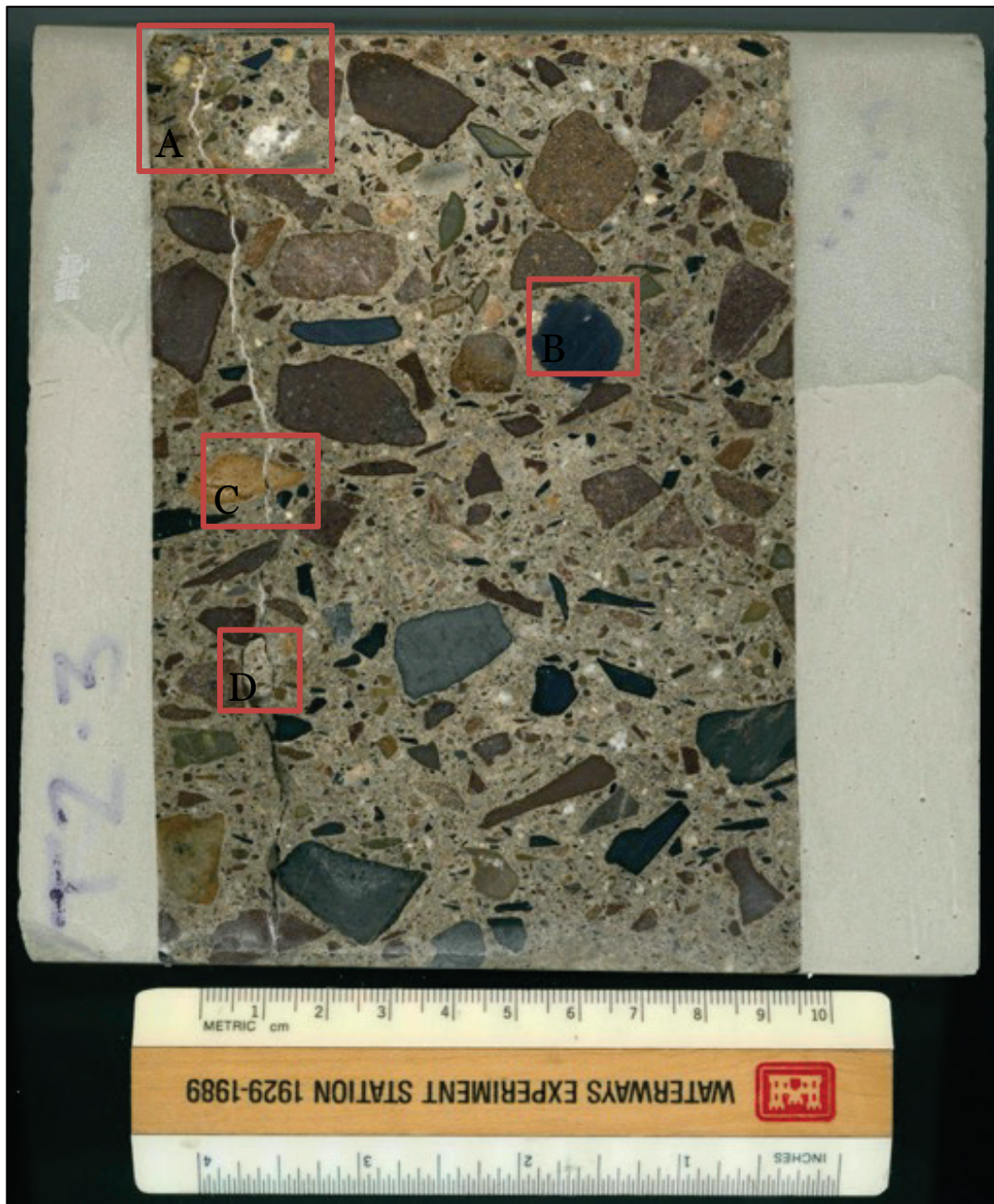


Figure C25. Photomicrographs of T2-3: (a) 5.0x photomicrograph of paste microstructure and surficial paste discoloration; (b) 10x photomicrograph of rebar with voids present at paste boundary; (c) 10x magnification showing vertical crack through a coarse aggregate; (d) 10x photomicrograph vertical crack with varied width.

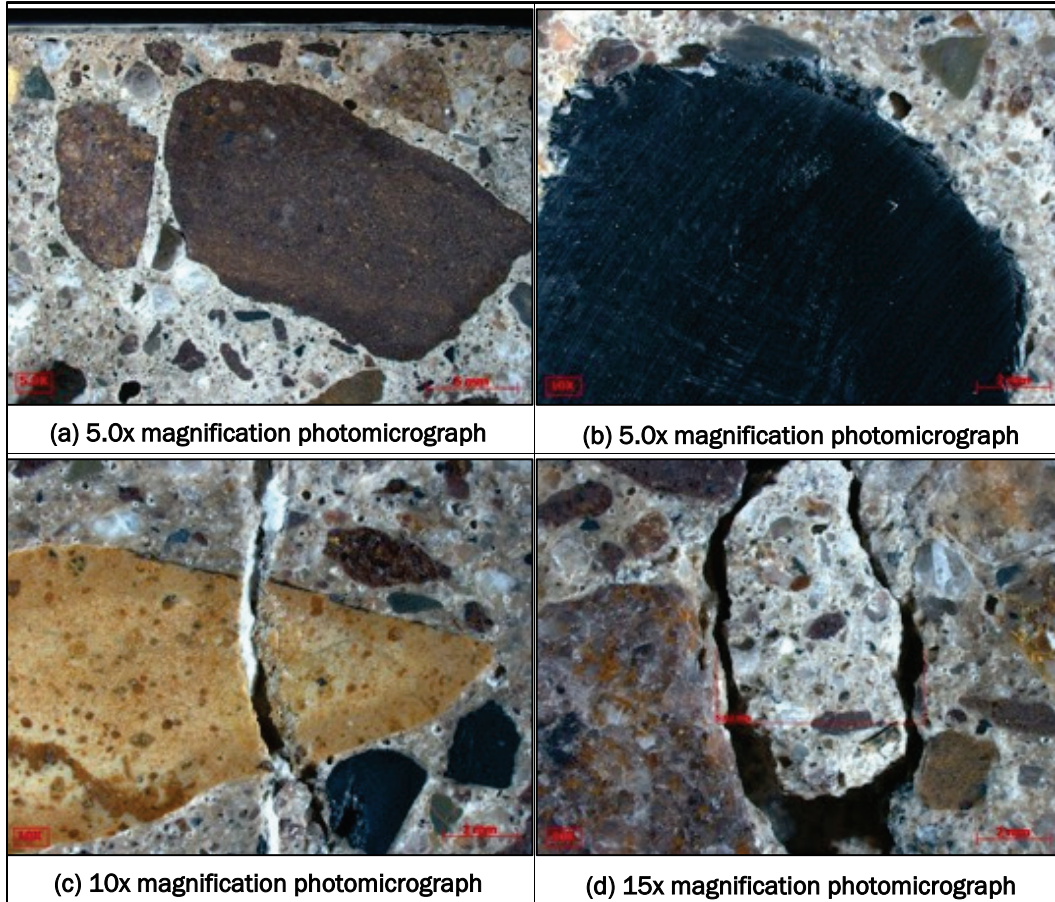
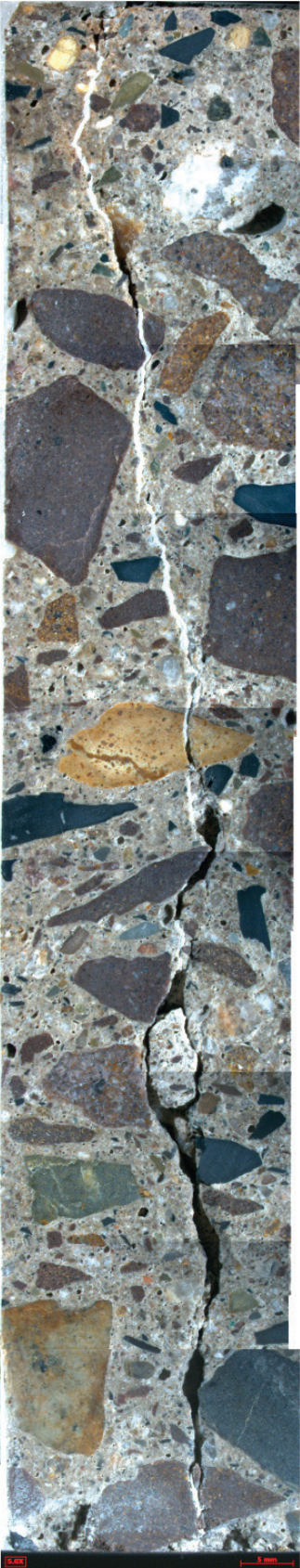


Figure C26. Map of crack observed in core T2-3.



SEM analysis

Electron photomicrographs were obtained at different locations of Tower 2, Core 3 and are shown in Figures C27 and C28.

Figure C27. Low magnification montage electron photomicrograph of T2-3 (200x magnification).

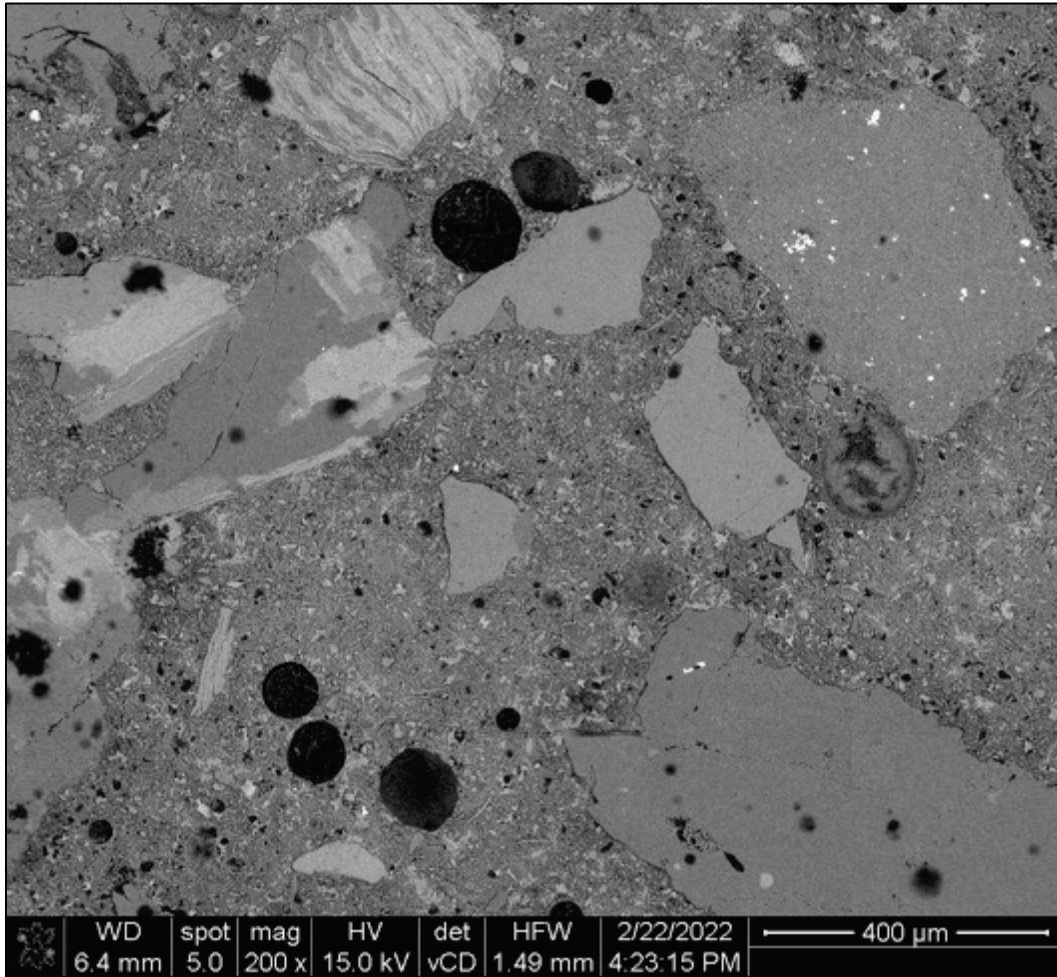
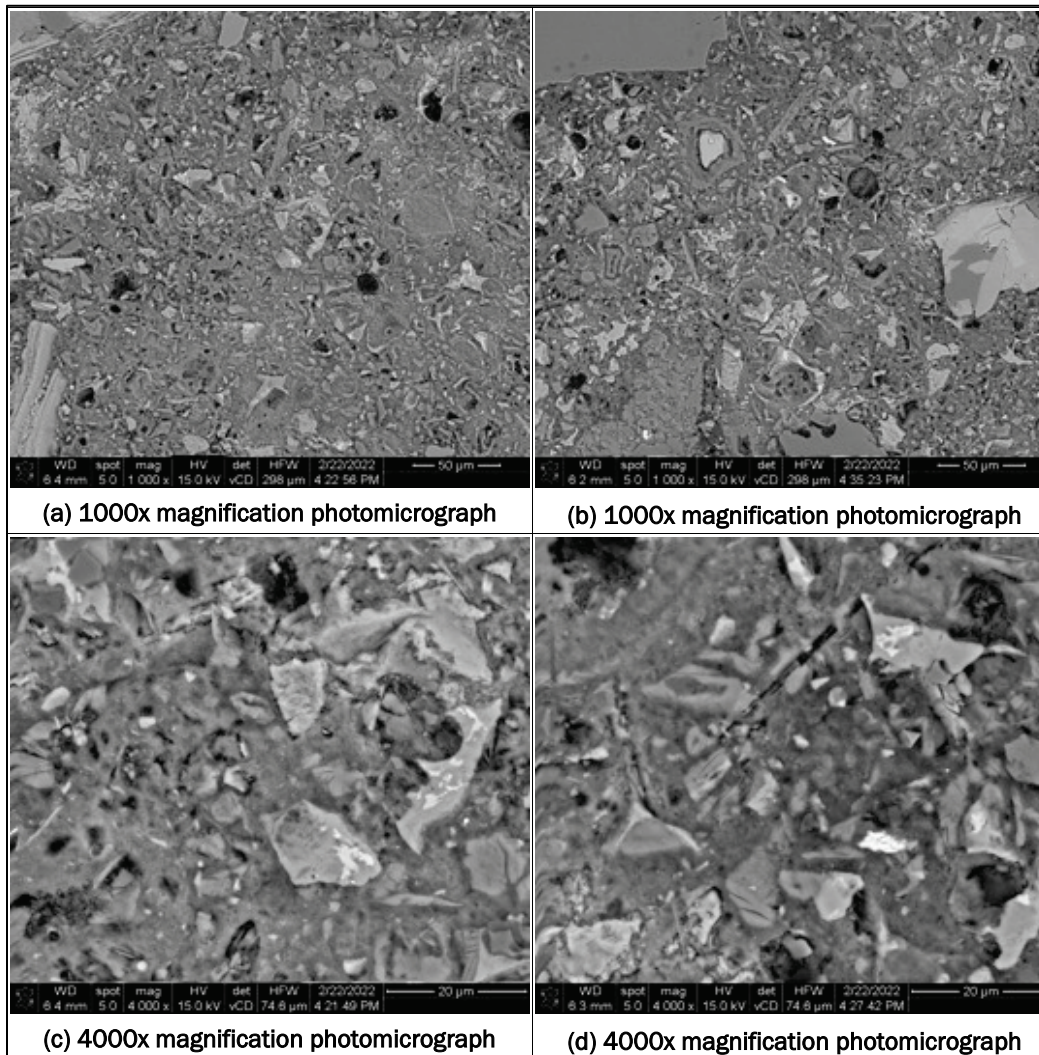


Figure C28. Electron photomicrographs of T2-3: (a) 1000x photomicrograph of paste microstructure; (b) 1000x photomicrograph of paste; (c) 4000x photomicrograph of paste; (d) 4000x photomicrograph of paste.



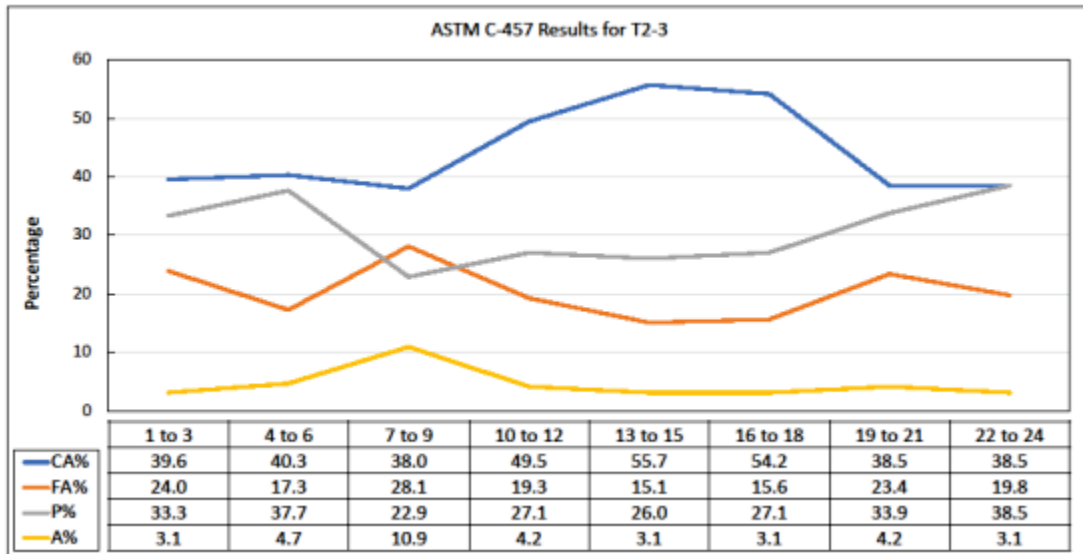
Air void/phase fraction analysis

Air void analysis was conducted on sample T2-3. To determine the minimum length of traverse and/or minimum number of points needed for accurate analysis, the nominal size of coarse aggregate used was 1.0 in. (as measured in initial petrographic analysis). The total traverse length needed was 95 in. or a minimum of 1425 points counted. Mixture proportions for each sample were calculated based on data gathered during from ASTM C-457.

The air content was 4.6% (entrained air was 2.3% and entrapped air was 2.2%), paste volume fraction was 30.8%, and the paste to air ratio was 6.8. Figure C29 shows a comparison of the concrete constituents for

every 1 cm, or 3 traverses into the sample. The phases do not have any discernible trend with depth.

Figure C29. Comparison of concrete phases in sample T2-3 with depth acquired during ASTM C-457 analysis. The x-axis represents traverse lines across the core, 3 of which equal approximately a centimeter.



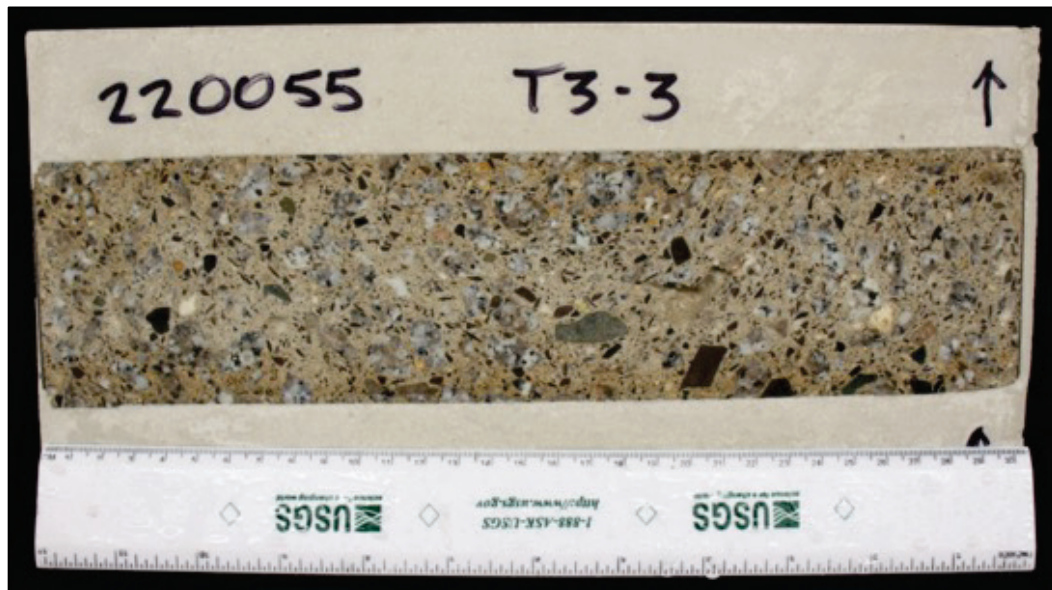
Tower 3, Core 3

The as-received core from Korea is shown in Figure C30 with the bisected half shown in Figure C31. The following provides a synopsis of the physical and durability related properties resulting from analysis of Tower 3, Core 3 (T3-3) (CMB# 220055).

Figure C30. As-received core T3-3.



Figure C31. Photo of bisected core T3-3.



Petrographic analysis

A scanned image from a polished section of the top 4 in. of the core is provided in Figure C32. Detailed photomicrographs of the core's microstructure are shown in Figure C33. The core was 12 in. in length, approximately 4.0 in. in diameter.

Examination of the core presented one extensive crack on the core surface that extended with depth over the entire length of the core. The crack varied in width from 0.25 to 2.50 mm and represented the only cracking present in the sample. The coarse aggregate was a crushed stone that had a maximum nominal size of 0.75 in. It consisted primarily of granitic mineralogies. The fine aggregate was a crushed stone and a quartz sand. The coarse aggregate was not uniformly dispersed, with some areas having a low concentration of coarse aggregate. These regions were concentrated on one side of the crack. Darkened rims were observed on some coarse aggregates, indicative of a reaction between the particles and paste; however, no disruption to the concrete was associated with this feature. Internal microfractures were observed in some coarse aggregates but are likely pre-existing features. No indicators of deleterious reactions, such as alkali-silica reaction (ASR), were observed within the sample. The paste was Yellowish Gray (5Y 8/1) in color and was air entrained. Entrapped air voids up to 0.5 in. in diameter were observed, but rare.

Figure C32. Scanned image of polished sections from core T3-3. Lettered boxes refer to locations of micrographs in Figure C33.

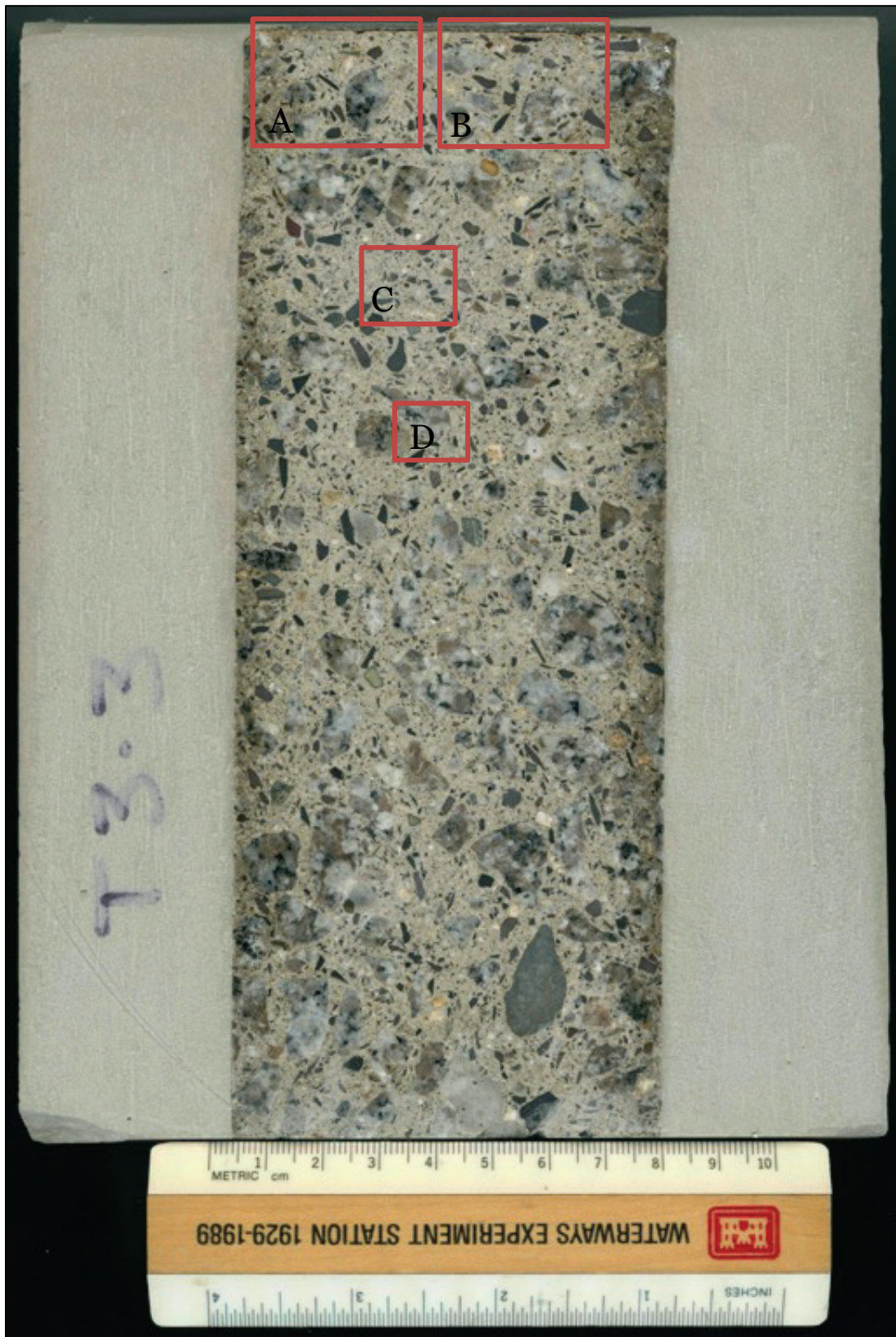
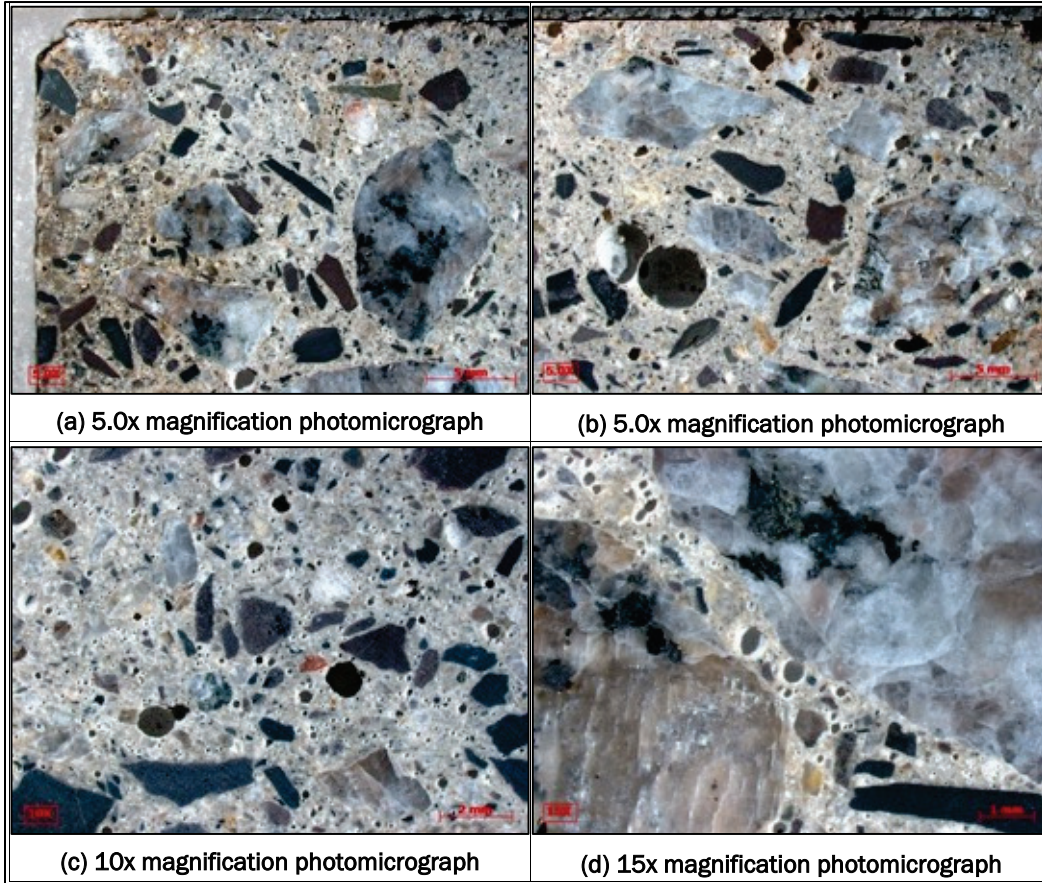


Figure C33. Photomicrographs of T3-3: (a) 5.0x photomicrograph of paste microstructure; (b) 5.0x photomicrograph of large entrapped air voids; (c) 10x magnification showing paste microstructure; (d) 15x photomicrograph showing air voids concentrated along aggregate boundaries.



SEM analysis

Electron photomicrographs were obtained at different locations of Tower 3, Shaft 3. Photomicrographs are illustrated in Figures C34–C35.

Figure C34. Low magnification montage electron photomicrograph of T3-3 (200x magnification).

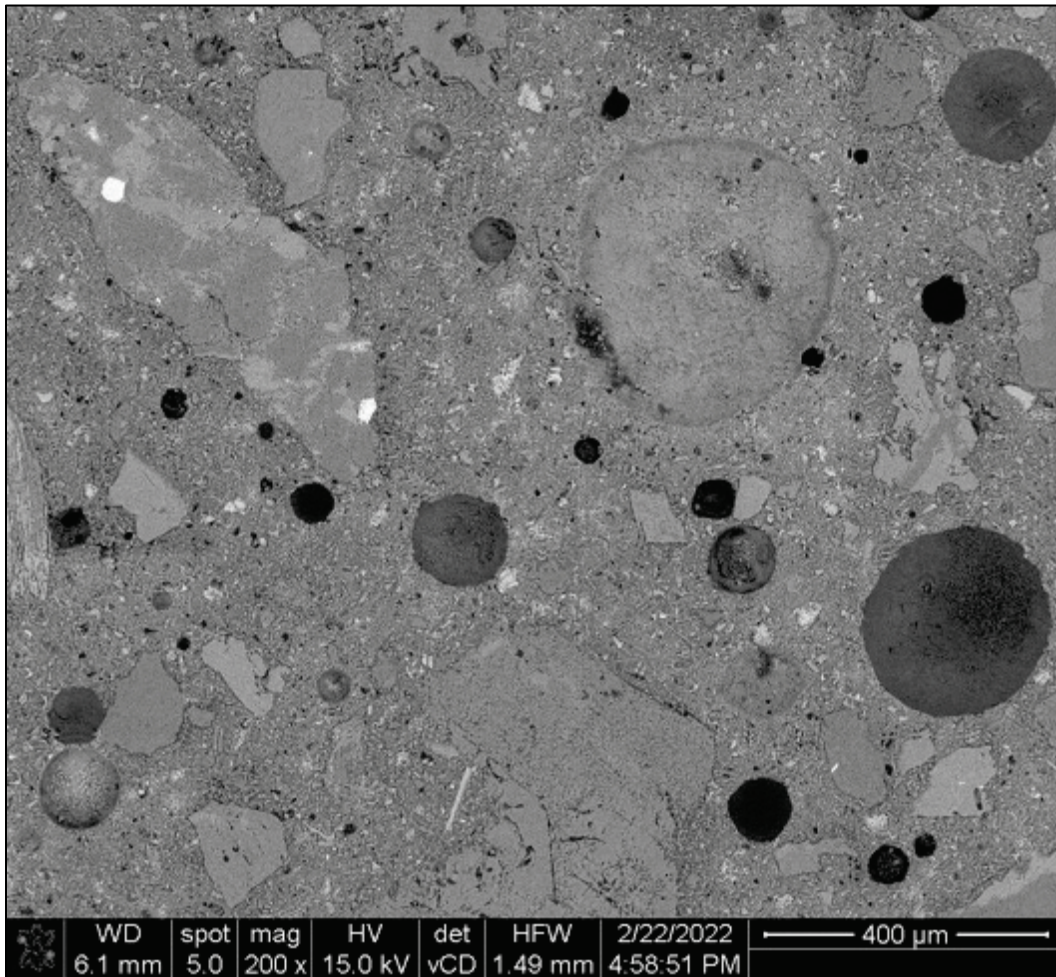
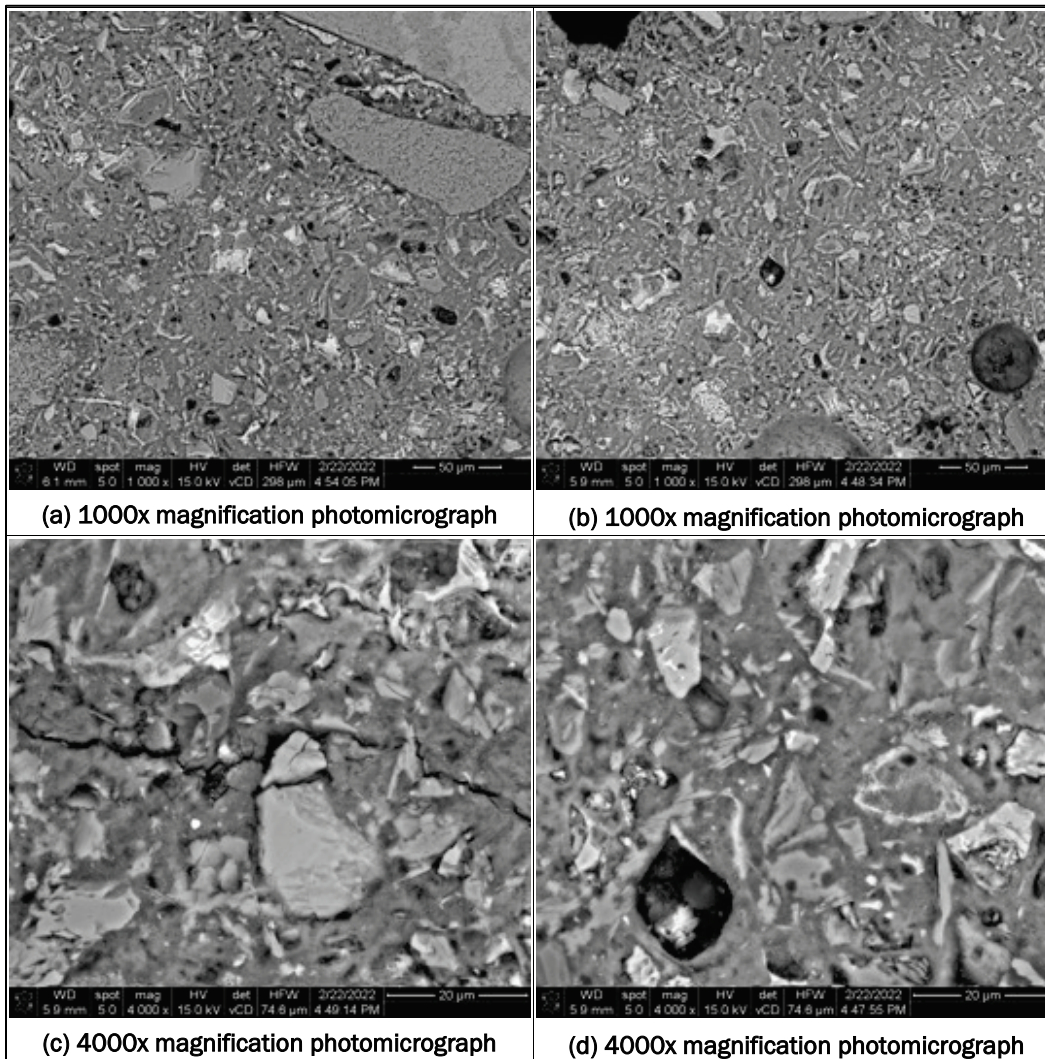


Figure C35. Electron photomicrographs of T3-3; (a) 1000x photomicrograph of paste microstructure; (b) 1000x photomicrograph of paste; (c) 4000x photomicrograph of paste; (d) 4000x photomicrograph of paste.



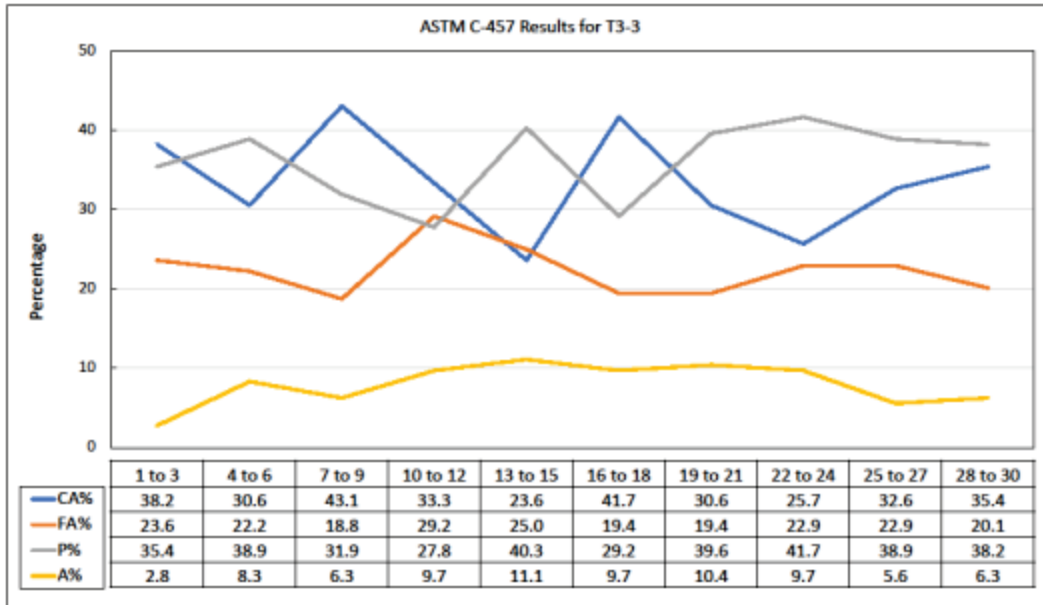
Air void/phase fraction analysis

Air void analysis was conducted on sample T3-3. To determine the minimum length of traverse and/or minimum number of points needed for accurate analysis, the nominal size of coarse aggregate used was 0.75 in. (as measured in initial petrographic analysis). The total traverse length needed was 90 in. or a minimum of 1350 points counted. Mixture proportions for each sample were calculated based on data gathered during from ASTM C-457.

The air content was 8.0% (entrained air was 5.1% and entrapped air was 2.9%), paste volume fraction was 36.2%, and the paste to air ratio was 4.5.

Figure C36 shows a comparison of the concrete constituents for every 1 cm, or 3 traverses into the sample. Air content was relatively high from 4 to 8 cm. Entrained air voids were often in clusters and some appeared infilled. The other phases did not have any discernible trend with depth.

Figure C36. Comparison of concrete phases in sample T3-3 with depth acquired during ASTM C-457 analysis. The x-axis represents traverse lines across the core, 3 of which equal approximately a centimeter.



Conclusions

This study examined concrete cores from recently constructed housing towers 1–3 at Camp Walker, South Korea. The assessment evaluated the samples for potential modes of concrete deterioration and durability issues through the use of petrographic analysis, SEM, and air void analysis. The results of the study included the following:

- Overall in-place concrete mixture proportions appeared to correspond, in bulk, to the approved mixture proportions for the project. The concrete was an air-entrained, straight portland cement mixture with no supplementary cementitious materials. Concrete in Towers 1 and 2 included maximum aggregate sizes of approximately 1 in. Concrete in Tower 3 included a smaller maximum aggregate size, corresponding to reported reductions in NMSA to improve workability for concrete placement and consolidation.
- Sample T1-3 contained a coarse aggregate with primarily silicate-based mineralogy with a maximum nominal size of 1.0 in. The fine aggregate

- was a crushed stone and quartz sand. An extensive crack was observed that extended with depth throughout the entire length of the core and varied in thickness from 0.25 to 2.50 mm. The coarse aggregate was not uniformly dispersed, creating potential durability concerns due to segregation. The concrete was air entrained and entrapped air voids were observed, but rare. Discoloration of the paste was observed near the surface, likely due to carbonation.
- Sample T1-2 contained a coarse aggregate with primarily silicate-based mineralogy with a maximum nominal size of 1.0 in. The fine aggregate was a crushed stone and quartz sand. An extensive crack was observed that extended with depth throughout the entire length of the core and varied in thickness from 0.10 to 2.0 mm. The coarse aggregate was not uniformly dispersed, creating potential durability concerns due to segregation. The concrete was air entrained and entrapped air voids were observed, but rare. Discoloration of the paste was observed near the surface, likely due to carbonation.
 - Sample T1-3 contained a coarse aggregate with primarily silicate-based mineralogy with a maximum nominal size of 1.25 in. The fine aggregate was a crushed stone and quartz sand. An extensive crack was observed that extended with depth throughout the entire length of the core and varied in thickness from 0.25 to 2.50 mm. The coarse aggregate was not uniformly dispersed, creating potential durability concerns due to segregation. Discoloration of the paste was observed near the surface, likely due to carbonation. Entrapped air voids were observed, especially frequent in the upper portion of the core. Entrained air occurred frequently in clusters and along aggregate boundaries, but no evidence of cracking or displacement was associated with them.
 - Sample T2-3 contained a coarse aggregate with primarily silicate-based mineralogy with a maximum nominal size of 1.0 in. The fine aggregate was a crushed stone and quartz sand. An extensive crack was observed that extended with depth throughout the entire length of the core and varied in thickness from 0.25 to 2.50 mm. Discoloration of the paste was observed near the surface, likely due to carbonation. The concrete was air entrained, although at a low level, and entrapped air voids were observed, but rare.
 - Sample T3-3 contained a coarse aggregate with primarily granitic mineralogies with a maximum nominal size of 3/4-in. The fine aggregate was a crushed stone and quartz sand. Discoloration of the paste was observed near the surface, likely due to carbonation. Entrapped air voids were observed, but rare. Entrained air voids

occurred often in clusters and along aggregate boundaries, but no evidence of cracking or displacement was associated with them.

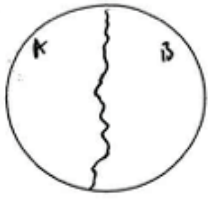
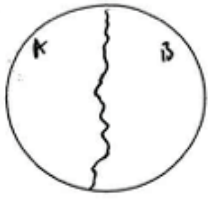
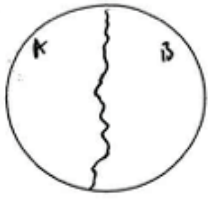






- Air void analysis of the samples resulted in the following phase fractions:

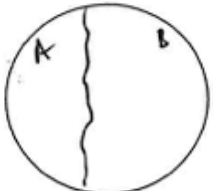


Sample	Paste (%)	Air (%)	Coarse Agg (%)	Fine Agg (%)	Paste/Air
T1-3	36.0	7.8	32.7	23.5	4.6
T2-3	30.8	4.6	44.3	20.3	6.8
T3-3	36.2	8.0	33.5	22.4	4.5

The concrete samples exhibited no signs of internal disruption of the coarse and fine aggregate portions, nor were other features associated with ASR expansion or freeze-thaw distress detected. Segregation of the coarse aggregate was observed in cores T1-1, T1-2, and T-3, causing potential durability issues and related cracking.

Overall, the concrete composition in bulk appeared to correspond to the approved mixture proportions. However, there are clear issues with construction procedures that have led to extensive segregation especially across cold joints or interruptions in the concrete placement. Cracking observed in the cores appeared to be caused by shrinkage at later stages given that in many instances the cracks intersected coarse aggregates. This is an indicator that the cracking was primarily caused by drying shrinkage at later stages when the concrete would have gained sufficient strength to have cracks extend through aggregates. No other durability or other mechanisms were noted as potential drivers for the observed distress.

Core logs

Location: Korea Core Name: T1-S-2, 220053-1 Investigator: CMS Date: 2-15-22	<table border="1" style="width: 100%; border-collapse: collapse;"> <tr> <td style="padding: 5px;">CORE SURFACE</td> <td style="text-align: center; vertical-align: middle;">  </td> </tr> <tr> <td colspan="2" style="padding: 5px;"> - crack down surface (0.25 - 2.50 mm) </td> </tr> </table>	CORE SURFACE		- crack down surface (0.25 - 2.50 mm)					
CORE SURFACE									
- crack down surface (0.25 - 2.50 mm)									
Core Length: 12" Bit Diameter: 4"									
<table border="1" style="width: 100%; border-collapse: collapse;"> <thead> <tr> <th style="width: 20%; padding: 5px;">DEPTH (in)</th> <th style="padding: 5px;">LEGEND</th> </tr> </thead> <tbody> <tr> <td style="padding: 5px; vertical-align: top;">  </td> <td style="padding: 5px; vertical-align: top;">  </td> </tr> </tbody> </table>	DEPTH (in)	LEGEND			<table border="1" style="width: 100%; border-collapse: collapse;"> <thead> <tr> <th style="padding: 5px;">REMARKS/COMMENTS</th> </tr> </thead> <tbody> <tr> <td style="padding: 5px;"> Max. aggregate size - 1" Aggregate type - mixed gravel, sandstone Max. entrapped air size - 0.5" Cracks visible? - Yes, one vertical crack that bisects the core - varies in thickness from 0.10 mm - 2.50 mm - minimal entrapped air voids - agg. looks well dispersed - agg to paste but appears strong </td> </tr> <tr> <td style="padding: 5px; text-align: center;">TESTS</td> </tr> <tr> <td style="height: 50px;"></td> </tr> </tbody> </table>	REMARKS/COMMENTS	Max. aggregate size - 1" Aggregate type - mixed gravel, sandstone Max. entrapped air size - 0.5" Cracks visible? - Yes, one vertical crack that bisects the core - varies in thickness from 0.10 mm - 2.50 mm - minimal entrapped air voids - agg. looks well dispersed - agg to paste but appears strong	TESTS	
DEPTH (in)	LEGEND								
									
REMARKS/COMMENTS									
Max. aggregate size - 1" Aggregate type - mixed gravel, sandstone Max. entrapped air size - 0.5" Cracks visible? - Yes, one vertical crack that bisects the core - varies in thickness from 0.10 mm - 2.50 mm - minimal entrapped air voids - agg. looks well dispersed - agg to paste but appears strong									
TESTS									


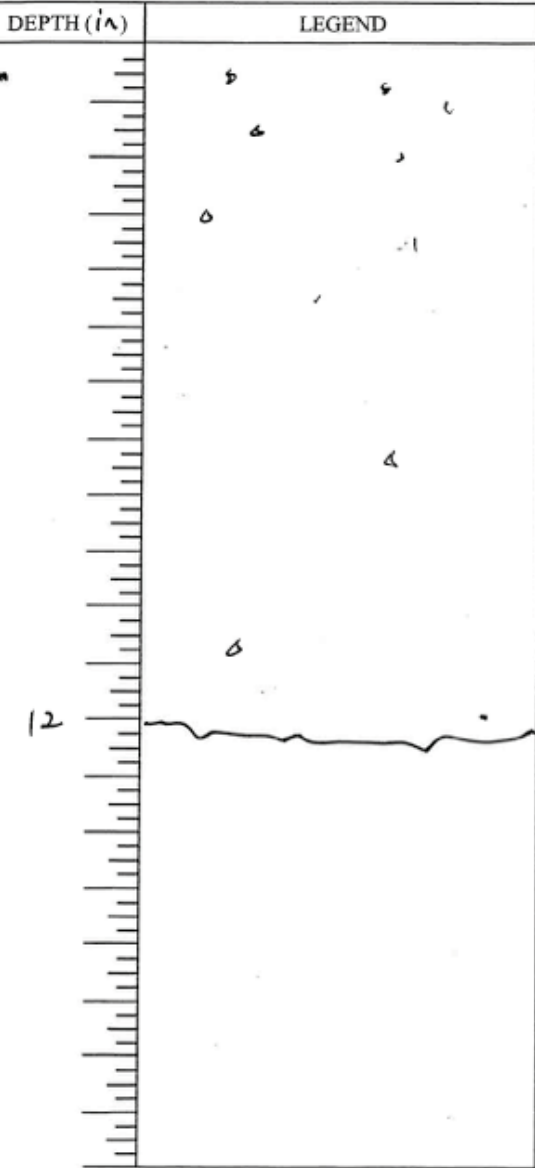
Location: Korea Core Name: T1-5-2, 220053-2 Investigator: CMG Date: 2-15-22		CORE SURFACE - bisected by thin crack (.2mm - 1.5mm)	
Core Length: 12" Bit Diameter: 4"			
DEPTH (ft)	LEGEND	REMARKS/COMMENTS	
		Max. aggregate size - 1" Aggregate type - Max. entrapped air size - 0.2" Cracks visible? - Yes, crack extends from the surface into depth up to 8" - Varied in thickness from (0.1 mm - 2.0 mm) - Large discrepancy in volume percentages of agg vs paste separated by the crack A side = coarse agg visible & well dispersed B side = little CA. in size & volume	
		- minimal entrapped air - agg - paste had appeared along	

Location: Korea
 Core Name: T1-3, 220053-3
 Investigator: CMC
 Date: 2-15-22

Core Length: 12"
 Bit Diameter: 3"

CORE SURFACE

- few large entrapped air voids (2.5mm)
- hairline cracks

REMARKS/COMMENTS

Max. aggregate size - 1 1/4"

Aggregate type -

Max. entrapped air size - 5mm

Cracks visible? - No cracks observed


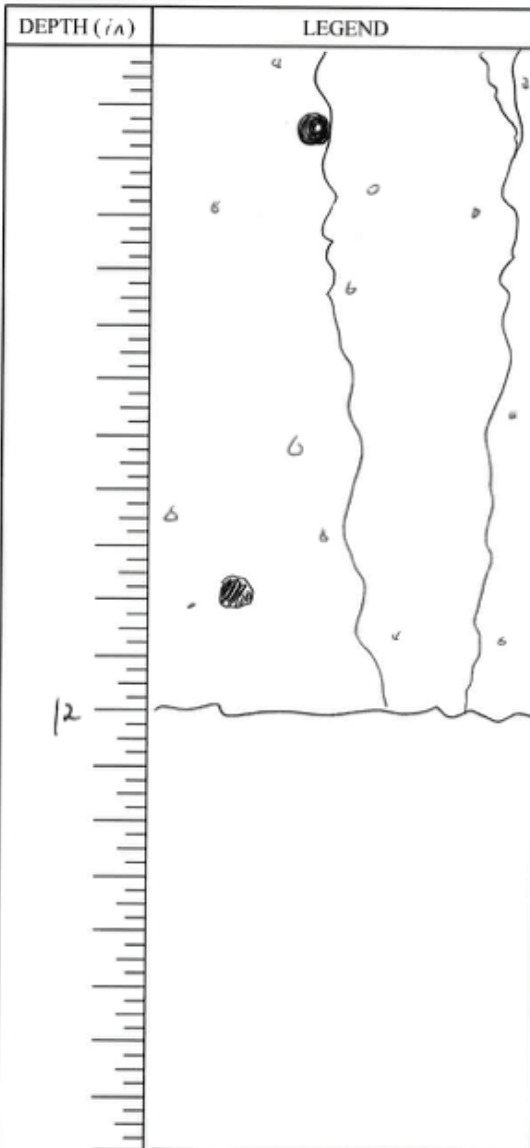
- minimal entrapped air
- some areas exhibit segregation
- eggs to paste bond appears strong

TESTS

Location: Korea
 Core Name: TR-3, 220054
 Investigator: CMC
 Date: 2/15/22
 Core Length: 12"
 Bit Diameter: 4"

CORE SURFACE

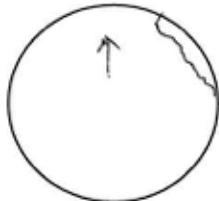

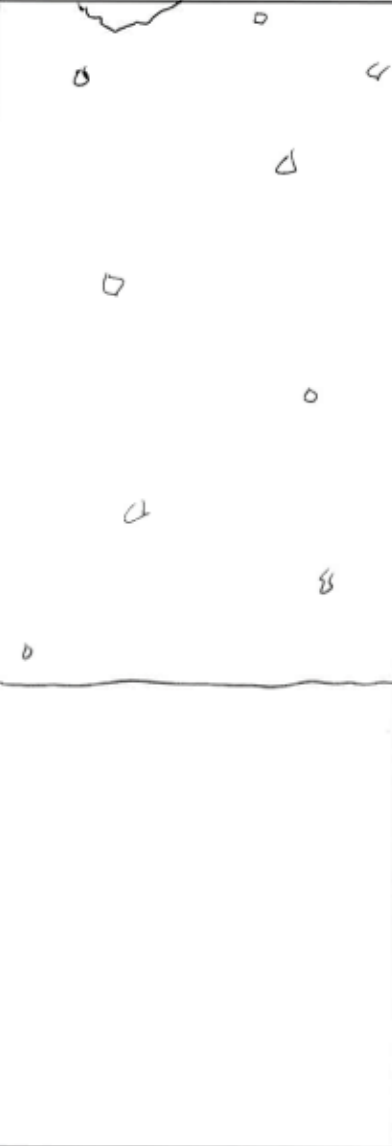
- large crack bisects surface (.4 - 1.5 mm)
- entrapped air voids

REMARKS/COMMENTS

- Max. aggregate size - 1 1/4"
- Aggregate type -
- Max. entrapped air size - 0.5 cm
- Cracks visible? - yes, surface crack extends w/ depth & bisects the core.
- width is 0.5 mm - 2.5 mm
- rebar present
- crack bisects some CA
- relatively high percentage of elongated CA

TESTS

Location: <i>Korea</i> Core Name: <i>T3-3, 220055</i> Investigator: <i>CMS</i> Date: <i>2/15/22</i>		CORE SURFACE 
Core Length: <i>12"</i> Bit Diameter: <i>3"</i>		
DEPTH (in)	LEGEND	REMARKS/COMMENTS
		Max. aggregate size - <i>1"</i> Aggregate type - Max. entrapped air size - <i>0.5 cm²</i> Cracks visible? <i>None</i> - CA phase percentage is very low, potential segregation or mix design issues
		TESTS

Air void data

Project: Camp Walker Korea FY22		Date: 22-Feb-22		Sample ID: T1-3		AIR Void TEST ASTM C 457			
CMS		Stop Interval: 1/16" > 1/8" ^		Job No:		Comments: Max agg of 1" = 95*/1425pts			
Traverse	Aggregate		Paste	Entrained		Entrapped		Total Stops	N Transected air voids
	Coarse	Fine		Empty	Filled	<1mm	>1mm		
1	20	5	11	2	0	0	10	48	10
2	17	4	13	1	0		12	47	4
3	18	7	15	1	0		6	47	6
4	18	10	18	1	0		0	47	10
5	28	6	12	1	0		0	47	5
6	19	11	17	0	0		0	47	4
7	14	12	17	2	0		2	47	11
8	25	6	10	1	0	1	4	47	7
9	25	8	13	1	0		0	47	8
10	21	7	18	1	0		0	47	9
11	19	6	20	2	0		0	47	10
12	15	15	13	4	0		0	47	4
13	13	15	15	2	0	1	1	47	13
14	18	9	18	1	0		1	47	11
15	7	18	18	4	0		0	47	14
16	6	12	27	2	0		0	47	13
17	10	15	18	2	0	1	1	47	7
18	21	12	13	0	0		1	47	8
19	17	7	18	1	0		4	47	11
20	15	15	15	1	0		1	47	16
21	14	13	14	3	0		3	47	10
22	8	12	23	3	0		1	47	19
23	4	16	22	2	0	1	2	47	18
24	13	10	20	2	0		2	47	8
25	20	11	14	1	0		1	47	7
26	15	16	14	1	0		1	47	8
27	4	14	25	2	0		2	47	17
28	12	16	16	1	0		2	47	13
29	14	8	21	2	0	1	1	47	15
30	10	14	21	1	0		1	47	20
31	16	13	15	1	0		1	46	9
32									
33									
34									
35									
36									
37									
38									
39									
40									
TOTAL	476	343	524	49	0	5	60	1457	325

Project: Camp Walker Korea - FY22		Date: 23-Feb-22		Sample ID: T3-3, 220055		AIR Void TEST ASTM C 457			
Operator: CMS		Stop Interval: 1/16" > 1/8" ^		Job No:		Comments: Max agg of 1" = 95"/1425pts			
Traverse	Aggregate		Paste	Entrained		Entrapped		Total Stops	N Transected air voids
	Coarse	Fine		Empty	Filled	<1mm	>1mm		
1	17	24	20	3		0	0	64	14
2	28	12	23	1		0	0	64	10
3	31	10	21	1		1	0	64	7
4	28	9	24	2		0	1	64	13
5	29	9	22	2		1	0	63	10
6	20	15	26	1		0	2	64	12
7	24	21	12	1		0	6	64	5
8	23	16	15	7		1	2	64	15
9	26	17	17	2		0	2	64	9
10	32	11	17	3		1	0	64	8
11	34	8	20	0		0	2	64	10
12	29	18	15	1		1	0	64	9
13	39	9	15	0		1	0	64	11
14	33	9	20	1		1	0	64	6
15	35	11	15	2		1	0	64	9
16	36	5	22	0		1	0	64	6
17	30	15	16	2		1	0	64	5
18	38	10	14	2		0	0	64	6
19	28	12	20	1		0	3	64	7
20	25	15	22	1		0	1	64	9
21	21	18	23	0		0	2	64	9
22	11	17	35	1		0	0	64	7
23	32	8	21	1		0	2	64	5
24	31	13	18	1		1	0	64	7
25									
26									
27									
28									
29									
30									
31									
32									
33									
34									
35									
36									
37									
38									
39									
40									
TOTAL	680	312	473	36	0	11	23	1535	209

Project: Camp Walker Korea EY22		Date: 24 Feb-22		Sample ID: T3-3		AIR Void TEST ASTM C 457			
CMS		Stop Interval: 1/16" > 1/8" ^		Job No:		Comments: Max Agg of 3/4" = 90"/1350pts			
Traverse	Aggregate		Paste	Entrained		Entrapped		Total Stops	N Transected air voids
	Coarse	Fine		Empty	Filled	<1mm	>1mm		
1	9	16	20	2	0	1	0	48	10
2	19	9	19	1			0	48	8
3	27	9	12	0			0	48	5
4	12	9	20	1			6	48	11
5	13	11	22	1			1	48	4
6	19	12	14	2			1	48	11
7	24	6	16	1			1	48	8
8	26	13	9	0			0	48	5
9	12	8	21	5			2	48	18
10	17	12	14	4		1	0	48	15
11	13	15	14	6			0	48	18
12	18	15	12	1		1	1	48	14
13	8	16	17	4			3	48	25
14	16	10	20	1		1	0	48	17
15	10	10	21	4		1	2	48	19
16	14	13	17	4			0	48	13
17	29	5	11	1			2	48	25
18	17	10	14	6			1	48	26
19	18	7	18	3			2	48	18
20	16	7	18	5		1	1	48	16
21	10	14	21	2			1	48	16
22	11	13	20	3			1	48	13
23	12	7	22	4			3	48	20
24	14	13	18	2			1	48	12
25	18	11	18	1			0	48	12
26	13	11	19	2			3	48	13
27	16	11	19	1			1	48	17
28	17	10	18	2			1	48	16
29	12	9	21	4			2	48	13
30	22	10	16	0				48	5
31									
32									
33									
34									
35									
36									
37									
38									
39									
40									
TOTAL	482	322	521	73	0	6	36	1440	423

Appendix D: Concrete Strength

Overview

During the on-site inspection, the ERDC team used a rebound hammer, commonly referred to as a Schmidt hammer, to non-destructively test bare areas of concrete in accordance with ASTM C805/C805M-18 (2018), *Standard Test Method for Rebound Number on Hardened Concrete*. The test provides a dimensionless rebound number that can be used to estimate in-place concrete strength. Because rebound hammer test results are influenced by the concrete surface, including the existence of a coating, tests were limited to areas within the towers and parking garages that were relatively smooth and free of a cementitious coating or paint. Ten rebound hammer impacts and photos of the test area were taken at each test location.

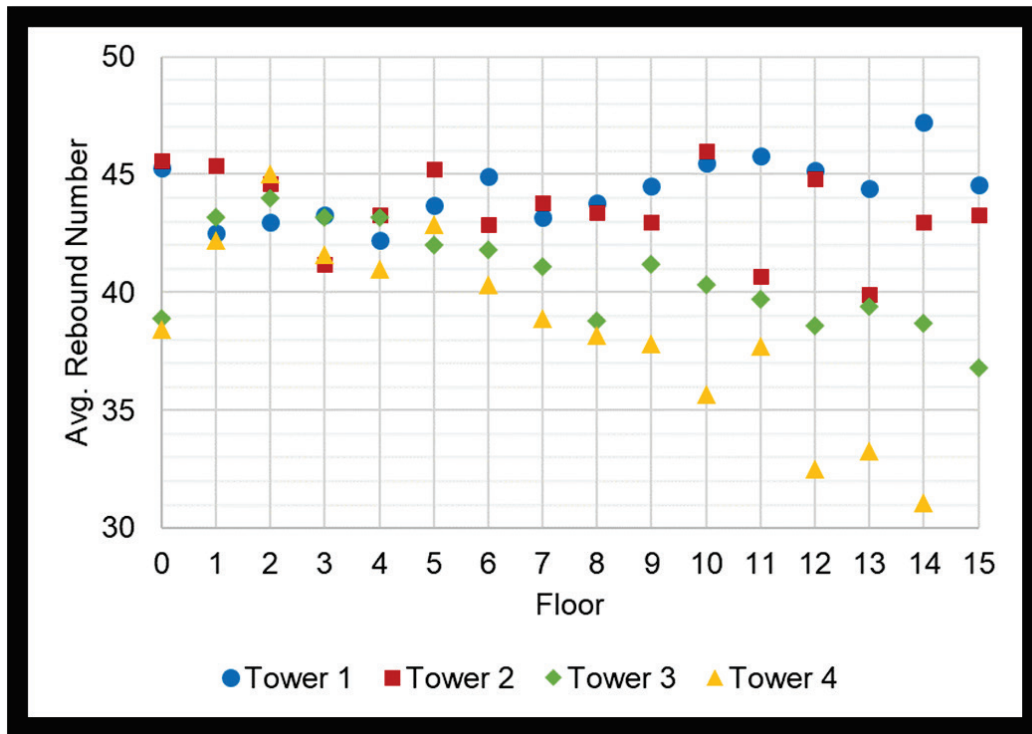
Concrete cores were drilled from the basement walls of Towers 1, 2, and 3. Three cores were taken from representative areas in each tower. Two cores from each representative area were delivered to the Far East District Environmental and Engineering Branch, Materials Testing Laboratory at Camp Humphreys to be tested in accordance with ASTM C39/C39M-21, *Standard Test Method for Compressive Strength of Cylindrical Concrete Specimens*. The third core of each area was transported back to the Concrete and Materials Branch at ERDC for petrographic analysis. In addition to those three cores, cores were taken on, above, and below a cold joint in Tower 1. In all cored locations, the surface coating layer was removed, rebound hammer tests were performed, and photos were taken before and after coring.

Rebound hammer tests

Rebound hammer tests were performed on bare concrete walls in shafts located behind the elevators on each floor in Towers 1, 2, and 3. The test wall locations in Tower 4 varied by floor depending on access to bare concrete. Figure D1 shows the average of the ten impacts taken in each test area for each floor of each tower. These areas do not necessarily include the cored areas. Those are presented and discussed separately. All rebound numbers ranged between 31 and 47. The concretes in Towers 1 and 2 generally produced higher rebound numbers than the concretes in Towers 3 and 4. Rebound numbers obtained in Tower 4

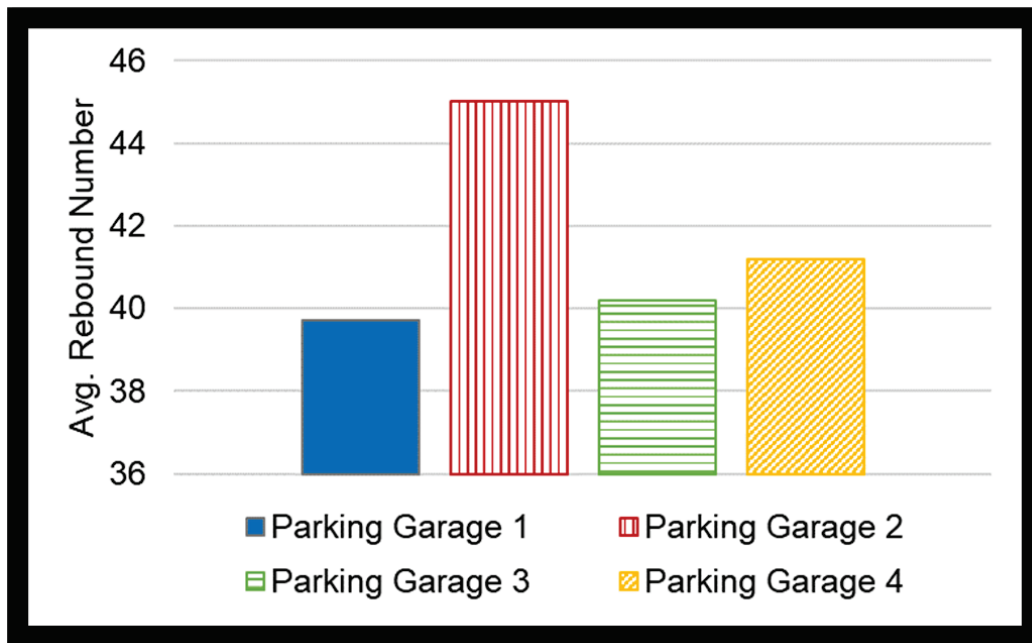
generally decreased as the floor level increased. Both of these trends can be attributed to the respective ages of the concretes.

Figure D1. Average rebound numbers obtained on each floor for each tower.



Rebound hammer tests were performed on bare concrete in beams, girders, and columns in the parking garages. The average rebound numbers obtained are shown in Figure D2. All values ranged between 38 and 47, and there appeared to be no trend regarding the age of the concretes. Overall, rebound numbers in Parking Garage 2 were higher than in the other parking garages.

Figure D2. Average rebound numbers obtained in each parking garage.



Concrete coring activities

Concrete cores were drilled from basement walls in Towers 1, 2, and 3 to be used in compressive strength testing and petrographic analysis. Prior to coring, the wall surface coating was removed and rebound hammer tests were performed on the bare concrete within the area. A ground-penetrating radar (GPR) device was used to identify locations of internal rebar. All cores used in compressive strength tests were 3 in. in diameter so as to avoid coring through reinforcement. Cores used for petrographic analysis were 4 in. in diameter if they were taken over a cold joint or crack to maintain the integrity of the cracked sections and 3 in. in diameter in areas where there was no defect. Table D1 provides a list of the areas cored and the wall designations in each tower. Wall designations are “Building-Floor-Lettered column line–Numbered column line.” When there are two numbers or letters (i.e., 16/17 or G/F) it indicates that the wall ran from between those column lines.

Table D1. Cored areas of each tower with corresponding wall designations.

Cored Area	Wall Designation
Tower 1 Representative Concrete	1-B-F-16/17
Tower 2 Representative Concrete	2-B-D.5-16/18
Tower 3 Representative Concrete	3-B-G/F-11
Tower 1 – Cold Joint	1-B-8-J/K

Two areas in the basement of Tower 1 were cored—one area deemed to be representative of the concrete quality throughout the structure and one area containing a cold joint within a shaft. Three 3-in.-diam cores were taken from the representative area of Tower 1. Figure D3 shows the prepared and cored area.

Figure D3. Prepared and cored (upper left insert) area of representative concrete in Tower 1. Red lines indicate locations of internal reinforcement.

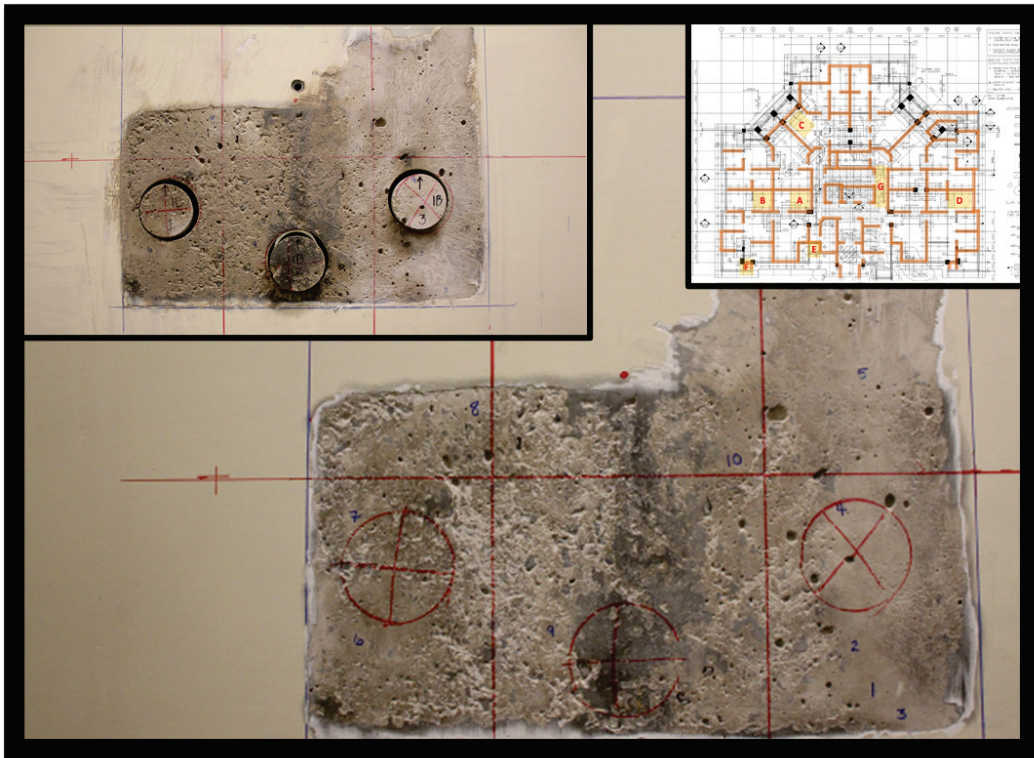


Figure D4 shows the prepared and cored cold joint in Tower 1. Two 3-in.-diam compressive strength cores were taken both above and below the cold joint for compressive strength testing, and two 4-in.-diam cores were taken over the cold joint for petrographic analysis.

Figure D4. Prepared and cored (upper left insert) area of wall containing a cold joint in Tower 1. Red lines indicate locations of internal reinforcement.



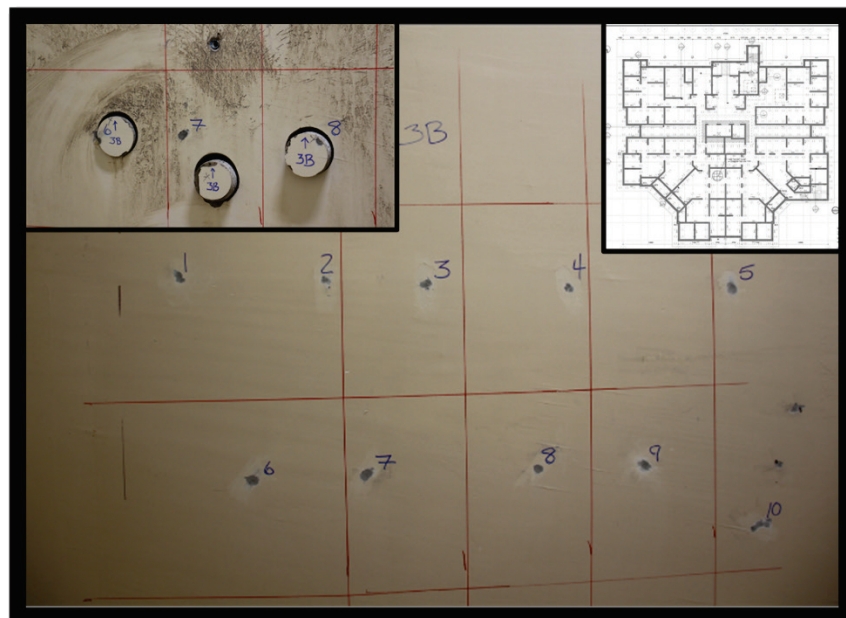
One area in the basement of Tower 2 was cored to provide two 3-in.-diam cores for compressive strength testing and one 4-in.-diam core taken over a crack for petrographic analysis. The crack was 0.4 mm wide and was selected for coring primarily to determine whether or not cracks of this magnitude penetrated the full depths of the walls. Another crack was visible in approximately the same location on the opposite side of the selected wall. Vertical reinforcement was located behind the crack by the GPR device. After coring, it was confirmed that the crack did in fact penetrate the full depth of the wall, and the assumption was made that the other cracks of this magnitude did as well. The cored area of Tower 2 is presented in Figure D5.

Figure D5. Prepared area for concrete coring in Tower 2. One core was taken over the crack, and two cores were taken to the sides of the crack to be representative concrete samples. Red lines indicate locations of internal reinforcement. Insert shows Schmidt hammer locations.



One representative area of Tower 3 was cored to provide two 3-in.-diam cores for compressive strength testing and one 3-in.-diam core for petrographic analysis. Figure D6 shows the prepared and cored area of Tower 3.

Figure D6. Prepared and cored (insert) area of representative concrete in Tower 3. Red lines indicate locations of internal reinforcement and numbers represent locations of Schmidt hammer testing.



Details of the compressive strength testing are provided under the USACE-POF strength report (Appendix E of this report), and the petrographic analyses of cores are provided in Appendix C of this report. No cores were taken from the parking garages because doing so would compromise the structural capacity of girders, beams, and columns or would puncture the moisture barrier on the outside of exterior basement walls, making the concrete susceptible to moisture ingress and future deterioration. Additionally, the same concrete mixtures that were used in the towers were also used in the respective parking garages.

Comparison of estimated and measured compressive strength

Obtaining direct compressive strength values from rebound testing is not possible. Correlations may be established if at least 12 cores are drilled and tested from six areas of each concrete mixture. However, the ERDC team decided that doing so would impose unnecessary damage on relatively new structures without sufficient evidence that the structural capacity of the concrete was in question. In absence of a direct correlation, inferences were made on the concretes using the chart provided by the rebound hammer manufacturer.

Values from the chart provided by the rebound hammer manufacturer were plotted to obtain a linear equation that could be used to easily estimate compressive strength based on rebound number. Table D2 presents the average rebound number obtained, the estimated compressive strength based on the rebound number, and the measured compressive strength on cores taken from specific areas of the towers. The first three rows show the areas of each tower considered to be representative of the concrete throughout each structure. Rows 4 and 5 show values for areas above (A) and below (B) the cold joint in the shaft (S) of Tower 1.

Table D2. Average rebound number, estimated compressive strength, and measured compressive strength for areas cored in each tower.

Coring Location	Average Rebound Number	Estimated Compressive Strength*, MPa	Measured Compressive Strength, MPa
Tower 1	46	51.6	43.0
Tower 2	41	43.2	34.5
Tower 3	39	39	41.6
Tower 1 S-A	45	49.7	31.8
Tower 1 S-B	43	46.6	34.6

* Values based on equation obtained from plotting values on chart provided by rebound hammer manufacturer, $[MPa] = 1.7435*[RN]-28.764$ where

MPa = Estimated compressive strength, MPa

RN = Average Rebound Number

All strength values measured for these areas exceeded the f'_c of 27 MPa. In every case except for one, estimated strengths were higher than the measured strengths. For Tower 3, the average rebound number was the lowest obtained for these areas, but the average measured compressive strength of the cores was high (41.6 MPa). This discrepancy is likely due to an atypically small rebound number obtained from one impact, even though it did not differ from the average enough to be excluded in accordance with the ASTM standard. Because the area of impact by the rebound hammer is relatively small, variations caused by impacting over small voids in the concrete are expected.

Summary

Except for the expected reduction in rebound number due to early age of the concretes in Towers 3 and 4, no areas tested provided low average values. Therefore, inferences on concrete strength throughout the structures made by comparing the estimated strengths to measured core strengths are valid.

Appendix E: Core Strength Report from Far East District

This appendix comprises the results of the unconfined compression strength tests performed on concrete cores from Towers 1–3 by USACE-POF.

Memorandum for ERDC. *Quality Assurance (QA) Concrete Strength Test for Drilled Core Samples, Family Housing Towers, Camp Walker, Korea (G&EE #22-024L/ L22-018) dated 17 February 2022.*

MEMORANDUM FOR ERDC

SUBJECT: Quality Assurance (QA) Concrete Strength Test for Drilled Core Samples, Family Housing Towers, Camp Walker, Korea (G&EE #22-024L/ L22-018)

1. The Far East District, Geotechnical and Environmental Engineering Branch, Materials Testing Laboratory (MTL) conducted ten concrete strength tests for the drilled core samples at Family Housing Towers in Camp Walker, Korea. The test results, calibration data sheets, and photographs of drilled core samples are enclosed for your use.
2. Ten 3-inch diameter drilled core samples were collected by the U.S. Army Engineer Research and Development Center (ERDC) and delivered to the MTL on 04 February 2022.
3. The original length of drilled core samples was measured in accordance with ASTM C42. The average length along the core axis line ranged from 10.00 in to 12.00 in. The measured lengths are summarized in Table 1.

Table 1. The Original Length of Drilled Core Samples

Specimen No.	Shortest (in)	Longest (in)	Average (in)	Specimen No.	Shortest (in)	Longest (in)	Average (in)
T1-1	11.79	11.79	11.75	T1-S-B2	10.06	10.10	10.00
T1-2	11.81	11.83	11.75	T2-1	11.85	11.87	11.75
T1-S-A	11.83	11.86	11.75	T2-2	11.88	11.90	12.00
T1-S-A1	11.88	11.89	12.00	T3-1	11.90	11.92	12.00
T1-S-B1	10.10	10.14	10.00	T3-2	11.90	11.91	12.00

4. The drilled core samples were cut and capped with a sulfur mortar compound in accordance with ASTM C617. The capped plainness of all specimens was less than 0.04 mm, which meets the tolerance requirement of within 0.05 mm in accordance with ASTM C39. The length-diameter ratio (L/D) was between 2.01 and 2.07.
5. Compressive strength tests were performed in accordance with ASTM C39. The average strength test results ranged from 4,610 psi (31.8 MPa) to 6,230 psi (42.9 MPa). The test results are summarized in Table 2.

Table 2. Compressive Strength Test Results

Specimen No.	L/D	Plainness (mm)	Individual Cylinder Strength, psi (MPa)	Average Strength, psi (MPa)	Date Tested	
1	T1-1	2.02	< 0.04	6,466 (44.6)	6,230 (42.9)	11 Feb 2022
	T1-2	2.03	< 0.04	5,990 (41.3)		
2	T1-S-A	2.03	< 0.04	5,296 (36.5)	5,020 (34.6)	
	T1-S-A1	2.02	< 0.04	4,744 (32.7)		
3	T1-S-B1	2.03	< 0.04	4,500 (31.0)	4,610 (31.8)	
	T1-S-B2	2.02	< 0.04	4,717 (32.5)		
4	T2-1	2.04	< 0.04	5,143 (35.5)	4,990 (34.4)	
	T2-2	2.01	< 0.04	4,846 (33.4)		
5	T3-1	2.03	< 0.04	5,687 (39.2)	6,030 (41.6)	
	T3-2	2.07	< 0.04	6,374 (43.9)		

6. Please contact Mr. Jaeung Yoon (DSN: 755-6626 / Jaeung.Yoon@usace.army.mil) or Mr. Minjae Park (DSN: 755-6105 / Minjae.Park@usace.army.mil) if additional clarification or assistance is needed.

Encl

SARAH H. WOO, P.E., PMP
 Chief, Geotechnical and Environmental
 Engineering Branch

Mr. Jaeung Yoon
 CEPOF-EDG-G

Mr. Minjae Park
 CEPOF-EDG-G

Ms. Sarah H. Woo
 CEPOF-EDG

MEMORANDUM FOR ERDC

SUBJECT: Quality Assurance (QA) Concrete Strength Test for Drilled Core Samples, Family Housing Towers, Camp Walker, Korea (G&EE #22-024L/ L22-018)

1. The Far East District, Geotechnical and Environmental Engineering Branch, Materials Testing Laboratory (MTL) conducted ten concrete strength tests for the drilled core samples at Family Housing Towers in Camp Walker, Korea. The test results, calibration data sheets, and photographs of drilled core samples are enclosed for your use.
2. Ten 3-inch diameter drilled core samples were collected by the U.S. Army Engineer Research and Development Center (ERDC) and delivered to the MTL on 04 February 2022.
3. The original length of drilled core samples was measured in accordance with ASTM C42. The average length along the core axis line ranged from 10.00 in to 12.00 in. The measured lengths are summarized in Table 1.

Table 1. The Original Length of Drilled Core Samples

Specimen No.	Shortest (in)	Longest (in)	Average (in)	Specimen No.	Shortest (in)	Longest (in)	Average (in)
T1-1	11.79	11.79	11.75	T1-S-B2	10.06	10.10	10.00
T1-2	11.81	11.83	11.75	T2-1	11.85	11.87	11.75
T1-S-A	11.83	11.86	11.75	T2-2	11.88	11.90	12.00
T1-S-A1	11.88	11.89	12.00	T3-1	11.90	11.92	12.00
T1-S-B1	10.10	10.14	10.00	T3-2	11.90	11.91	12.00

4. The drilled core samples were cut and capped with a sulfur mortar compound in accordance with ASTM C617. The capped plainness of all specimens was less than 0.04 mm, which meets the tolerance requirement of within 0.05 mm in accordance with ASTM C39. The length-diameter ratio (L/D) was between 2.01 and 2.07.
5. Compressive strength tests were performed in accordance with ASTM C39. The average strength test results ranged from 4,610 psi (31.8 MPa) to 6,230 psi (42.9 MPa). The test results are summarized in Table 2.

Table 2. Compressive Strength Test Results

Specimen No.	L/D	Plainness (mm)	Individual Cylinder Strength, psi (MPa)	Average Strength, psi (MPa)	Date Tested	
1	T1-1	2.02	< 0.04	6,466 (44.6)	6,230 (42.9)	11 Feb 2022
	T1-2	2.03	< 0.04	5,990 (41.3)		
2	T1-S-A	2.03	< 0.04	5,296 (36.5)	5,020 (34.6)	
	T1-S-A1	2.02	< 0.04	4,744 (32.7)		
3	T1-S-B1	2.03	< 0.04	4,500 (31.0)	4,610 (31.8)	
	T1-S-B2	2.02	< 0.04	4,717 (32.5)		
4	T2-1	2.04	< 0.04	5,143 (35.5)	4,990 (34.4)	
	T2-2	2.01	< 0.04	4,846 (33.4)		
5	T3-1	2.03	< 0.04	5,687 (39.2)	6,030 (41.6)	
	T3-2	2.07	< 0.04	6,374 (43.9)		

6. Please contact Mr. Jaeung Yoon (DSN: 755-6626 / Jaeung.Yoon@usace.army.mil) or Mr. Minjae Park (DSN: 755-6105 / Minjae.Park@usace.army.mil) if additional clarification or assistance is needed.

Encl

SARAH H. WOO, P.E., PMP
 Chief, Geotechnical and Environmental
 Engineering Branch

Appendix F: Initial ERDC Assessment Memorandum

This appendix comprises the preliminary assessment submitted to CEPOD.

Memorandum for Commander (CEPOD-DE/BG Kirk E. Gibbs), Pacific Ocean Division, U.S. Army Corps of Engineers. *Initial ERDC Assessment of Camp Walker Family Housing Towers 1 and 2 and their Parking Garages* dated 28 January 2022.



[REDACTED]

DEPARTMENT OF THE ARMY
U.S. ARMY CORPS OF ENGINEERS, ENGINEER RESEARCH AND DEVELOPMENT CENTER
WATERWAYS EXPERIMENT STATION, 3909 HALLS FERRY ROAD
VICKSBURG, MISSISSIPPI 39180-6199

CEERD-ZA

28 January 2022

MEMORANDUM FOR Commander (CEPOD-DE/BG Kirk E. Gibbs), Pacific Ocean Division, U.S. Army Corps of Engineers, 573 Bonney Loop, Building 525, Suite A300, Fort Shafter, HI 96858

(U) SUBJECT: Initial ERDC Assessment of Camp Walker Family Housing Towers 1 and 2 and their Parking Garages

(U) BLUF: The US Army Engineer Research and Development Center (ERDC) Evaluation Team (the ERDC Team) has evaluated Towers 1 and 2 plus corresponding parking garages at Camp Walker, Daegu, South Korea, to assess the impact of observed cracking in the concrete structures, as initially reported by CEPOF. The ERDC Team has not observed any life safety concerns in Towers 1 and 2 or their connected parking garages. The ERDC Team recommends that on-site personnel continue to conduct regular monitoring for cracking and displacements in the structures and that the CEPOF Team continues to work, as planned, to engage an expert structural forensics consultant to further assess long-term impacts of this cracking on the service life of the structure and to develop remediation plans.

(U) Introduction and Scope:

[REDACTED] This memorandum furnishes the ERDC Team's initial findings on the structural condition of Family Housing Towers 1 and 2 and appurtenant Parking Garages at Camp Walker, Daegu, South Korea. The ERDC scope of work covers four areas: a) the identification of any life safety concerns, b) potential intermediate considerations for monitoring and additional analysis, c) potential long-term durability concerns in the structures, and d) support to CEPOF as they seek additional services for forensic analysis and repair activities. This memorandum reports on the first area, a) life safety concerns. Areas b and c, intermediate and long-term structural and durability concerns, will be addressed in ERDC's final assessment report to be delivered on 11 March 2022. Area d support will be provided until CEPOF no longer needs the ERDC Team assistance.

[REDACTED]

CEERD-ZA

(U) SUBJECT: Initial ERDC Assessment of Camp Walker Family Housing Towers 1 and 2 and their Parking Garages

█ The ERDC Team has evaluated Towers 1 and 2 plus corresponding parking garages to assess the impact of observed cracking in the concrete structures, as initially reported by CEPOF. Our evaluation included on-site visual inspection of accessible areas, review of CEPOF documentation on the structures' condition, and an abridged review of the extensive design and construction records. Seventeen ERDC engineers, scientists and technicians with subject matter expertise in Structural Engineering, Concrete Materials, Geotechnical Engineering, Forensic Analysis, and Construction Practices have been engaged since 17 January 2022 to evaluate the available data and perform our initial assessment. Four of these personnel, Dr. C. Kennan Crane, PE, Dr. Oliver-Denzil S. Taylor, PE, Dr. Stephanie G. Wood, and Mr. Jason A. Morson have been onsite at Camp Walker to conduct independent ERDC inspections and testing.

█ The on-site team was able to visually inspect all concrete not covered by architectural finishings in Towers 1 and 2. Based upon these inspections, it was deemed unnecessary to conduct further destructive investigations behind wall coverings. The on-site team also performed a visual geotechnical and foundation assessment. The results of the foundation inspection and design review indicate that the cracking identified in these structures is not related to foundation distress. The following paragraphs provide more detail on the structural, geotechnical, and foundation observations and findings.

(U) Inspection Observations and Findings (Structural):

█ The structural tower designs utilize cast-in-place reinforced concrete slab and wall construction with a centrally located elevator shaft. According to the design documentation, progressive collapse resistance was incorporated per the requirements of Unified Facilities Criteria 4-023-03. These important design features enhance overall structural robustness and provide redundancy and resilience for load transfer and load redistribution through the structures.

CEERD-ZA

(U) SUBJECT: Initial ERDC Assessment of Camp Walker Family Housing Towers 1 and 2 and their Parking Garages

█ The on-site team visually inspected all concrete not covered by architectural sheetrock in Tower 1 and 2, which correlates to approximately 75% of Tower 1 and 2 basements and 15% to 20% of the upper floors (primarily in the stair wells, elevator shafts, and inter-floor space). Cracking was observed in a majority of the inspected areas and generally consisted of hairline cracks in multiple orientations with width of 0.2 mm or less. Hairline cracks were observed in the basement ceiling, which are accounted for by the reinforcement steel in standard design. Cracking was more prevalent in Tower 2 than in Tower 1. The on-site team did identify isolated cracks wider than 0.2mm, but no crack widths were observed in excess of 0.7mm. The predominately narrow crack widths, distribution, and orientation is largely consistent with non-structural shrinkage cracking and corroborates the findings of initial assessments made by CEPOF¹. These types of cracks represent more of a long-term durability challenge including potential for corrosion, freeze/thaw action, or other modes of deterioration.

█ The parking garages are cast-in-place reinforced concrete beam-column construction with monolithic slabs. The on-site team was able to visually inspect both structures and observed cracks in walls, beams, and slabs. In several instances, crack widths exceeded the width above which long-term durability is a concern (ie, 0.2 mm). Field observations of concrete cracking in the parking garages indicated restrained shrinkage cracking. Our analysis suggests that these cracks were not caused by structural deficiencies. However, due to their nature and orientation, and in order to maintain design factors of safety, it is prudent to address the recommend repairs in the near term as noted in the CEPOF memorandum².

█ Similar structural concrete was used across all structures and the reported QA/QC testing results for these materials are in accordance with design specifications. Additional testing is being conducted to confirm that in-place concrete strengths and compositions conform to design requirements and project specifications. The concrete mixture proportions as designed do not have clear indicators of potential severe shrinkage issues like those observed in the structures. The observed shrinkage and resultant cracking is likely the product of significant restraint provided by the heavily reinforced robust structural system coupled with (reportedly) poor quality curing practices. The ERDC Team's field observations, along with QA documentation, report extensive issues with concrete honeycombing and improper termination of concrete placements within walls and on slabs during construction, all of which have resulted in the presence of unintended cold joints in the columns and wall systems. However, this presents largely a long-term durability concern that should be addressed in the near term versus a structural concern.

CEERD-ZA

(U) SUBJECT: Initial ERDC Assessment of Camp Walker Family Housing Towers 1 and 2 and their Parking Garages

(U) Inspection Observations and Findings (Geotechnical and Foundations):

█ The on-site team performed a visual geotechnical and foundation assessment of interior and exterior areas of Towers 1 and 2 and their Parking Garages for evidence of foundation distress. The ERDC Team also reviewed the construction and design documents including the results of static and dynamic load tests performed on the pile foundations. The results of the foundation inspection and design review indicate that the cracking identified in these structures is not related to foundation distress or excessive movement of the foundation.

(U) Recommendations:

█ Based on the above observation and analysis, the ERDC Team has not observed any life safety concerns in Towers 1 and 2 or their connected parking garages. Cracking and defects observed in Towers 1 and 2 appear to be the result of concrete shrinkage cracking and are not a structural concern. Cracking observed in Parking Garages 1 and 2 do not present a life safety concern, but they should be addressed as noted within the CEPOF memorandum dated 19 January 2022². As a precautionary measure, until the expert consultant forensics evaluation is completed, the ERDC Team recommends that on-site personnel continue to conduct regular monitoring for cracking and displacements in the structures and that the CEPOF continues to work, as planned, to engage an expert structural forensics consultant to further assess long-term impacts of this cracking on the service life of the structure and to develop remediation plans to ensure intended factors of safety are maintained. For Towers 1 and 2 and associated parking garages, the ERDC Team's initial assessment is that the observed issues will not degrade the near-term extreme event performance (earthquake, wind, progressive collapse) below the original design levels. However, the follow-on detailed analyses by the third-party evaluator should address this question in detail.

CEERD-ZA

(U) SUBJECT: Initial ERDC Assessment of Camp Walker Family Housing Towers and Parking Garages 1 and 2

(U) If you or your team have any additional questions or concerns we will be glad to discuss. The ERDC will continue their analysis of Towers 3 and 4 and associated parking garages as well as conducting additional sampling with the goal of providing a full analysis by 11 March 2022.

AUTHORITY LINE:



BARTLEY P. DURST, SES
Director, Geotechnical and Structures
Laboratory



DAVID W. PITTMAN, PE, PhD, SES
ERDC Director

1 Encls
The ERDC Team Personnel List

Acronyms and Abbreviations

Term	Definition
ACI	American Concrete Institute
AE	Architectural/Engineering
AFCEC	Air Force Civil Engineer Center
ASTM	American Society for Testing and Materials
CEPOD	USACE Pacific Ocean Division
DA	Department of the Army
ERDC	Engineer Research and Development Center
FED	Far East District
FHWA	Federal Highway Administration
GPR	Ground-Penetrating Radar
GSL	Geotechnical and Structures Laboratory
HRWA	High Range Water Reducing Admixture
NAS	National Academy of Sciences
NAVFAC	Naval Facilities Engineering Command
NDT	Nondestructive Testing
NMSA	Nominal Maximum Size Aggregate
PCA	Portland Cement Association
PLT	Point Load Test
POD	Pacific Ocean Division
QA/QC	Quality Assurance/Quality Control
QAR	Quality Assurance Representative
SCM	Supplementary Cementitious Material
UC	Unconfined Compression
UFC	Unified Facilities Criteria
USACE-POF	U.S. Army Corps of Engineers Far East District

Unit Conversion Factors

Multiply	By	To Obtain
cubic yards	0.7645549	cubic meters
feet	0.3048	meters
inches	0.0254	meters
microinches	0.0254	micrometers
microns	1.0 E-06	meters
pounds (force)	4.448222	newtons
pounds (force) per square inch	6.894757	kilopascals

REPORT DOCUMENTATION PAGE

Form Approved
OMB No. 0704-0188

Public reporting burden for this collection of information is estimated to average 1 hour per response, including the time for reviewing instructions, searching existing data sources, gathering and maintaining the data needed, and completing and reviewing this collection of information. Send comments regarding this burden estimate or any other aspect of this collection of information, including suggestions for reducing this burden to Department of Defense, Washington Headquarters Services, Directorate for Information Operations and Reports (0704-0188), 1215 Jefferson Davis Highway, Suite 1204, Arlington, VA 22202-4302. Respondents should be aware that notwithstanding any other provision of law, no person shall be subject to any penalty for failing to comply with a collection of information if it does not display a currently valid OMB control number. **PLEASE DO NOT RETURN YOUR FORM TO THE ABOVE ADDRESS.**

1. REPORT DATE (DD-MM-YYYY) April 2022		2. REPORT TYPE Final		3. DATES COVERED (From - To)	
4. TITLE AND SUBTITLE Report on Evaluation of Apartment Towers 1–4 and Parking Garages 1–4 at Camp Walker, Daegu, South Korea				5a. CONTRACT NUMBER	
				5b. GRANT NUMBER	
				5c. PROGRAM ELEMENT NUMBER	
6. AUTHOR(S) C. Kennan Crane, Omar Esquilin-Mangual, Bradley W. Foust, Andrew B. Groeneveld, William F. Heard, John M. Hoemann, Kyle L. Klaus, Jason A. Morson, Robert D. Moser, James C. Ray, M. Jason Roth, Cody M. Strack, Lucas A. Walshire, Stephanie G. Wood, and Stanley C. Woodson				5d. PROJECT NUMBER	
				5e. TASK NUMBER	
				5f. WORK UNIT NUMBER	
7. PERFORMING ORGANIZATION NAME(S) AND ADDRESS(ES) Geotechnical and Structures Laboratory U.S. Army Engineer Research and Development Center 3909 Halls Ferry Road Vicksburg, MS 39180				8. PERFORMING ORGANIZATION REPORT NUMBER ERDC/GSL TR-22-5	
12. DISTRIBUTION / AVAILABILITY STATEMENT Approved for public release; distribution is unlimited.				10. SPONSOR/MONITOR'S ACRONYM(S)	
				13. SUPPLEMENTARY NOTES Pacific Ocean Division (POD) funding	
14. ABSTRACT In August of 2021, unexpected cracking was discovered in the concrete of newly constructed apartment towers and parking garages at Camp Walker, Daegu, South Korea. Initial evaluation by USACE Far East District (USACE-POF) determined the towers to be safe for continued occupation. Out of an abundance of caution a team from the Engineer Research and Development Center (ERDC) conducted an independent evaluation of these structures to further verify life safety. Additionally, this evaluation sought to determine the potential causes of this cracking and remediation schemes both to inform future construction, but also to lay the groundwork for a more in-depth lifecycle evaluation by an Architectural/Engineering (AE) firm specializing in structural forensics. The ERDC evaluation consisted of on-site inspection, nondestructive testing, materials sampling and testing, and review of particular design and construction documentation provided by the Far East District. The results of the evaluation confirmed the Far East District's findings that there was not a threat to life safety in these structures. Furthermore, the results of the ERDC evaluation indicated that drying shrinkage was the most likely causes of the observed cracking. In the areas where this cracking was the most severe, repair with epoxy injection was recommended for continued structural safety. In areas with moderate cracking, sealing of cracks was recommended to prevent long-term durability issues decreasing the lifespan of the structures.					
15. SUBJECT TERMS Forensic analysis Structural inspection			Reinforced concrete Concrete shrinkage Construction practices Concrete--Cracking		Geotechnical evaluation Military bases—Korea (South) Buildings—Structural health monitoring Buildings—Maintenance and repair
16. SECURITY CLASSIFICATION OF:			17. LIMITATION OF ABSTRACT SAR	18. NUMBER OF PAGES 226	19a. NAME OF RESPONSIBLE PERSON
a. REPORT Unclassified	b. ABSTRACT Unclassified	c. THIS PAGE Unclassified			19b. TELEPHONE NUMBER (include area code)

